10

LEVEL

GENERAL ✷ ELECTRIC

AD A056283

(10)

(6)

AN/TPS-59(XN-1) EDM
RADAR SET, MARINE LIGHTWEIGHT TACTICAL 3D
ENGINEERING DEVELOPMENT MODEL .

PRE-SERVICE ACCEPTANCE TEST REPORT.

VOLUME I.

(11) 29 Apr 1977

A056284
V 2

(12) 197 p.

CONTRACT DATA REQUIREMENTS LIST
SEQUENCE LINE ITEM 0005 SEQUENCE NO. C005

(15)
Prepared Under
Contract N00039-72-C-0356
G. E. Requisition EH-88274

DDC
RECEIVED
JUL 13 1978
A

(14) EH-88274-VOL-I

Prepared for

Department of the Navy
Naval Electronics Systems Command
Washington, DC 20360

149 500

TABLE OF CONTENTS

Paragraph	Title	Page

TABLE OF CONTENTS (Continued)

TABLE OF CONTENTS (Continued)

LIST OF ILLUSTRATIONS

LIST OF ILLUSTRATIONS (Continued)

LIST OF TABLES

LIST OF TABLES (Continued)

1.0. INTRODUCTION.

This document contains the test results obtained in performing the Pre-Service performance tests in accordance with the approved Acceptance Test Procedures, Section 4.0. The pre-service testing was done at a test site at Verona, New York to demonstrate the electrical performance, reliability, maintainability and RF Compatibility of the AN/TPS-59(XN-1) in relation to the Specifications of ELEX-R-50.

The test report is submitted in three volumes. Volume I contains the summarized data and results obtained. Volume II contains the Appendices. The third volume, submitted separately, contains all the classified portions of the data.

1.1. PURPOSE.

The purpose of this pre-service test acceptance test report is to summarize and document the results obtained in performance of the pre-service tests on the AN/TPS-59(XN-1) tactical 3-D radar. This document is submitted in response to contract data requirements list, item 005, sequence number C005.

1.2. SCOPE.

A summary of the performance demonstrations which comprise the Pre-Service Acceptance Test Procedures is shown in Table 1-1. In accordance with Contract Modification P00028, modification or deferment of certain tests or substitution of data obtained during prior phases of the contract in lieu of certain other tests were implemented as indicated in the comments column of Table 2-1. Details of the modification, deferments, or substitutions are given in the appropriate test report paragraph. The material in this report has been arranged in the same sequence and, as much as possible, in the same format as the Pre-Service Acceptance Test Procedures.

1-3. SUMMARY.

The significant test results are summarized below. A Lear jet with an average cross section of 0.7 square meters Swerling Case III was used as the test vehicle during the flight tests.

Table 1-1. Pre-Service Performance Tests

Performance Tests	Acceptance Test Procedure Para. No.	Test Report Para. No.	Comments
Electrical Performance Tests	4.1	2.0	Tests Modified (See Para 2.2 for details).
Reliability Demonstration Test	4.2	3.0	Test Modified.
Maintainability and Inter-Changeability Demonstration Test	4.3	4.0	Test Modified.
Power Test	4.4	5.0	Prior data substituted.
Supply Line Voltage and Frequency Tests	4.5	6.0	Prior data substituted.
Preliminary Heat Test	4.6	7.0	Test Modified.
Enclosure Test	4.7	8.0	Prior data substituted.
Assembly/Disassembly	4.8	7.0	Prior data substituted.
Weights and Dimensions	4.9	10.0	
Preliminary Road Test	4.10	11.0	Prior data substituted.
RF Antenna Measurements	4.11	12.0	
Noise Test	4.12	13.0	
Preliminary EMI Test	4.13	14.0	Refer to Vol. III (Classified Data)
Interchangeability Demonstration	4.14	15.0	Deferred to future effort.
Surface Examination	4.15	16.0	
Salt Spray Test	4.16	17.0	Prior Test substituted.
TAOC Integration Demonstration	4.17	18.0	Deferred to future effort.

1) <u>Probability of Detection (P$_D$) in the Clear</u>

A P$_D$ of 0.906 averaged over a 0 to 200 nmi range was obtained on the Lear
jet that flew ten flight paths at altitudes that varied from 2000 feet to 40,000 feet.
The individual P$_D$ for range intervals 0 to 20 nmi, 80 to 100 nmi, and 180 to 200 nmi
were 0.725, 0.879, and 0.781 respectively and recommendations are included in this
report on how to increase this to the 0.90 specification.

2) <u>Probability of Detection (P$_D$) in Ground Clutter</u>

A P$_D$ of 0.960 (0.9 specification) averaged over a 0 to 100 nmi range was
obtained on the test aircraft which flew at speeds of 160 to 400 knots at altitudes of
5000 and 10,000 feet.

The average number of false alarms per scan on noise and clutter residue was
less than six where the specification allowed 10.

3) <u>Range Accuracy and Minimum Range Test</u>

A range accuracy of 49.4 feet averaged over 0 to 100 nmi and 124.6 feet
averaged over 100 to 200 nmi was obtained on the test target which flew ten flight
paths at altitudes that varied from 2000 to 40,000 feet. The specified accuracies
were 100 feet for 0 to 100 nmi and 400 feet for 100 to 300 nmi. The measured data
exceed the specification substantially.

The minimum reported range, averaged over six flights, was 3.75 nmi compared
to the 4.0 nmi specification.

4) <u>Range Resolution</u>

The range resolution was determined for simulated aircraft spacings of 200 feet
for the 0 to 100 nmi range and 800 feet for the 100 to 300 nmi range.

For the 200 foot spacing, two detections were obtained 32% of the time.
Theoretical calculations show that this is the expected value. For the 800 foot
spacing, two detections were obtained 42% of the time; this agrees quite closely
with the expected 43% value.

5) Azimuth Accuracy

An azimuth accuracy of 4.41 mr averaged over a 0 to 200 nmi range, was obtained on the test aircraft on ten flight paths at altitudes that varied from 200 to 40,000 feet. The measured accuracy is degraded from the specified value of 3 mr by 47%. The azimuth accuracy is relatively constant with range and recommended software modifications to improve the accuracy are included in this report.

6) Height Accuracy

The height accuracy was determined by measuring the height of the test aircraft over the flight paths at altitudes that varied from 2000 to 40,000 feet.

The accuracy was better than the specified 1000 feet for all ranges and altitudes out to 80 nmi except for the 40,000 feet altitude in the 20 to 40 nmi range interval. Spoiled beams in this region degraded the height accuracy.

Beyond 80 nmi, the height accuracy is degraded by about 60% from the specified accuracy except for the 20,000 to 30,000 feet altitudes in the 100 to 120 nmi range interval where the specified accuracy was met. Post flight data indicated that a 1.5 mr elevation bias existed at the time of the flights. Removal of this bias would improve the height accuracy to the point where it is only degraded about 35% from the specified accuracy.

Recommendations on how to improve the height accuracy are included in this report.

7) Reliability Demonstration

The AN/TPS-59(XN-1) was operated from June 21, 1976 to July 17, 1976 for 546 hours of operation without a relevant failure. Extrapolation of 546 hours of operation to 1000 hours indicates that a MTBF of 1000 hours with a 60% confidence level can be expected.

8) Maintainability and Interchangeability Demonstration Test

A number of failures were induced in both the shelter and platform equipments. The Fault Location program successfully determined where the simulated failures occurred.

9) <u>Control and Control Circuits Demonstration</u>

This demonstration indicated that the AN/TPS-59(XN-1) will operate in both the GCI and MTDS modes and that the ancillary mode controls are functional.

10) <u>Power and Supply Line Voltage and Frequency Test</u>

Two years of AN/TPS-59(XN-1) operation with standard Marine Corps motor generators indicates satisfactory operation is achievable with standard power equipment used in the field.

11) <u>Preliminary Heat Test</u>

The shelter equipment operated satisfactorily for 3.5 hours with only one air conditioner before an over temperature condition resulted. Additional air baffling in the Radar Console was added to correct this problem.

Four rows of electronics operated satisfactorily for 4 hours in a sealed 50°C environment. One row power supply failed, but subsequent analysis indicated a HIC inverter had failed because of a process problem.

2.0. ELECTRICAL PERFORMANCE TESTS.

2.1. PURPOSE.

Electrical performance tests were conducted as part of the Pre-Service Acceptance Test Procedures to verify the performance parameters of the AN/TPS-59(XN-1) Radar Set. The general scope of the tests and a description of the test method used for the majority of the tests is given in paragraphs 2.2 and 2.3. The detailed scope, results, conclusions and recommendations, if any, for each individual test are contained in appropriate subparagraphs under paragraphs 2.4 through 2.11.

2.2. SCOPE.

A summary of the performance demonstrations and their constituent subtests which comprise the electrical performance tests specified in the Pre-Service Acceptance Test Procedures is shown in Table 2-1. In accordance with Contract Modification P00028, modification of certain test procedures; deferment of weather, ECCM, and 2D mode testing to a future phase of the contract; and substitution of tests conducted during prior phases of the contract in lieu of certain tests specified in the acceptance test procedures were implemented in the Electrical Performance Tests as indicated in the comments column of Table 2-1. Details of the test procedure modifications, test deferments, or test substitutions are given in the appropriate test report paragraphs.

2.3. TEST METHOD.

With the exception of the range resolution and control circuit subtests, analytical data for the AN/TPS-59(XN-1) electrical performance demonstrations were obtained through the use of controlled flight tests conducted at the USAF RADC Verona Test Annex, Verona, New York on 1 June 1976 through 4 June 1976. The flights described in the Pre-Service Acceptance Test Procedure (paragraph 4.1.2) and designated as F1 through F10, F12, and F13, are repeated for reference in Table 2-2.

Table 2-1. Electrical Performance Tests

Performance Demonstration	Acceptance Test Procedure Para. No.	Test Report Para. No.	Comments
Detectability	4.1.4.1	2.4	
1) Aircraft Detectability Subtest	4.1.4.1.3	2.4.1	
2) Min. Range Subtest	4.1.4.1.5	2.4.2	
Resolution	4.1.4.2	2.5	
1) Angular Resolution Subtest	4.1.4.2.3	2.5.1	Prior test substituted
2) Range Resolution Subtest	4.1.4.2.5	2.5.2	Test procedure modified
Accuracy	4.1.4.3	2.6	
1) Range Accuracy Subtest	4.1.4.3.3	2.6.1	
2) Azimuth Accuracy Subtest	4.1.4.3.3	2.6.2	
3) Height Accuracy Subtest	4.1.4.3.5	2.6.3	
Anti-Clutter	4.1.4.4	2.7	
1) Anti-Ground Clutter Subtest	4.1.4.4.3	2.7.1	
2) Anti-Weather Clutter Subtest	4.1.4.4.5	2.7.2	Deferred to future effort
ECCM	4.1.4.5	2.8	Deferred to future effort
IFF	4.1.4.6	2.9	Deferred to future effort
Control and Control Circuits	4.1.4.7	2.10	
1) GCI Operation Subtest	4.1.4.7.2	2.10.1	
2) MTDS-Mated Operation Subtest	4.1.4.7.3	2.10.2	
3) Ancillary Controls Subtest	4.1.4.7.4	2.10.3	Modified test procedure
Alternate Modes	4.1.4.8	2.11	Deferred to future effort

Table 2-2. Aircraft Flights

F1	A radial flight path at 40K ft altitude; 20 nmi to 120 nmi range limits; 4 legs (2 up range and 2 down) at a speed of approximately 400 knots.
F2, F3, F4	Radial flight paths at 40K ft altitude; 120 to 220 nmi range limits; 4 legs each flight (12 legs total) at speed of approximately 400 knots.
F5, F6	Radial flight paths at 30K ft altitude; 60 to 200 nmi range limits; 3 legs each flight at a speed of 400 knots.
F7	A radial flight path at 20K ft altitude; 10 to 120 nmi range limits; 3 legs at a speed of 320 knots.
F8	A radial flight path at 10K ft altitude; from 5 to 120 nmi and back; 3 legs at a speed of 250 knots.
F9	A radial flight path at 5K ft altitude; from overhead to 80 nmi and back; 3 legs at a speed of 250 knots.
F10	A radial flight path at 2K ft altitude; from overhead to 50 nmi and back; 5 legs at a speed of 250 knots.
F12	A radial flight path from overhead to 80 nmi and return at an altitude of 5K ft; through heavy ground clutter; 1 leg at 160 knots, 1 leg at 200 knots and 2 legs at 240 knots.
F13	A radial flight path from overhead to 80 nmi and return at an altitude of 10K ft; through heavy ground clutter; 1 leg at 300 knots, 1 leg at 350 knots, 1 leg at 375 knots and 1 leg at 400 knots.

In accordance with Contract Modification P00028, flight F11 (range resolution test) was cancelled and flights F14 through F16 (weather and ECCM tests) were deferred to a future phase of the contract. In addition, the AN/TPS-59(XN-1) was operated during all flights with the MTI, Normalizer, and SET 1 functions enabled and with the SET 2 and SET 3 functions disabled.

A flight test procedure (Appendix A) was prepared and used to determine the pre- and post- "flight day" status of the AN/TPS-59(XN-1) Radar Set as well as the blip/scan data for each flight. The "flight day" logs containing the radar status and blip/scan data are provided as Appendix B.

The flight tests were conducted using the AN/TPS-59(XN-1), an AN/FPS-16 Tracking Radar calibrated and maintained by the Verona Test Annex, and a Lear jet aircraft equipped with a C-band beacon. As described in the Pre-Service Acceptance Test Procedures (paragraph 4.1.3), data concerning the AN/TPS-59(XN-1) estimates of range, azimuth and height were recorded on magnetic tape. Simultaneous recordings of range, azimuth and elevation estimates of the AN/FPS-16 tracking radar were also made. The data was reduced (data association, coordinate transformation, etc.) offline with differences between the AN/TPS-59(XN-1) and AN/FPS-16 position estimates used to determine the accuracy of the AN/TPS-59(XN-1).

Only valid AN/FPS-16 and AN/TPS-59(XN-1) detections were used in determining the radar accuracies. If the AN/TPS-59(XN-1) data indicated that a conflict existed in tagging the target, the data was ignored for accuracy evaluation. Instances when the AN/TPS-59(XN-1) data were on the wrong aircraft, as verified in the blip/scan data, were also eliminated from the accuracy statistics. Also, data points collected from the AN/FPS-16 when it had "broken track" were eliminated. These were most readily identified by reviewing computer plots of the trajectory of the target aircraft. In addition, the blip/scan data was used to assist in determining probability-of-detection.

The processed data, reduced and purged as described above, were summarized and are presented in Tables 2-3, 2-5, 2-6, 2-7, 2-9, 2-11, 2-12, 2-14, and 2-15. Magnetic tapes of the AN/FPS-16 and AN/TPS-59(XN-1) raw flight data and the computer printouts of the processed data have been retained at General Electric for reference purposes.

2.4. DETECTABILITY DEMONSTRATION.

This demonstration consisted of the aircraft detectability and minimum range subtests given below.

2.4.1. Aircraft Detectability Subtest.

2.4.1.1. Scope.

This subtest was conducted to determine the clutter-free (in-the-clear) probability-of-detection for the AN/TPS-59(XN-1) over a specified number of range intervals. The subtest was performed in accordance with the procedures given in paragraph 4.1.4.1.3 of the Pre-Service Acceptance Test Procedures.

Flights F1 through F10 were employed to collect data used in determining the detectability of the radar in the clear out to a range of 220 nautical miles (nmi). Probability-of-detection for range intervals beyond 200 nmi was extrapolated from the curves given in Figure 4.1-4a of the Pre-Service Test Procedures using the radar performance at 200 nmi as a base.

The AN/TPS-59(XN-1) shall have passed this subtest if all the average detection probabilities (P_D) defined as number of detections divided by the number of scans) equals or exceeds 90% for all range intervals less than 200 nmi and 70% for all range intervals exceeding 200 nmi.

2.4.1.2. Results.

Processed detection data collected from flights F1 through F10 along with applicable flight blip/scan data extracted from Appendix B was summarized as explained below and is shown in Table 2-3. Each leg of each flight was divided into 20 nmi range intervals. The number of detections (N_D) and scans (N_S) for each flight were summed vertically for each range interval; then, the total N_D was divided by the total N_S to determine the average probability-of-detection (P_D) for each interval.

Table 2-3. Probability-o

Range	0-20					20-40					40-60				
Flights (Processed Data Printout No.)	N_S	N_D	N_C	P_D	P_D'	N_S	N_D	N_C	P_D	P_D'	N_S	N_D	N_C	P_D	P_D'
1A (ATR 1-1)						17	17	6	1.000	0.647	23	23	0	1.000	1.(
1B (ATR 1-2)						16	16	4	1.000	0.750	18	18	0	1.000	1.
1C (ATR 1-3)						19	19	7	1.000	0.632	24	24	0	1.000	1.
1D (ATR 1-7)						18	18	6	1.000	0.667	18	18	0	1.000	1.
Subtotal						70	70	23	1.000	0.671	83	83	0	1.000	1.
5A (ATR 3-9)															
5B (ATR 4-1)											6	6	0	1.000	1.
5C (ATR 4-2)											2	2	0	1.000	1.
5A (ATR 4-3)											2	2	0	1.000	1.
5B (ATR 4-4)											2	2	0	1.000	1.
5C (ATR 4-5)															
Subtotal											12	12	0	1.000	1.
7A (ATR 2-1)						26	26	0	1.000	1.000	26	26	0	1.000	1.
7B (ATR 2-2)	11	5	0	0.455	0.455	24	24	2	1.000	0.917	25	25	0	1.000	1.
7C (ATR 2-5)	2	1	0	0.500	0.500	26	26	0	1.000	1.000	27	26	0	0.963	0.
Subtotal	13	6	0	0.462	0.462	76	76	2	1.000	0.974	78	77	0	0.987	0.
8A (ATR 2-6)	22	12	0	0.545	0.545	31	31	2	1.000	0.935	31	31	0	1.000	1.
8B (ATR 6-1)	22	16	0	0.727	0.727	30	30	1	0.909	0.879	34	33	0	0.971	0.
8C (ATR 7-1)	14	9	0	0.643	0.643	33	32	5	0.970	0.818	32	32	0	1.000	1.
Subtotal	58	37	0	0.638	0.638	97	93	8	0.959	0.876	97	96	0	0.990	0.
9A (ATR 7-2)	27	20	0	0.741	0.741	31	30	2	0.968	0.903	26	20	0	0.769	0.
9B (ATR 7-3)	18	9	0	0.500	0.500	31	30	1	0.968	0.935	23	19	0	0.826	0.
9C (ATR 7-4)	27	19	0	0.704	0.704	33	31	1	0.939	0.909	18	17	0	0.944	0.
Subtotal	72	48	0	0.667	0.667	95	91	4	0.958	0.916	67	56	0	0.836	0.
10A (ATR 5-1)	28	20	0	0.714	0.714	20	18	1	0.900	0.850	8	8	0	1.000	1.
10B (ATR 5-2)	31	23	0	0.742	0.742	15	15	2	1.000	0.867					
10C (ATR 5-3)	24	22	0	0.917	0.917	20	20	1	1.000	0.95					
10D (ATR 5-3)	30	25	0	0.833	0.833	33	32	1	0.970	0.939					
10E (ATR 5-5)	24	22	0	0.917	0.917	38	36	0	0.947	0.947	2	2	0	1.000	1.
Subtotal	137	112	0	0.818	0.818	126	121	5	0.960	0.921	10	10	0	1.000	1.
Total	280	203	0	0.725	0.725	464	451	42	0.972	0.881	347	334	0	0.963	0.

/

obability-of-Detection Data

0-60		60-80					80-100					100-120				
P_D	P_D'	N_S	N_D	N_C	P_D	P_D'	N_S	N_D	N_C	P_D	P_D'	N_S	N_D	N_C	P_D	P_D'
1.000	1.000	22	22	0	1.000	1.000	23	22	0	0.957	0.957	21	21	0	1.000	1.000
1.000	1.000	17	17	0	1.000	1.000	17	16	0	0.941	0.941	17	17	1	1.000	0.941
1.000	1.000	24	24	0	1.000	1.000	24	24	0	1.000	1.000	23	23	0	1.000	1.000
1.000	1.000	17	17	0	1.000	1.000	18	17	0	0.944	0.944	17	17	0	1.000	1.000
1.000	1.000	80	80	0	1.000	1.000	82	79	0	0.963	0.963	78	78	1	1.000	0.987
		22	22	0	1.000	1.000	23	23	1	1.000	0.957	22	22	0	1.000	1.000
1.000	1.000	25	24	0	0.960	0.960	22	21	0	0.955	0.955	23	23	1	1.000	0.957
1.000	1.000	22	22	0	1.000	1.000	22	19	0	0.864	0.864	22	22	0	1.000	1.000
1.000	1.000	27	27	0	1.000	1.000	23	22	0	0.957	0.957	23	23	0	1.000	1.000
1.000	1.000	21	21	1	1.000	0.952	20	18	0	0.900	0.900	21	21	0	1.000	1.000
		20	18	0	0.900	0.900	23	22	0	0.957	0.957	23	23	1	1.000	0.957
1.000	1.000	137	134	1	0.978	0.971	133	125	1	0.940	0.952	134	134	2	1.000	0.985
1.000	1.000	27	24	0	0.889	0.889	26	21	0	0.808	0.808	26	26	1	1.000	0.962
1.000	1.000	24	24	0	1.000	1.000	24	22	0	0.917	0.917	23	23	0	1.000	1.000
0.963	0.963	28	27	0	0.964	0.964	27	17	0	0.630	0.630	28	28	0	1.000	1.000
0.987	0.987	79	75	0	0.949	0.949	77	60	0	0.779	0.779	77	77	1	1.000	0.987
1.000	1.000	32	28	0	0.875	0.875	21	14	0	0.667	0.667					
0.971	0.971	31	25	0	0.806	0.806	3	2	0	0.667	0.667					
1.000	1.000	31	25	0	0.806	0.806	6	4	0	0.667	0.667					
0.990	0.990	94	78	0	0.830	0.830	30	20	0	0.667	0.667					
0.769	0.769															
0.826	0.826															
0.944	0.944															
0.836	0.836															
1.000	1.000															
1.000	1.000															
1.000	1.000															
0.963	0.963	390	367	1	0.941	0.938	322	284	1	0.882	0.879	289	289	4	1.000	0.986

2

Table 2-3. Probability-of-D

Flights (Processed Data Printout No.)	Range 120-140					140-160					160-180				
	N_S	N_D	N_C	P_D	P_D'	N_S	N_D	N_C	P_D	P_D'	N_S	N_D	N_C	P_D	
2A (ATR 1-1)	22	22	0	1.000	1.000	22	21	1	1.000	0.955	21	16	0	0.762	0.
2B (ATR 1-2)	18	18	1	1.000	0.944	17	17	0	1.000	1.000	17	15	0	0.882	0.
2C (ATR 1-3)	23	23	2	1.000	0.913	23	21	0	0.913	0.913	22	22	0	1.000	1.
2D (ATR 1-4)	17	17	0	1.000	1.000	17	16	0	0.941	0.941	18	18	0	1.000	1.
3A (ATR 3-8)	22	22	0	1.000	1.000	22	22	0	1.000	1.000	21	18	0	0.857	0.
3B (ATR 1-7)	17	17	1	1.000	0.941	17	16	0	0.941	0.941	17	16	1	0.941	0.
3C (ATR 4-6)	19	19	0	1.000	1.000	19	19	0	1.000	1.000	20	19	0	0.950	0.
3D (ATR 3-3)	18	18	1	1.000	0.944	19	19	0	1.000	1.000	18	18	0	1.000	1.
4A (ATR 3-4)	24	24	0	1.000	1.000	23	23	0	1.000	1.000	22	22	1	1.000	0.
4B (ATR 3-5)	18	18	0	1.000	1.000	19	17	0	0.895	0.895	18	17	0	0.944	0.
4C (ATR 3-6)	25	24	2	0.960	0.880	23	22	0	0.957	0.957	22	22	0	1.000	1.
4D (ATR 3-7)	17	17	0	1.000	1.000	18	17	0	0.944	0.944	17	17	0	1.000	1.
Subtotal	240	239	7	0.996	0.967	239	230	1	0.962	0.958	233	220	3	0.944	0.
5A (ATR 3-9)	23	23	0	1.000	1.000	22	22	0	1.000	1.000	6	6	0	1.000	1.
5B (ATR 4-1)	24	24	0	1.000	1.000	24	23	1	0.958	0.917	4	4	1	1.000	0.7
5C (ATR 4-2)	22	22	1	1.000	0.955	24	24	0	1.000	1.000	11	10	1	0.909	0.8
6A (ATR 4-3)	23	23	1	1.000	0.957	22	22	0	1.000	1.000	6	4	0	0.667	0.6
6B (ATR 4-4)	21	21	0	1.000	1.000	22	22	1	1.000	0.955	11	7	1	0.636	0.5
6C (ATR 4-5)	22	22	0	1.000	1.000	22	22	1	1.000	0.955	17	14	0	0.824	0.8
Subtotal	135	135	2	1.000	0.985	136	135	3	0.993	0.971	55	45	3	0.818	0.7
Total	375	374	9	0.997	0.973	375	365	4	0.973	0.963	288	265	6	0.920	0.8

1

Table 2-3. Probability-of-Detection Data (Continued)

P_D'	160-180					180-200					200-220				
	N_S	N_D	N_C	P_D	P_D'	N_S	N_D	N_C	P_D	P_D'	N_S	N_D	N_C	P_D	P_D'
0.955	21	16	0	0.762	0.714	22	15	0	0.682	0.682	8	7	1	0.875	0.750
1.000	17	15	0	0.882	0.882	20	14	0	0.700	0.700	1	1	0	1.000	1.000
0.913	22	22	0	1.000	1.000	21	16	0	0.762	0.762					
0.941	18	18	0	1.000	1.000	8	8	0	1.000	1.000					
1.000	21	18	0	0.857	0.857	20	18	1	0.900	0.850	1	1	0	1.000	1.000
0.941	17	16	1	0.941	0.882	18	13	0	0.722	0.722					
1.000	20	19	0	0.950	0.950	25	13	1	0.520	0.480	3	1	0	0.333	0.333
1.000	18	18	0	1.000	1.000	16	14	0	0.875	0.875					
1.000	22	22	1	1.000	0.955	21	17	1	0.810	0.762	6	5	0	0.833	0.833
0.895	18	17	0	0.944	0.944	18	18	0	1.000	1.000	3	1	0	0.333	0.333
0.957	22	22	0	1.000	1.000	21	17	0	0.810	0.810	19	15	1	0.789	0.737
0.944	17	17	0	1.000	1.000	18	18	0	1.000	1.000	7	6	0	0.857	0.857
0.958	233	220	3	0.944	0.931	228	181	3	0.799	0.781	48	36	2	0.750	0.708
1.000	6	6	0	1.000	1.000										
0.917	4	4	1	1.000	0.750										
1.000	11	10	1	0.909	0.818										
1.000	6	4	0	0.667	0.667										
0.955	11	7	1	0.636	0.545										
0.955	17	14	0	0.824	0.824										
0.971	55	45	3	0.818	0.764										
0.963	288	265	6	0.920	0.899	228	181	3	0.794	0.781	48	36	2	0.750	0.708

2

The P_D for each leg of each flight and for each flight as a total was also determined. As additional information, the number of times a multiple declared target mark (N_C) occurred was also recorded. From this data, a modified probability-of-detection (P_D') that considered multiple declared target marks as misses was also determined $[(N_D - N_C) \div N_S]$. The results $(P_D$ and $P_D')$ are summarized in Table 2-4 and shown graphically $(P_D$ only) in Figure 2-1.

2.4.1.3. Conclusions.

As can be seen from Table 2-4, the AN/TPS-59(XN-1) achieved an over-all P_D of 0.927 and a P_D' of 0.906 in the region of 0 to 200 nmi, both of which surpassed the over-all specification P_D requirement of 0.900 for this region. In the region of 200 to 300 nmi, the over-all average P_D for the AN/TPS-59(XN-1), extrapolated from the 180 to 200 nmi P_D data, exceeded 0.670 which very nearly approaches the over-all specification P_D requirement of 0.700. for this region.

Examination of Figure 2-1 will show that while the AN/TPS-59(XN-1) exceeded the P_D requirement of 0.900 for the overall region from 0 to 200 nmi, the individual P_D for range intervals 0 to 20 nmi, 80 to 100 nmi, and 180 to 200 nmi fell somewhat short of the 0.900 P_D requirement. The significance is that these range intervals coincide with the maximum range of a given waveform used in the AN/TPS-59(XN-1) transmit template (simple pulse in the 0 to 20 nmi interval, short-range LFM pulse in the 20 to 100 nmi interval, and two long-range LFM pulses in the 100 to 200 nmi interval). Performance in the 0 to 20 nmi interval is attributable to the reluctance of some of the predrivers in the array row transceivers to "turn-on" during the short simple pulse, a fact that was known prior to the start of flight tests. Performance in the 80 to 100 nmi and 180 to 200 nmi intervals is not as easily explainable, but it appears to be relatable directly to system sensitivity and target cross section.

Comparison of the flight data with an analytical prediction which assumes a $0.7m^2$ steady (i.e., nonfluctuating) target, indicates that the radar is 2 dB low in sensitivity relative to its condition as determined in our April sensitivity evaluation (presented to NRL on 21 April 1976). The conclusion of a lack of sensitivity is hard to accept in face of the exhaustiveness of the April evaluation. An alternative explanation is that the target is not steady, but actually fluctuates. For example, the signal-to-noise ratio required to achieve a 90% detection probability on a $0.7m^2$ (Swerling Case I) fluctuating target is 8.0 dB greater than that required against a $0.7m^2$ steady reflector.

Table 2-4. Probability-of-Detection (P_D) and Modified
Probability-of-Detection (P_D') Vs Range

Range Measured Data	Scans (N_S)	Detection (N_D)	Multiples (N_C)	P_D	P_D'
0-20	280	203	0	0.725	0.725
20-40	464	451	42	0.972	0.881
40-60	347	334	0	0.963	0.963
60-80	390	367	1	0.941	0.938
80-100	322	284	1	0.882	0.879
100-120	289	289	4	1.000	0.986
120-140	375	374	9	0.997	0.973
140-160	375	365	4	0.973	0.963
160-180	288	265	6	0.920	0.899
180-200	228	181	3	0.794	0.781
Total 0-200	3358	3113	70	0.927	0.906
200-220	48	36	2	0.750	0.708
Extrapolated Data					
200-220				0.770	
220-240				0.720	
240-260				0.700	
260-280				0.630	
280-300				0.570	
Total 200-300				>0.670	
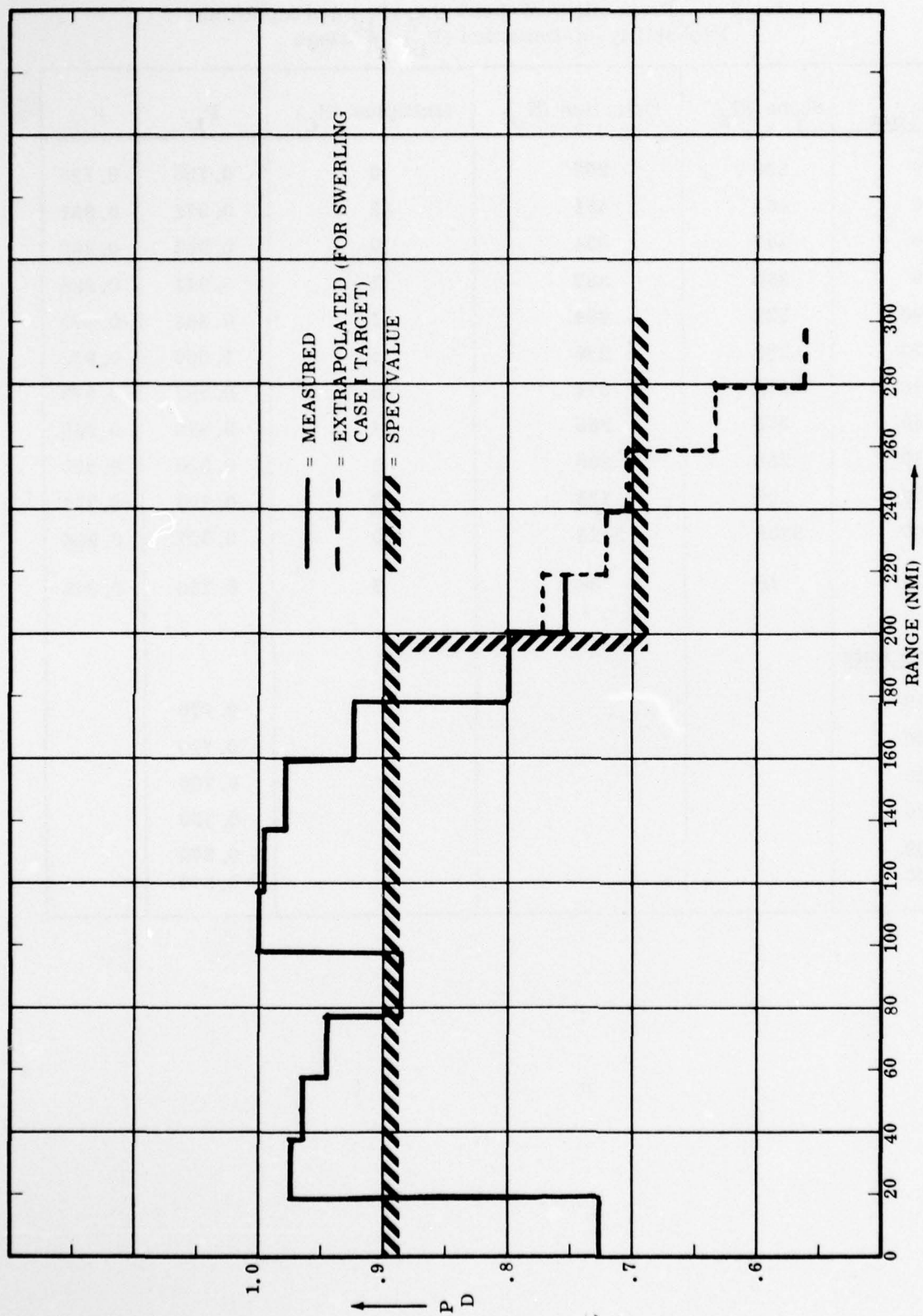
Figure 2-1. Probability of Detection vs Range

One argument supporting the notion that the target cross section fluctuates stems from a comparison between the performance achieved at 80 to 100 nmi and 180 to 200 nmi. At the longer range, including the higher atmospheric absorption loss, 12.3 dB more energy is required to achieve the same signal-to-noise ratio. The long range pulse has four times the energy of the short range pulse, hence the signal-to-noise ratio achieved at 200 nmi is less by 6.3 dB.

Now against a nonfluctuating target (an 88% detection probability), the value actually achieved in flight testing in the 80 to 100 nmi range interval requires a single pulse signal-to-noise ratio of 13.1 dB. In the 180 to 200 nmi interval, two transmissions provide a cumulative 78% detection probability when a 53% detection probability is achieved on each. With a two pulse waveform, the per pulse signal-to-noise ratio required to achieve a 53% detection probability is 9.0 dB. Hence, if the targets were nonfluctuating, the performance actually achieved would indicate a difference in signal-to-noise ratio of 4.1 dB. This is 2.2 dB less than the range and pulse width differences indicate it should be.

Under the assumption of a Swerling Case I fluctuating target, the measured probability of detections would indicate a difference in signal-to-noise ratio between the 200 and 100 nmi returns of 8.4 dB, or 2.1 dB greater than it should be. Under the assumption of a Swerling Case III fluctuating target, the indicated difference in signal-to-noise ratio between the 200 and 100 nmi returns is 6.3 dB, exactly the proper value.

Thus, the Swerling Case III target model is the only one consistent with the performance actually achieved. This model seems reasonable from another point of view. It is associated with a target consisting of one dominant return (ala the steady reflector) plus Rayleigh scattering (ala the Swerling I target). As a result, the fluctuations are not as severe as in Swerling I. They are like those which might be anticipated from an aircraft flying at a near constant aspect with respect to the radar. In our April sensitivity evaluation presentation, General Electric indicated that the signal-to-noise ratio which would be achieved on a return from a $0.7m^2$ reflector is 15.9 dB. This was under the assumption of a 2 dB field degradation loss. Since the actual loss experienced in the flight test was only about 0.5 dB, we should have actually achieved a signal-to-noise ratio of 17.4 dB. Under the assumption that the Lear jet is a $0.7m^2$

Swerling III fluctuating target, the predicted detection probability at 100 nmi becomes 89%, only 1% more than that actually realized. At 200 nmi, the per-pulse signal-to-noise ratio the radar should have achieved during flight testing is 11.1 dB. The associated detection probability against a Swerling Case III target is 79%, almost the value actually realized.

Thus, it appears that the radar sensitivity exhibited during flight testing is very nearly that predicted as a result of the April sensitivity evaluation. There are, however, several simple changes that can be made to the transmit template which should enhance performance in the range intervals beyond 180 nmi for a Swerling Case III target as well as overcome the turn-on difficulties associated with predrivers in the 0 to 20 nmi range interval. These changes are given in the recommendations paragraph below.

Note that improvements of the P_D for the 180 to 200 nmi range interval will cause a corresponding increase in the extrapolated P_D (based on Swerling Case I target) for the 200 to 300 nmi region. The resulting increases should cause the average P_D to meet or exceed the overall specification P_D requirement of 0.700 for the 200 to 300 nmi region.

Two other points are worth noting. In Figure 2-1, both extrapolated and actual P_D data are presented for the 200 to 220 nmi range interval, which employs the three-pulse portion of the transmit template. Unfortunately, the target aircraft, flying at 40,000 ft, was at or below the radar horizon at this range and only sporadic detection was achieved. This accounts for the actual P_D being lower than the extrapolated value at this range. The other point worth noting is the high number of declared target marks in the 20 to 40 nmi range interval. A review of the blip/scan data (Appendix B) shows that these primarily occur in the 40,000-foot flights. This region of coverage uses two broadened (spoiled) elevation beams and it appears that target returns entering through the high-angle sidelobes associated with these beams are the cause of the extra target marks. It will be seen in the height accuracy subtests results that this also effects height accuracy. A suggestion is offered in the recommendations given below to alleviate the multiple declared target marks and enhance height accuracy in this region.

2.4.1.4.   Recommendations.

2.4.1.4.1.   180 to 300 nmi Range Interval .

The following changes to the transmit template should be made to enhance the P_D in the 180 to 300 nmi region against a Swerling Case III target.

1)   Change the two-to-three pulse transition range from 200 nmi to 180 nmi.

2)   Change the three-to-four pulse transition range from 250 nmi to 220 nmi.

The three pulse waveform will increase the P_D at the 180 to 200 nmi range interval from 0.794 to a value that meets or exceeds 0.900. (Refer to Figure 2-2.) The P_D at 250 nmi will correspondingly increase from approximately 0.48 to 0.60 for the Swerling Case III target. Note that the P_D extrapolated for the Swerling Case I target shown in Table 2-4 and Figure 2-1 will also increase by some corresponding amount.

2.4.1.4.2.   80 to 100 nmi Range Interval .

Since the P_D for this range interval is nearly 0.900 for the Swerling Case III target, no changes are recommended. However, assuming that resultant increase in clutter returns would not be excessive and a slight degradation of range accuracy for this interval is not objectionable, the one-to-two pulse transition range could be shifted from 100 nmi to 80 nmi to enhance the P_D in this range interval, if desired.

2.4.1.4.3.   4 to 40 nmi Range Interval .

Two software changes are recommended to enhance detectability and height accuracy in this region.

1)   Replace the two spoiled beams used at the upper elevations of the short range interval with three unspoiled beams.

2)   If further investigation proves feasible, eliminate simple short pulse and use short range LFM pulse from 4 to 100 nmi (for XN-1 only).

It appears that the spoiled beams are the cause of the multiple declared target marks and degraded height accuracy in the 20 to 40 nmi range interval. Replacement of the two spoiled beams by three unspoiled beams can be accomplished with the addition of just under 1 ms to the elevation scan time. The associated increase in azimuth beam crossover is negligible.
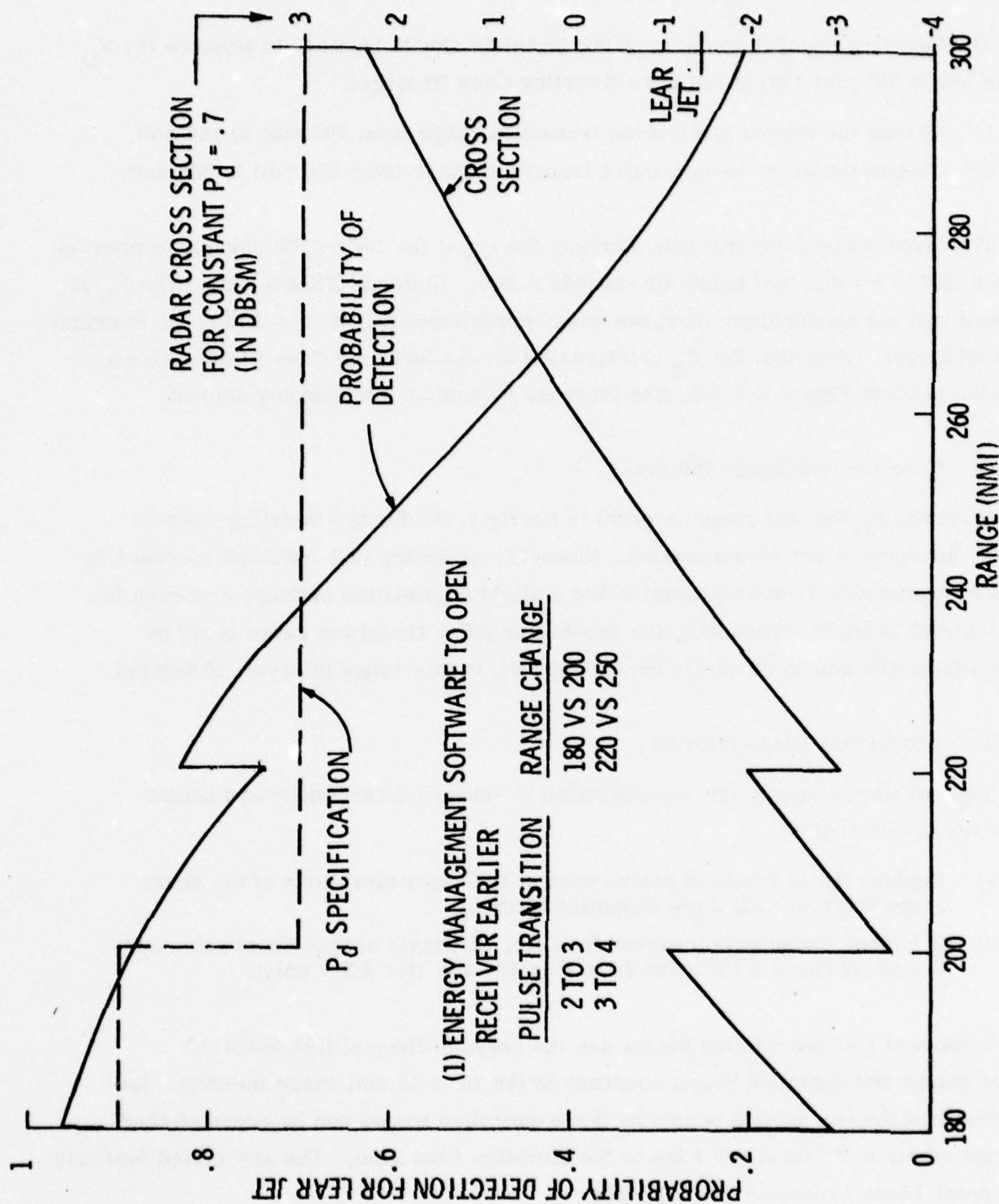
Figure 2-2. Detection Extrapolations for High Altitude Targets

To improve the detectability in the 0 to 20 nmi range interval, the previously known turn-on difficulties associated with the row transceiver predrivers must be overcome. Since the predriver has been substantially modified in the design of the next-generation, low-cost row transceiver scheduled for future production, improving the present predriver seems to be of questionable value. A possible solution that requires additional investigation is to eliminate the simple short pulse in the transmit template and use the 102.4 μs, short-range LFM pulse for the 0 to 100 nmi region. This solution, applicable only to the XN-1 model of AN/TPS-59, may have several minor complications. One is a definite, but slight loss of range resolution between 4 and 9 nmi due to truncation of the receive pulse. The other is a possibility of a high false alarm rate. Since the short-range LFM pulse has such high energy relative to the simple pulse (256 times as much), very short range clutter returns may cause false alarms, especially when entering through the sidelobes of the upper beams which do not employ MTI. Prior investigations of this change using the spoiled beams were not encouraging. Another investigation should be made after the spoiled beams have been eliminated. The unspoiled beams have lower sidelobes, to the extent that few clutter returns should be detectable and these should be eliminated by subsequent signal processing. If the investigation indicates improvement in short range performance, then this solution should be adopted for the AN/TPS-59(XN-1) to overcome the predriver turn-on difficulties.

2.4.2. Minimum Range Subtest.

2.4.2.1. Scope.

This subtest was conducted to determine the minimum detection range of the AN/TPS-59(XN-1). Flights F9 and F10 were employed to collect data for this subtest. The subtest was performed in accordance with the procedures given in paragraph 4.1.4.1.5 of the Pre-Service Acceptance Test Procedures except that only the inbound legs of the flights were used. Manual delays inherent in acquisition and initiation of data recording permitted the aircraft to exceed the minimum detection range before valid data could be recorded on the outbound legs of the flights.

The AN/TPS-59(XN-1) shall have passed this subtest if the average inbound minimum detection range (by radar) for the test flights is not greater than 4 nmi.

2.4.2.2. Results.

The minimum range reported on each of six flights is given in Table 2-5. The average of these six flights is 3.75 nmi.

Table 2-5. Minimum Range Data

Flight	Minimum Reported Range (nmi)
ATR 7-2	4.23
ATR 7-4	3.70
ATR 7-6	3.64
ATR 7-8	3.65
ATR 5-2	3.39
ATR 5-4	3.92
Average Minimum Range = 3.75 nmi	

2.4.2.3. Conclusions.

The AN/TPS-59(XN-1) is instrumented to detect targets to a minimum range of 3.0 nmi. The results of these flights (Flight ATR 5-2) and others indicate that aircraft can be detected to the instrumented minimum range and thus easily meet the specification value of 4.0 nmi.

2.5. RESOLUTION DEMONSTRATION.

This demonstration consisted of the angular and range resolution subtests given below.

2.5.1. Angular Resolution Subtest.

In accordance with Contract Modification P00028, this subtest was not conducted based on the results of resolution tests conducted during prior phases of the contract which are considered to demonstrate that the AN/TPS-59(XN-1) meets the requirement that the 6 dB round-trip beamwidth does not exceed 3.4° in azimuth and 1.7° in elevation at any point within the band from 1215 to 1345 MHz.

2.5.2. Range Resolution Subtest.

2.5.2.1. Scope.

This test was conducted in accordance with the Acceptance Test Plan, Rev. 5, dated 5/18/76, Para 4.1.4.2.5 to determine the AN/TPS-59(XN-1) range resolution. A sample copy of a portion of the Loop D 1538 hard copy data obtained for tests conducted on the short range mode is given in Figure 2-3.

The AN/TPS-59(XN-1) shall have passed this subtest if the range resolution probability is greater than 0.39 for simulated aircraft spacings of 200 feet and 800 feet in short and long range regions, respectively.

2.5.2.2. Results.

The data obtained in conducting this test was reduced and is summarized in Table 2-6 . In addition to the simulated aircraft spacing of 200 feet, tests were also conducted for simulated spacings of 250 feet. These results are also presented in Table 2-6. .

2.5.2.3. Conclusions.

For the signal-to-noise ratios used in this subtest, the theoretical range resolution probabilities should be increased in the long range region by the factor $1/0.9$ (1.1) where the 0.9 was the probability of detecting the aircraft. Thus, the 0.39 pass fail criteria becomes 0.43. The actual 0.42 value obtained is seen to correlate very

400 m.s. spacing   Equal Amplitude

#2

1-8-76

LOOP D
THIS PROGRAM PROCESSES SHORT RANGE REPLYS
ACTIVE TEST NUMBERS ARE
12A THROUGH D 14A AND 14B

RECPOND--14a
AUTOMATIC FAULT STATUS
0010100000000210000000000000AC0

NO	OCT	ID	RANGE	ACP	SI Σ_z	SQ Σ_q	MS $|\Sigma|$	AZI A_{Zc}	AZQ A_{Zq}	ELI EL_s	ELQ EL_q	AZM	ELM
1	0		279.2	12026	5	64	64	3	61	2	74	0.02	0.05
1	0		279.2	12029	80	29	85	79	33	83	31	0.04	0.20
	0		279.2	12033	37	-49	61	39	-46	40	-53	0.05-	0.00
1	0		279.0	12036	-48	30	56	-48	27	-55	29	0.04	0.07
2	0		279.6	12036	36	41	54	37	38	40	37	-0.05-	0.10
1	0		279.2	12043	59	61	84	59	60	61	61	-0.00-	0.01
1	0		279.2	12044	75	-25	79	74	-21	75	-26	0.04-	0.01
	0		279.0	12047	-49	-35	60	-45	-34	-59	-38	0.02-	0.04
2	0		279.6	12047	41	18	44	41	22	52	26	0.07	0.04
1	0		279.2	12051	28	67	72	23	63	29	73	0.04	0.01
1	0		279.2	12054	81	16	82	82	20	84	16	0.04-	0.20
	0		279.0	12058	-3	-62	62	1	-59	-1	-67	0.04	0.01
	0		279.0	12062	-43	37	56	-43	34	-47	39	0.04	0.01
2	0		279.6	12062	36	39	53	38	39	39	42	-0.02-	0.02
1	0		279.2	12065	70	47	84	65	49	68	46	0.02	0.00
1	0		279.2	12069	68	-32	75	68	-30	69	-34	0.02-	0.01
	0		279.0	12072	-58	-21	61	-55	-25	-65	-27	0.07	-0.04
2	0		279.6	12072	37	22	43	38	25	46	24	0.04-	0.05
1	0		279.2	12076	28	71	76	26	70	28	74	0.02	0.01
1	0		279.2	12080	84	5	84	83	8	85	4	0.03-	0.01
	0		279.0	12083	-17	-60	62	-13	-60	-21	-62	0.06-	0.05
2	0		279.6	12083	46	7	46	48	12	51	12	0.09	0.06
1	0		279.2	12087	-12	54	55	-15	54	-18	64	0.05	0.05
1	0		279.2	12094	75	43	86	70	46	72	48	0.06	0.01
1	0		279.2	12094	51	-41	65	52	-36	58	-45	0.07	0.01
	0		279.0	12097	-68	5	68	-59	3	-65	3	0.03	0.03
2	0		279.6	12097	36	33	48	38	32	44	33	-0.04-	0.03

Figure 2-3. Loop D Test 1538 Hard Copy Data Sample

close to the value expected in this region. By the same token, the relatively high signal-to-noise ratios used for this test insert an additional weighting filter in the digital path for short range signals to reduce the range lobes for high level signals, thus the 0.39 pass-fail criteria should be modified by the ratio 0.942/0.9 (1.04) where the factor is due to broading of the time domain response due to the additional weighting filter. The 0.32 value obtained is seen to also agree closely with the theoretical value expected. Since the digital weighting filter is not inserted for signals below the short range rescaling region, the range resolution probability can be expected to increase to the value 0.42 as obtained for the long range region. (No rescaling is accomplished in long range.)

Table 2-6. Range Resolution Data

LR/SR	Target 2 Target 1	Spacing ft (μsec)	No. Total Detections	% Total Multi Det.	% Total Averaged
SR	Leads	200(400)	117	30	
SR	Leads	200(400)	256	38	
SR	Lags	200(400)	111	41	
SR	Lags	200(400)	384	26	
			868		32
SR	Leads	250(500)	113	37	
SR	Leads	250(500)	512	40	
SR	Lags	250(500)	103	57	
SR	Lags	250(500)	512	37	
			1240		39.9
LR	Leads	800(1600)	68	25	
LR	Leads	800(1600)	21	33	
LR	Leads	800(1600)	61	43	
LR	Leads	800(1600)	61	46	
LR	Lags	800(1600)	63	35	
LR	Lags	800(1600)	51	63	
LR	Lags	800(1600)	61	44	
LR	Lags	800(1600)	58	48	
			444		42.1

Summary

Range Separation (Feet)	Estimated Range Resolution Probability (%)
200	32
250	39.9
800	42.1

2-19

2.6.   ACCURACY DEMONSTRATION.

This demonstration consisted of the range, azimuth, and height accuracy subtests given below.

2.6.1.   Range Accuracy Subtest.

2.6.1.1.   Scope.

This subtest was conducted to determine the range accuracy of the AN/TPS-59(XN-1).   Flights F1 through F10 were employed to collect the data.   The subtest was performed in accordance with the procedures given in paragraph 4.1.4.3.3 of the Pre-Service Acceptance Test Procedures.

The AN/TPS-59(XN-1) shall have passed this subtest if the averaged range errors for each 20 nmi range interval throughout the region covered jointly by the AN/TPS-59(XN-1) and AN/FPS-16 satisfy the following inequalities:

$$\text{Average range error (ft)} \quad \leq \sqrt{(100 \text{ ft})^2 + \epsilon_r^2} \text{ for ranges} \leq 100 \text{ nmi}$$

$$\leq \sqrt{(400 \text{ ft})^2 + \epsilon_r^2} \text{ for ranges} \leq 100 \text{ nmi}$$

where ϵ_r is the rms range error (in ft) associated with the AN/FPS-16 data.

2.6.1.2.   Results.

Processed range data collected from flights F1 through F10 were summarized as explained below and are shown in Table 2-7.   For each valid AN/FPS-16 and AN/TPS-59(XN-1) detection, the range difference was calculated and then averaged ($\overline{\text{RE}}$) over all detections (N) in each applicable 20 nmi range interval for each leg of flights F1 through F10.   The standard deviation (σ_{RE}) of the difference (RE) is the range error for a given leg in a given range interval.   The range errors for different legs within the same range interval were combined using the equation:

$$\text{Total range error} = \left[\frac{(N_1-1)\ \sigma_{\text{RE}_1}^2 + (N_2-1)\ \sigma_{\text{RE}_2}^2 + \dots}{N_1 + N_2 + \dots\ ^{-1}} \right]^{\frac{1}{2}}$$

where N_i is the number of detections used to determine the range error for a given leg in a given range interval.

Table 2-7. Range Accuracy Data

Flight (Tape)	0–20 N	$\overline{RE}$	σ_{RE}	20–40 N	$\overline{RE}$	σ_{RE}	40–60 N	$\overline{RE}$	σ_{RE}	60–80 N	$\overline{RE}$	σ_{RE}	80–100 N	$\overline{RE}$	σ_{RE}
1A & 2A (ATR 1-1)				9	-84	57.6	23	-96.6	54	22	-105.6	31.2	20	-109.8	62.4
1B & 2B (ATR 1-2)				12	-27	45	18	-30.6	44.4	15	-27.6	33.6	16	-45.6	43.8
1C & 2C (ATR 1-3)				11	-114.6	34.8	24	-111	40.2	24	-121.2	48.6	24	-124.8	47.4
2D (ATR 1-4)															
1D & 3B (ATR 1-7)				6	-31.2	36.0	14	-59.4	46.8	17	-12	76.2	16	-57.6	45.6
3A (ATR 3-8)															
3C (ATR 4-6)															
3D (ATR 3-3)															
4A (ATR 3-4)															
4B (ATR 3-5)															
4C (ATR 3-6)															
4D (ATR 3-7)															
5A (ATR 3-9)										22	-71.4	33	22	-90.6	37.2
5B (ATR 4-1)							6	-140.4	55.2	24	-119.4	45	21	-130.2	51
5C (ATR 4-2)										21	-78	54	19	-85.2	44.4
6A (ATR 4-3)										27	-124.2	55.2	16	-130.8	52.2
6B (ATR 4-4)										20	-72.6	40.8	18	-85.8	45.6
6C (ATR 4-5)										11	-112.2	33.6	21	-152.4	62.4
7A (ATR 2-1)				20	-91.2	49.8	25	-88.8	40.8	24	-89.4	43.2	21	-113.4	48.6
7B (ATR 2-2)	5	-175.2	70.8	22	-41.4	46.2	25	-51.6	61.2	24	-73.8	48.0	22	-80.4	53.4
7C (ATR 2-5)				25	-115.8	42	26	-112.8	36.6	26	-121.8	45.6	15	-118.8	34.2
8A (ATR 2-6)	12	-180.6	39.0	29	-56.4	46.2	31	-66	46.2	28	-75.6	45.6	12	-93.6	51.0
8B (ATR 6-1)	15	-147.6	46.8	29	-45.6	49.8	33	-57	38.4	16	-49.8	51.6			
8C (ATR 7-1)	9	-181.2	42.6	27	-106.2	61.2	32	-117	43.8	25	-136.2	54	4	-152.4	48.6
9A (ATR 7-2)	20	-184.8	50.4	28	-84.6	48	20	-95.4	42.6						
9B (ATR 7-3)	9	-223.2	41.4	28	-102	52.2	17	-105.6	58.2						
9C (ATR 7-4)	17	-174.6	53.4	30	-65.4	47.4	17	-75.6	49.8						
10A (ATR 5-1)	19	-256.2	47.4	14	-185.4	195.6									
10B (ATR 5-2)	22	-207	54	13	-103.8	41.4									
10C (ATR 5-3)	22	-235.2	55.8	18	-115.8	43.8									
10D (ATR 5-4)	25	-216	50.4	31	-100.2	39.6									
10E (ATR 5-5)	18	-232.2	43.8	30	-147	52.2									
Total	193		48.42	382		58.54	311		45.47	346		46.54	267		48.1

cy Data

80-100		100-120			120-140			140-160			160-180			180-200		
$\overline{RE}$	σ_{RE}	N	$\overline{RE}$	σ_{RE}	N	$\overline{RE}$	σ_{RE}	N	$\overline{RE}$	σ_{RE}	N	$\overline{RE}$	σ_{RE}	N	$\overline{RE}$	σ_{RE}
-109.8	62.4	20	-150	213	20	-104.4	114.6	21	-101.4	182.4	13	-73.8	125.4	10	-138.6	75.6
-45.6	43.8	15	-4.2	114.6	16	-42	150.6	13	69	130.2	15	54	184.2	9	198	112.8
-124.8	47.4	23	-108	88.2	21	-137.4	112.8	21	-110.4	120	20	-163.2	134.4	12	168	100.2
					17	10.8	103.8	14	-10.8	115.8	17	36.6	61.8	7	-22.8	138.6
-57.6	45.6	17	-48	93.6	16	-40.8	116.4	15	-9.6	166.8	15	-22.8	113.4	10	79.8	161.4
					22	-151.8	114.6	22	-99.6	139.8	14	-168	133.2	8	-210.6	288.6
					19	15.6	111.6	19	-28.2	109.2	19	-34.2	115.8	12	46.2	506.4*
					17	-10.8	94.8	19	-26.4	116.4	16	-28.8	124.8	8	-33.6	140.4
					17	-134.4	81.6	22	-122.4	147.6						
					18	-40.2	111.6	17	-26.4	161.4	17	0	143.4	18	-27.6	118.2
					20	-148.8	111	22	-148.8	103.8	21	-118.8	123.0	17	-140.4	145.8
					17	-34.2	105	17	-9.6	135	17	-34.8	137.4	18	-26.4	102.6
-90.6	37.2	21	-14.4	187.8	23	-21	199.2	21	4.2	221.4	6	-5.4	76.8			
-130.2	51	22	-198	96	24	-121.2	165	22	-168.6	90						
-85.2	44.4	22	-12.6	76.8	17	-27	121.2	24	-15.6	109.8	9	4.8	85.8			
-130.8	52.2	23	-105	120	22	-133.2	111	22	-147.6	89.4	4	-127.2	91.2			
-85.8	45.6	21	-45	112.2	21	-26.4	126.6	21	-12.6	111.6	5	49.2	74.4			
-152.4	62.4	22	-129	134.4	22	-143.4	109.8	21	-150.6	127.8	14	-189	215.4			
-113.4	48.6	20	-102.6	106.8												
-80.4	53.4	19	44.4	117												
-118.8	34.2	24	-125.4	124.8												
-93.6	51.0															
-152.4	48.6															
	48.1	269		124.4	349		121.76	353		132.21	222		128.1	129		189.1
														(128)		(124.7)

*Question AN/FPS-16 Break Track
on Scan 25
11, -94.2, 147.0 with 1 detection
deleted

The summary of range accuracy (error) versus range is given in Table 2-8. and is shown graphically in Figure 2-4.

2.6.1.3. Conclusions.

Assuming that the rms range error of the AN/FPS-16 is negligible, the most stringent case, than the inequalities given in paragraph 2.6.1.1 reduce to a range accuracy requirement of 100 ft from 0 to 100 nmi and 400 ft beyond 100 nmi for the AN/TPS-59(XN-1). Examination of Table 2-8 or Figure 2-4 shows that the AN/TPS-59(XN-1) is nearly twice as accurate as required from 0 to 100 nmi and over three times as accurate as required beyond 100 nmi.

2.6.2. Azimuth Accuracy Subtest.

2.6.2.1. Scope.

This subtest was conducted to determine the azimuth accuracy of the AN/TPS-59(XN-1). Flights F1 through F10 were employed to collect the data. The subtest was performed in accordance with the procedures given in paragraph 4.1.4.3.3 of the Pre-Service Acceptance Test Procedure.

The AN/TPS-59(XN-1) shall have passed this subtest if the averaged azimuth errors for each 20 nmi range interval throughout the region covered jointly by the AN/TPS-59(XN-1) and AN/FPS-16 satisfy the following inequality:

Average Azimuth Error (mils) $\leq (3)^2 + \epsilon_A$ where ϵ_A is azimuth error (in mils) associated with the AN/FPS-16 data.

2.6.2.2. Results.

Processed azimuth data collected from flights F1 through F10 were summarized as explained below and are shown in Table 2-9. For each valid AN/FPS-16 and AN/TPS-59(XN-1) detection, the azimuth difference was calculated and then averaged $(\overline{AE})$ over all detections (N) in each applicable 20 nmi range interval for each leg of flights F1 through F10. The standard deviation (σ_{AE}) of the difference $(\overline{AE})$ is the

2-22

Table 2-8. Range Accuracy

Range	Range Accuracy (ft)
0 - 20	48.4
20 - 40	58.5
40 - 60	45.5
60 - 80	46.5
80 - 100	48.1
100 - 120	124.4
120 - 140	121.8
140 - 160	132.2
160 - 180	120.1
180 - 200	124.7
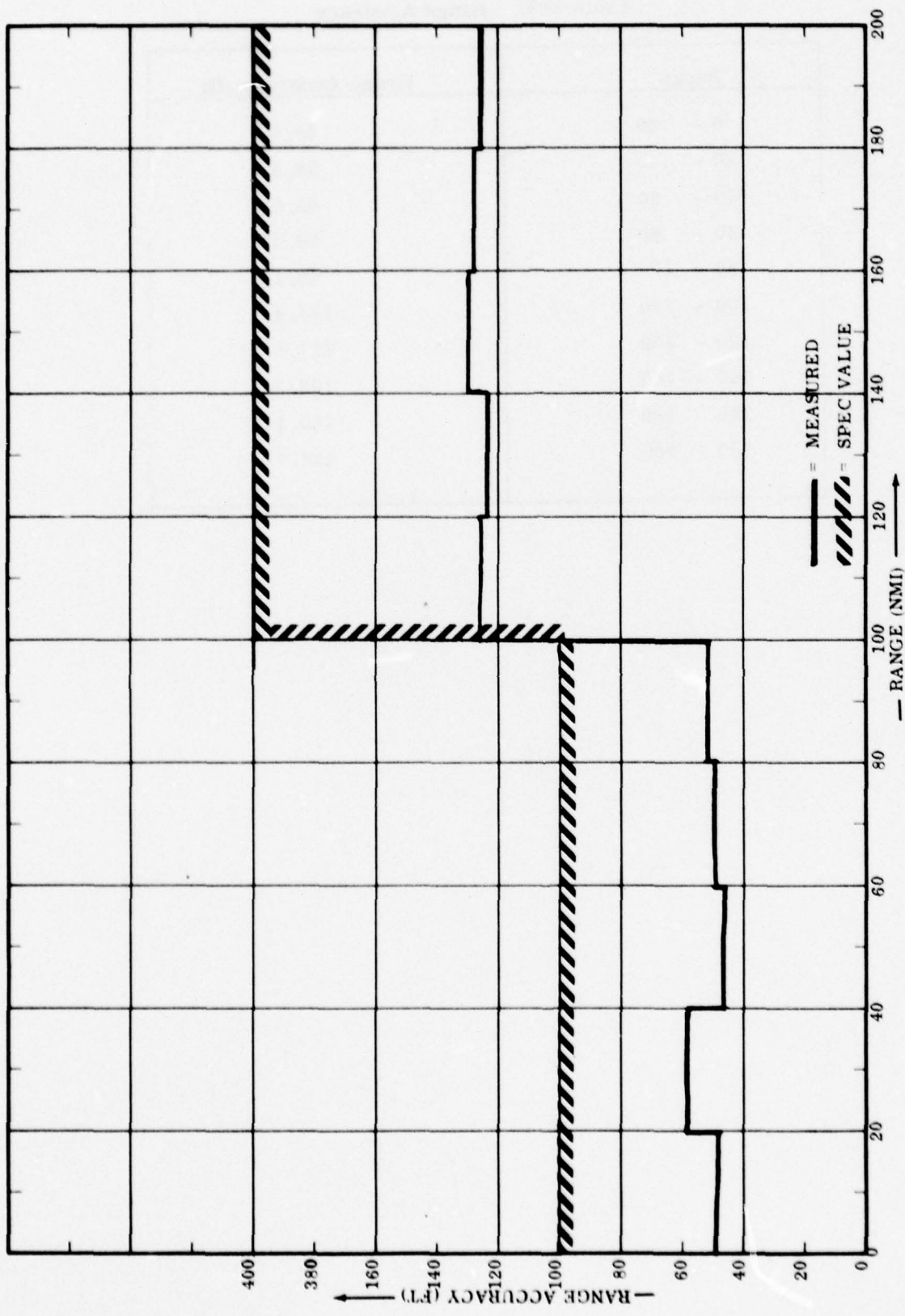
Figure 2-4. Range Accuracy vs Range

Table 2-9. Azimuth Acc

Range	0-20			20-40			40-60			60-80			80-100		
Flight (Tape)	N	$\overline{AE}$	σ_{AE}	N	$\overline{AE}$	σ_{AE}	N	$\overline{AE}$	σ_{AE}	N	$\overline{AE}$	σ_{AE}	N	$\overline{AE}$	σ_A
1A & 2A (ATR 1-1)				9	1.83	4.98	23	54	4.07	22	1.19	4.17	20	.38	3.
1B & 2B (ATR 1-2)				12	-2.07	7.37	18	80	4.35	15	-0.48	5.37	16	2.59	4.
1C & 2C (ATR 1-3)				11	128	3.48	24	-17	4.65	24	0.22	3.35	24	-1.63	5.
2D (ATR 1-4)															
1D & 3B (ATR 1-7)				6	1.1	5.92	14	-1.64	3.86	17	-1.54	3.8	16	-2.49	4.
3A (ATR 3-8)															
3C (ATR 4-6)															
3D (ATR 3-3)															
4A (ATR 3-4)															
4B (ATR 3-5)															
4C (ATR 3-6)															
4D (ATR 3-7)															
5A (ATR 3-9)										22	0.86	3.55	22	2.13	6.
5B (ATR 4-1)							6	3.95	4.81	24	5.48	3.83	21	3.91	3.
5C (ATR 4-2)										21	3.13	5.40	19	0.90	4.
6A (ATR 4-3)										27	4.41	3.45	16	2.49	4.
6B (ATR 4-4)										20	-0.09	4.20	18	1.70	3.
6C (ATR 4-5)										11	3.04	3.29	21	3.15	5.
7A (ATR 2-1)				20	-1.39	4.91	25	0.70	5.15	24	2.50	3.30	21	4.48	3.
7B (ATR 2-2)	5	3.74	6.76	22	-3.60	5.49	25	-1.13	5.37	24	-0.44	3.29	22	0.25	5.
7C (ATR 2-5)				25	-2.46	4.92	26	-0.29	5.65	26	1.90	3.92	15	4.28	2.
8A (ATR 2-6)	12	2.81	5.07	29	-1.50	4.00	31	-1.39	4.70	28	0.37	3.70	12	2.48	5.
8B (ATR 6-1)	15	8.33	3.73	29	5.31	3.93	33	6.37	3.28	16	7.89	2.67			
8C (ATR 7-1)	9	9.02	3.03	27	5.97	3.55	32	5.75	4.35	25	8.83	3.56	4	11.05	2.
9A (ATR 7-2)	20	9.62	2.81	28	7.32	4.56	20	8.75	4.07						
9B (ATR 7-3)	9	9.76	4.75	28	6.40	5.65	17	7.23	3.88						
9C (ATR 7-4)	17	7.92	4.35	30	6.94	3.23	17	5.78	4.85						
10A (ATR 5-1)	19	3.58	4.68	14	1.77	4.67									
10B (ATR 5-2)	22	5.25	4.33	13	1.22	3.91									
10C (ATR 5-3)	22	4.3	4.23	18	0.53	5.64									
10D (ATR 5-4)	25	4.29	3.31	31	3.55	4.91									
10E (ATR 5-5)	18	3.68	5.18	30	0.66	5.17									
Total	193		4.11	382		4.64	311		4.45	346		3.75	267		4.

Grand average - 4.43
(28.21)

Azimuth Accuracy Data (MILS)

80-100			100-120			120-140			140-160			160-180			180-200		
N	$\overline{AE}$	σ_{AE}	N	$\overline{AE}$	σ_{AE}	N	$\overline{AE}$	σ_{AE}	N	$\overline{AE}$	σ_{AE}	N	$\overline{AE}$	σ_{AE}	N	$\overline{AE}$	σ_{AE}
	.38	3.97	20	-1.68	5.54	20	-1.46	7.02	21	1.09	7.95	13	0	5.89	10	2.65	6.74
	2.59	4.42	15	0.63	3.48	16	-0.26	2.73	13	0.60	4.91	15	-0.73	4.15	9	-0.33	5.96
	-1.63	5.45	23	-3.18	5.48	21	-2.79	3.88	21	0.29	4.95	20	-5.69	4.66	12	-1.25	6.15
						17	-2.62	3.75	14	1.08	4.05	17	-1.74	4.90	7	-4.32	4.48
	-2.49	4.0	17	-3.61	3.91	16	-4.22	4.21	15	-1.30	4.96	15	-1.09	4.37	10	-5.82	5.11
						22	0.11	4.91	22	0.82	4.28	14	-0.55	3.70	8	3.44	1.87
						19	2.2	4.26	19	1.08	4.24	19	-0.64	5.94	12	3.66	5.01
						17	1.07	3.66	19	1.47	4.74	16	-2.18	5.31	8	0.25	4.22
						17	-0.98	3.69	22	-1.96	4.83						
						18	1.07	3.12	17	3.50	5.67	17	1.55	5.46	18	-0.08	3.03
						20	-0.41	3.89	22	-0.54	5.28	21	-0.14	5.05	17	2.29	2.89
						17	-0.89	3.93	17	3.17	4.81	17	-0.16	3.28	18	-0.55	3.54
	2.13	6.36	21	-0.04	3.36	23	-0.06	4.87	21	-2.62	4.82	6	-0.8	4.98			
	3.91	3.87	22	2.77	3.97	24	4.04	5.19	22	0.32	5.75						
	0.90	4.33	22	2.2	5.02	17	2.06	4.77	24	-0.37	4.95	9	1.99	4.45			
	2.49	4.85	23	2.28	4.00	22	2.33	2.97	22	2.79	3.85	4	-0.1	6.41			
	1.70	3.94	21	1.51	4.25	21	0.76	4.12	21	0.97	4.55	5	1.73	4.07			
	3.15	5.12	22	2.66	2.79	22	1.64	4.72	21	2.52	3.32	14	5.30	4.74			
	4.48	3.95	20	-6.43	5.39												
	0.25	5.61	19	-5.89	4.41												
	4.28	2.72	24	-4.99	6.12												
	2.48	5.00															
	11.05	2.93															
		4.56	269		4.48	349		4.26	353		4.87	222		4.7	129		4.32

azimuth error for a given leg in a given range interval. The azimuth errors for different legs within the same range interval were combined using the equation:

$$\text{Total Azimuth Error} = \left[\frac{(N_1-1)\,\sigma_{AE_1}^{\,2} + (N_2-1)\,\sigma_{AE_2}^{\,2} + \ldots}{N_1 + N_2 + \ldots^{-1}} \right]^{\frac{1}{2}}$$

where N_i is the number of detections used to determine the range error for a given leg in a given range interval.

The summary of azimuth accuracy (error) versus range is given in Table 2-10. and is shown graphically in Figure 2-5.

2.6.2.3. Conclusions.

Assuming that the azimuth error of the AN/FPS-16 is negligible, the most stringent case, then the inequality given in paragraph 2.6.1.1 reduces to an azimuth accuracy requirement of 3 mils for all measured range intervals of the AN/TPS-59(XN-1). Examination of Table 2-10 or Figure 2-5 shows that the AN/TPS-59(XN-1) nearly achieved the azimuth accuracy requirement. The deviation experienced does not appear related to radar sensitivity since it is relatively constant over all the range intervals.

It is believed that the azimuth accuracy can be enhanced by several software changes in the monopulse signal processing and calibration (discussed in height accuracy subtest, paragraph 5.6.3). In addition, it appears that some modification of the azimuth encoder may be required since it is estimated that the present encoder is introducing a certain amount of azimuth deviation into the system, although how much or how often is not known.

2.6.2.4. Recommendations.

Two changes are recommended to enhance the azimuth accuracy of the AN/TPS-59(XN-1).

1) Investigate deviations, if any, associated with the present azimuth encoder. If the deviations are significant, modify the encoder.
2) Implement software changes to monopulse signal processing and calibration.

Table 2-10. Azimuth Accuracy

Range	Azimuth Accuracy (Mils)
0 - 20	4.11
20 - 40	4.64
40 - 60	4.45
60 - 80	3.75
80 - 100	4.56
100 - 120	4.48
120 - 140	4.26
140 - 160	4.81
160 - 180	4.70
180 - 200	4.32

Since the present azimuth encoder has been the source of several deficiencies in the past, it appears to be an excellent area for investigation to see if the azimuth accuracy can be enhanced.

The monopulse signal processing and calibration software changes, which are relatively simple in nature, are explained fully in the height accuracy subtest (paragraph 2.6.3).

2.6.3. Height Accuracy Subtest.

2.6.3.1. Scope.

This subtest was conducted to determine the height accuracy of the AN/TPS-59(XN-1) at both high and low elevation angles, the transition being 1.5°. Flights F1 through F10 were employed to collect the data.
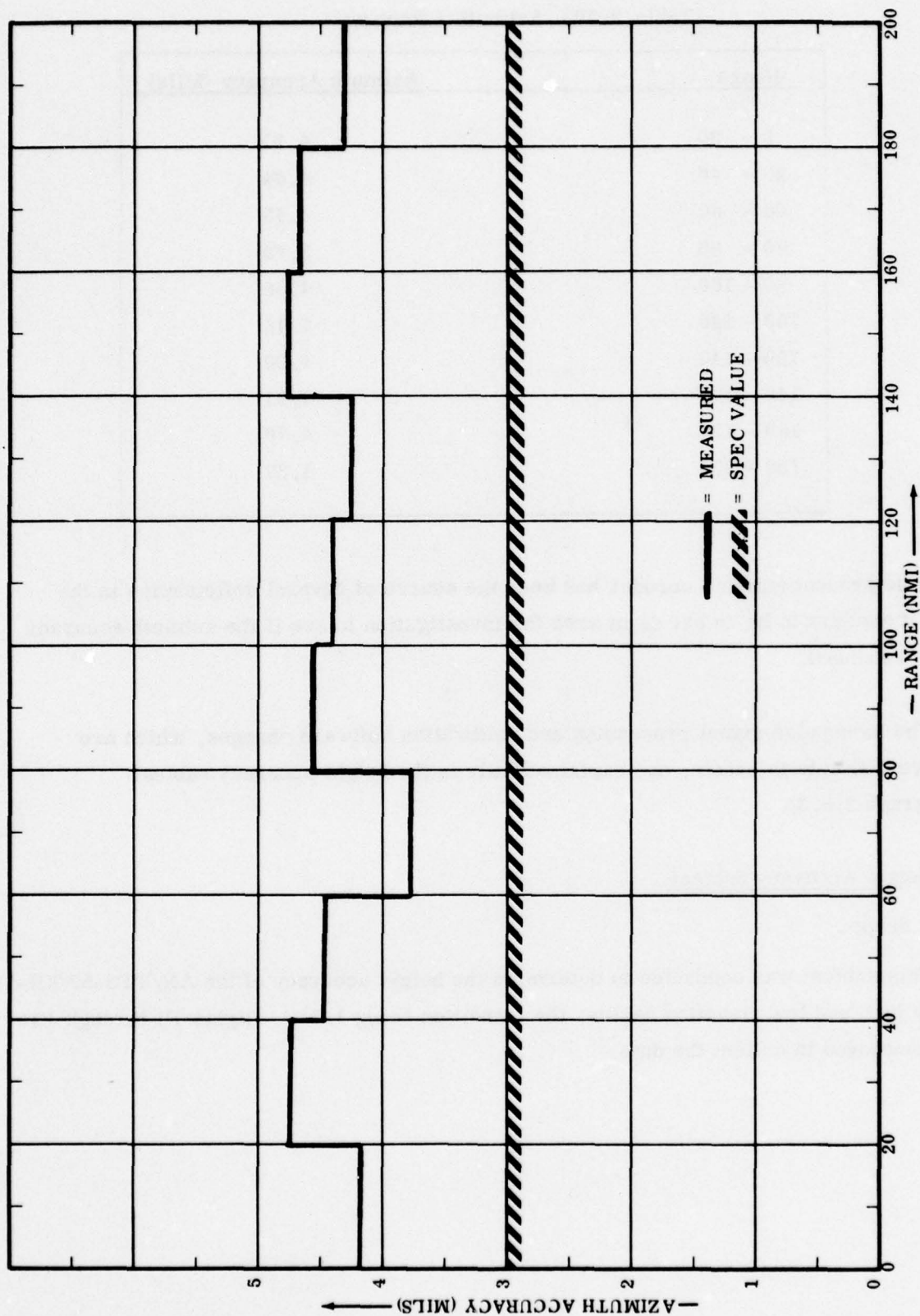
Figure 2-5. Azimuth Accuracy vs Range

2-28

The AN/TPS-59(XN-1) shall have passed this subtest if the averaged height errors for each 20 nmi range interval within the high (above 1.5°) and normal (between 0.8° and 1.5°) elevation regions satisfy the following inequalities:

Average height error (ft) $\leq \sqrt{(1000)^2 + \epsilon_H^2}$ for range $\leq$ 100 nmi

$\leq \sqrt{(1500)^2 + \epsilon_H^2}$ for range > 100 and $\leq$ 150 nmi

$\leq \sqrt{(2000)^2 + \epsilon_H^2}$ for range > 150 and $\leq$ 200 nmi

$\leq \sqrt{(2500)^2 + \epsilon_H^2}$ for range > 200 and $\leq$ 250 nmi

where ϵ_H is the rms height error (ft) associated with the reference data (AN/FPS-16 or IFF).

2.6.3.2.   Results.

Processed height data collected from flights F1 through F10 were summarized as explained below and are shown in Tables 2-11 and 2-12. To account for any elevation bias errors, the following technique was used to determine the AN/TPS-59(XN-1) height accuracy for a given leg in a given range interval in both tables. The mean heights of the AN/TPS-59(XN-1) data $(\overline{H_{59}})$ and the AN/FPS-16 data $(\overline{H_{16}})$ were computed along with the standard deviation of the AN/TPS-59(XN-1) height (σ_{59}). These were then combined using the following equation to yield the height error for the flight and range bin of interest.

$$\sigma_{HE} = \left[\sigma_{59}^2 + \frac{N}{N-1} (\overline{H_{59}} - H_{16}^2) \right]^{\frac{1}{2}}$$

where N is the number of data points used in calculating the statistics of the AN/TPS-59(XN-1) height.

Height errors (σ_{HE}) for different legs, but at the same altitude and within the same range bin were then combined (from both Tables 2-11 and 2-12) in a manner similar to that shown in the range and azimuth accuracy subtests. This resulted in a total height accuracy as a function of range and altitude for the AN/TPS-59(XN-1) and is shown in Table 2-13 and graphically in Figures 2-6 through 2-9.

2-29

Table 2-11. Low Angle Height Ac

Range	0-20					20-40					40-60						
Flight (Tape)	N	σ_{59}	$\overline{H_{59}}$	$\overline{H_{16}}$	σ_{HE}	N	σ_{59}	$\overline{H_{59}}$	$\overline{H_{16}}$	σ_{HE}	N	σ_{59}	$\overline{H_{59}}$	$\overline{H_{16}}$	σ_{HE}	N	σ
5A (ATR 3-9)																	
5B																	
5C																	
6A																	
6B																	
6C																	
Total																	
7A (ATR 2-1)																	
7B (ATR 2-2)																	
7C (ATR 2-5)																	
Total																	
8A (ATR 2-6)												20	416	10,213	10,334	434	26	7
8B (ATR 6-1)												23	440	10,033	10,081	443	19	7
8C (ATR 7-1)												22	530	9,994	10,173	561	20	9
Total												65	458	10,075	10,190 115	476	65	7
9A (ATR 7-2)						22	365	5,102	5,096	365		6	350	5,833	5,252	726		
9B (ATR 7-3)						23	286	5,130	5,117	286		5	428	5,475	5,189	534		
9C (ATR 7-4)						24	221	5,047	5,053	221		3	260	5,833	5,157	868		
Total						69	296	5,072	5,083 -4	290		14	337	5,705	5,207 -496	637		
10A (ATR 5-1)	11	185	2,500	2,511	185	3	132	2,583	2,542	141								
10B (ATR 5-2)	11	152	2,557	2,485	170	4	204	2,750	2,657	231								
10C (ATR 5-3)	15	203	2,508	2,573	203	5	296	2,675	2,545	312								
10D (ATR 5-4)	12	171	2,417	2,450	174	2	177	2,500	2,716	353								
10E (ATR 5-5)	15	209	2,492	2,449	214	6	95	2,667	2,798	172								
Total	64	182	2,494	2,481	186	20	169	1,656	2,600	213								

$$\sigma_{HE} = \left[\sigma_{59}^2 + \frac{N}{N-1} (H_{54} - H_{16})^2 \right]^{\frac{1}{2}}$$

-11. Low Angle Height Accuracy Data

0-60			60-80					80-100					100-120				
$\overline{H}_{59}$	$\overline{H}_{16}$	σ_{HE}	N	σ_{59}	$\overline{H}_{59}$	$\overline{H}_{16}$	σ_{HE}	N	σ_{59}	$\overline{H}_{59}$	$\overline{H}_{16}$	σ_{HE}	N	σ_{59}	$\overline{H}_{59}$	$\overline{H}_{16}$	σ_{HE}
								13	1,572	19,385	21,054	2,343	25	1,317	20,575	21,985	1,951
								15	1,154	20,242	20,948	1,366	22	1,184	20,835	21,219	1,246
								9	752	20,722	20,982	801	28	932	20,603	21,217	1,122
								37	124	20,058 / 936	20,994	1,643	75	1,030	20,662 / 810	19,972	1,461
213	10,334	434	26	735	10,255	10,659	843										
033	10,081	443	19	733	10,026	10,132	741										
994	10,173	561	20	954	10,700	10,548	967										
075	10,190 / 115	476	65	795	10,325 / 146	10,471	842										
833	5,252	726															
475	5,189	534															
833	5,157	868															
705 / -496	5,207	637															

2-30

Table 2-11. Low Angle Hei

Range	120-140					140-160						
Flight (Tape)	N	σ_{59}	$\overline{H_{59}}$	$\overline{H_{16}}$	σ_{HE}	N	σ_{59}	$\overline{H_{59}}$	$\overline{H_{16}}$	σ_{HE}	N	σ
2A (ATR 1-1)						13	2,250	41,087	42,259	2,559	15	1,
2B (ATR 1-2)						10	1,228	40,988	42,714	2,195	15	1,
2C (ATR 1-3)						16	2,339	41,055	41,581	2,401	22	1,
2D (ATR 1-4)						8	3,796	39,516	42,499	4,958	18	1,
3A (ATR 3-8)						13	2,008	40,433	42,402	2,869	18	2,
3B (ATR 1-7)						9	2,073	42,708	41,932	2,230	15	2,
3C (ATR 4-6)						12	1,564	41,490	42,371	1,815	19	2,
3D (ATR 3-3)						11	2,006	40,034	42,756	3,489	18	2,
4A (ATR 3-4)						14	1,934	40,946	42,635	2,610		
4B (ATR 3-5)						10	2,483	41,238	42,387	2,763	17	1,
4C (ATR 3-6)						14	1,870	41,848	42,520	1,996	22	3,
4D (ATR 3-7)						11	3,165	39,125	42,170	4,496	17	1,
Total						141	2,166	40,902	42,334	2,788	196	2,
5A (ATR 3-9)	22	1,604	31,631	32,524	1,846	21	2,406	31,988	32,652	2,500	6	1,
5B (ATR 4-1)	24	1,608	31,464	32,462	1,904	22	2,316	31,364	32,801	2,744		
5C (ATR 4-2)	16	1,094	30,915	32,530	1,995	24	1,203	31,245	33,427	2,533	6	3,
6A (ATR 4-3)	21	1,372	31,292	32,258	1,692	22	3,270	31,676	32,711	3,437	4	4,
6B (ATR 4-4)	20	1,626	31,769	32,356	1,734	21	1,978	32,363	33,025	2.091	6	3,
6C (ATR 4-5)	22	1,126	31,955	32,124	1,139	20	2,207	32,450	32,430	2,207	4	7,
Total	125	1,408	31,529	32,371	1,695	130	2,257	31,824	32,856	2,580	26	2,
		842					1,032					

/

Table 2-11. Low Angle Height Accuracy Data (Continued)

0-160			160-180					180-200				
$\overline{H}_{59}$	$\overline{H}_{16}$	σ_{HE}	N	σ_{59}	$\overline{H}_{59}$	$\overline{H}_{16}$	σ_{59}	N	σ_{59}	$\overline{H}_{59}$	$\overline{H}_{16}$	σ_{59}
1,087	42,259	2,559	15	1,939	40,992	43,183	2,984	12	2,513	40,844	43,545	3,778
0,988	42,714	2,195	15	1,964	39,950	43,140	3,842	11	4,086	43,398	42,625	4,165
1,055	41,581	2,401	22	1,975	41,108	42,471	2,417	14	4,199	42,643	42,292	4,215
9,516	42,499	4,958	18	1,928	40,431	42,067	2,559	8	2,728	39,219	42,007	4,040
0,433	42,402	2,869	18	2,743	41,222	42,839	3,208	11	1,349	43,727	43,182	1,465
2,708	41,932	2,230	15	2,581	41,375	43,178	3,185	11	4,637	41,886	42,306	4,658
1,490	42,371	1,815	19	2,363	40,743	42,727	3,121	10	3,737	41,600	42,623	4,303
0,034	42,756	3,489	18	2,173	40,722	42,698	2,976	13	2,774	42,981	41,960	2,971
0,946	42,635	2,610										
1,238	42,387	2,763	17	1,725	41,199	42,504	2,187	12	2,447	40,656	43,612	3,940
1,848	42,520	1,996	22	3,135	40,852	42,603	3,611	13	3,357	41,510	42,693	3,576
9,125	42,170	4,496	17	1,566	39,375	42,772	3,836	15	2,146	43,067	43,444	2,181
0,902	42,334	2,788	196	2,204	40,737	42,717	3,033	130	3,094	42,064	42,859	3,497
1,988	32,652	2,500	6	1,787	33,313	32,419	2,038					
1,364	32,801	2,744										
1,245	33,427	2,533	6	3,090	35,875	33,554	4,002					
1,676	32,711	3,437	4	4,182	35,625	33,875	4,654					
2,363	33,025	2.091	6	3,389	33,250	33,624	3,414					
2,450	32,430	2,207	4	7,875	32,875	32,658	1,874					
1,824	32,856	2,580	26	2,714	34,178	33,220	3,062					
	1,032					-958						

Table 2-12. Normal Monopulse Heig[...]

Flight (Tape)	0-20					20-40					40-60					N
Range	N	σ_{59}	H_{59}	H_{16}	σ_{HE}	N	σ_{59}	H_{59}	H_{16}	σ_{HE}	N	σ_{59}	H_{59}	H_{16}	σ_{HE}	N
1A (ATR 1-1)						9	1,565	42,430	41,945	1,647	23	522	41,766	41,898	539	22
1B (ATR 1-2)						12	1,472	42,385	41,837	1,579	18	298	41,326	41,779	553	1
1C (ATR 1-3)						12	2,035	42,969	41,818	2,364	24	567	41,630	41,797	592	2
1D (ATR 1-7)						11	1,459	42,636	41,956	1,624	18	509	41,375	41,880	727	1
Total						44	1,601	42,605	41,889	1,785	83	485	41,546	41,839	591	7
													293			
5A (ATR 3-9)																2
5B (ATR 4-1)											6	282	31,313	31,803	606	2
5C (ATR 4-2)																2
6A (ATR 4-3)																2
6B (ATR 4-4)																2
6C (ATR 4-5)																1
Total											6	282	31,313	31,803	606	13
													490			
7A (ATR 2-1)						25	264	20,215	20,471	371	25	432	20,155	20,563	600	2
7B (ATR 2-2)	5	244	20,325	20,336	244	22	319	20,205	20,407	380	25	471	20,120	20,505	613	2
7C (ATR 2-5)						25	197	20,240	20,502	332	26	694	19,889	20,482	921	2
Total	5	244	20,325	20,336	244	72	258	20,221	20,462	356	76	540	20,052	20,516	720	7
													241			
8A (ATR 2-6)	12	195	10,042	10,055	195	29	314	9,922	10,164	399	11	547	10,273	10,334	551	
8B (ATR 6-1)	15	192	10,158	10,158	192	29	288	9,897	10,179	407	10	329	10,325	10,081	418	
8C (ATR 7-1)	9	125	10,083	10,124	132	27	372	9,889	10,103	431	10	305	9,975	10,173	370	
Total	36	174	10,101	10,115	175	85	321	9,903	10,150	407	31	400	10,194	10,200	441	
			14					247					6			
9A (ATR 7-2)	20	131	5,006	5,011	131	6	184	4,854	5,096	323						
9B (ATR 7-3)	9	141	4,944	5,072	196	5	209	4,925	5,117	300						
9C (ATR 7-4)	19	117	5,013	5,027	118	6	258	5,083	5,053	260						
Total	48	125	4,997	5,029	137	17	206	4,956	5,087	276						
			32					131								
10A (ATR 5-1)	9	55	2,472	2,511	69											
10B (ATR 5-2)	12	94	2,469	2,485	95											
10C (ATR 5-3)	7	159	2,446	2,513	175											
10D (ATR 5-4)	13	65	2,442	2,450	66											
10E (ATR 5-5)	7	95	2,464	2,449	96											
Total	48	90	2,458	2,479	96											
			21.													

$$\sigma_{HE} = \left[\sigma_{54}^2 + \frac{N}{N-1} (H_{59} - H_{16})^2 \right]$$

	0-60			60-80					80-100					100-120			
	H_{16}	σ_{HE}	N	σ_{59}	H_{59}	H_{16}	σ_{HE}	N	σ_{59}	H_{59}	H_{16}	σ_{HE}	N	σ_{59}	H_{59}	H_{16}	σ_{HE}
6	41,898	539	22	646	41,585	41,971	757	22	976	41,796	42,193	1,300	21	1,009	41,161	42,308	1,549
6	41,779	553	15	1,048	41,425	41,813	1,122	16	1,187	40,586	41,807	1,732	15	1,496	40,735	41,773	1,842
0	41,797	592	24	758	41,589	41,937	837	24	1,239	41,375	42,067	1,426	23	1,872	40,310	42,075	2,600
75	41,880	727	17	732	41,243	41,925	1,015	16	1,484	41,086	41,873	1,692	17	1,196	39,890	42,143	2,612
16	41,839	591	78	772	41,481	41,920	899	78	1,192	41,273	42,009	1,487	76	1,403	40,535	42,095	2,171
293					439					736					1,560		
			22	625	31,171	31,803	899	22	1,196	30,852	31,909	1,613	21	1,205	31,113	32,001	1,510
13	31,803	606	24	550	31,234	31,873	854	21	690	31,196	32,066	1,127	22	825	31,051	32,261	1,488
			22	1,072	31,142	31,815	1,274	19	1,797	30,592	31,938	2,268	22	794	30,722	36,985	1,517
			27	1,061	31,788	31,788	1,061	18	1,008	30,722	31,692	1,419	23	1,194	30,734	32,117	1,851
			20	562	31,394	31,836	722	18	1,546	30,764	31,915	1,948	21	1,065	30,435	32,007	1,931
			18	676	31,236	31,906	966	22	1,020	30,994	31,998	1,311	21	739	31,167	31,937	1,081
13	31,803	606	133	790	31,343	31,833	965	120	1,221	30,864	31,884	1,607	130	971	30,870	32,053	1,560
490					490					1025					1,183		
55	20,563	600	24	719	19,771	20,832	1,301	8	672	20,500	21,054	896					
60	20,505	613	24	599	20,209	20,616	729	7	1,366	21,500	20,948	1,490					
89	20,482	921	27	688	20,157	20,667	862	8	1,120	20,813	20,982	1,134					
52	20,516	720	75	662	20,050	20,703	976	23	1,025	20,913	20,997	1,127					
241					653					84							
73	10,334	551															
25	10,081	418															
75	10,173	370															
94	10,200	441															

$$\left[\frac{N}{N-1} \left(H_{59} - H_{16}\right)^2 \right]^{\frac{1}{2}}$$

Range	120-140					140-160			
Flight (Tape)	N	σ_{59}	$\overline{H_{59}}$	$\overline{H_{16}}$	σ_{HE}	N	σ_{59}	$\overline{H_{59}}$	$\overline{H_{16}}$
2A (ATR 1-1)	22	1,569	40,750	42,078	2,076	8	2,877	40,297	42,25
2B (ATR 1-2)	17	1,133	40,735	42,201	1,889	7	1,926	42,500	42,714
2C (ATR 1-3)	21	1,900	40,661	42,123	2,419	5	2,281	40,500	41,59
2D (ATR 1-4)	17	1,614	40,346	42,405	2,666	8	1,860	40,500	42,49
3A (ATR 3-8)	22	1,755	40,227	42,366	2,806	9	2,640	40,542	42,40
3B (ATR 1-7)	16	1,681	41,070	42,156	2,021	7	2,892	41,375	41,93
3C (ATR 4-6)	19	1,486	39,980	42,074	2,615	7	1,576	40,411	42,37
3D (ATR 3-3)	17	1,252	41,081	42,572	1,982	8	1,976	39,625	42,75
4A (ATR 3-4)	24	1,513	40,880	42,421	2,183	9	848	41,194	42,63
4B (ATR 3-5)	18	1,761	40,076	42,462	3,021	7	2,273	40,125	42,38
4C (ATR 3-6)	22	1,607	40,608	42,263	2,335	8	1,989	40,875	42,52
4D (ATR 3-7)	17	2,327	39,927	42,182	3,289	6	2,325	40,750	42,17
Total	232	1,617	40,532	42,274	2,411	89	2,036	40,718	42,38
			1,742					1,668	

Table 2-12. Normal Monopulse Height Accuracy Data (Continued)

			140-160			
$\overline{H_{16}}$	σ_{HE}	N	σ_{59}	$\overline{H_{59}}$	$\overline{H_{16}}$	σ_{HE}
42,078	2,076	8	2,877	40,297	42,259	3,560
42,201	1,889	7	1,926	42,500	42,714	1,940
42,123	2,419	5	2,281	40,500	41,591	2,581
42,405	2,666	8	1,860	40,500	42,499	2,833
42,366	2,806	9	2,640	40,542	42,402	3,296
42,156	2,021	7	2,892	41,375	41,932	2,954
42,074	2,615	7	1,576	40,411	42,371	2,639
42,572	1,982	8	1,976	39,625	42,756	3,887
42,421	2,183	9	848	41,194	42,635	1,748
42,462	3,021	7	2,273	40,125	42,387	3,337
42,263	2,335	8	1,989	40,875	42,520	2,653
42,182	3,289	6	2,325	40,750	42,170	2,797
42,274	2,411	89	2,036	40,718	42,386	2,740
2			1,668			

Table 2-13. Height Accuracy

Range	2500	5000	10,000	20,000	30,000	40,000
0 - 20	153 (1001)	137 (1001)	175 (1000)	244 (1000)		
20 - 40	213 (1032)	286 (1006)	407 (1005)	356 (1006)		1785 (1014)
40 - 60		637 (1054)	463 (1007)	720 (1028)	606 (1007)	591 (1027)
60 - 80			842 (1079)	976 (1079)	965 (1007)	899 (1015)
80 - 100				1456 (1175)	1607 (1028)	1487 (1014)
100 - 120				1461 (1653)	1560 (1560)	2171 (1539)
120 - 140					1695 (1562)	2411 (1609)
140 - 160					2580 (1879)	2764 (1929)
160 - 180					3062 (2451)	3033 (2181)
180 - 200						3497 (2466)
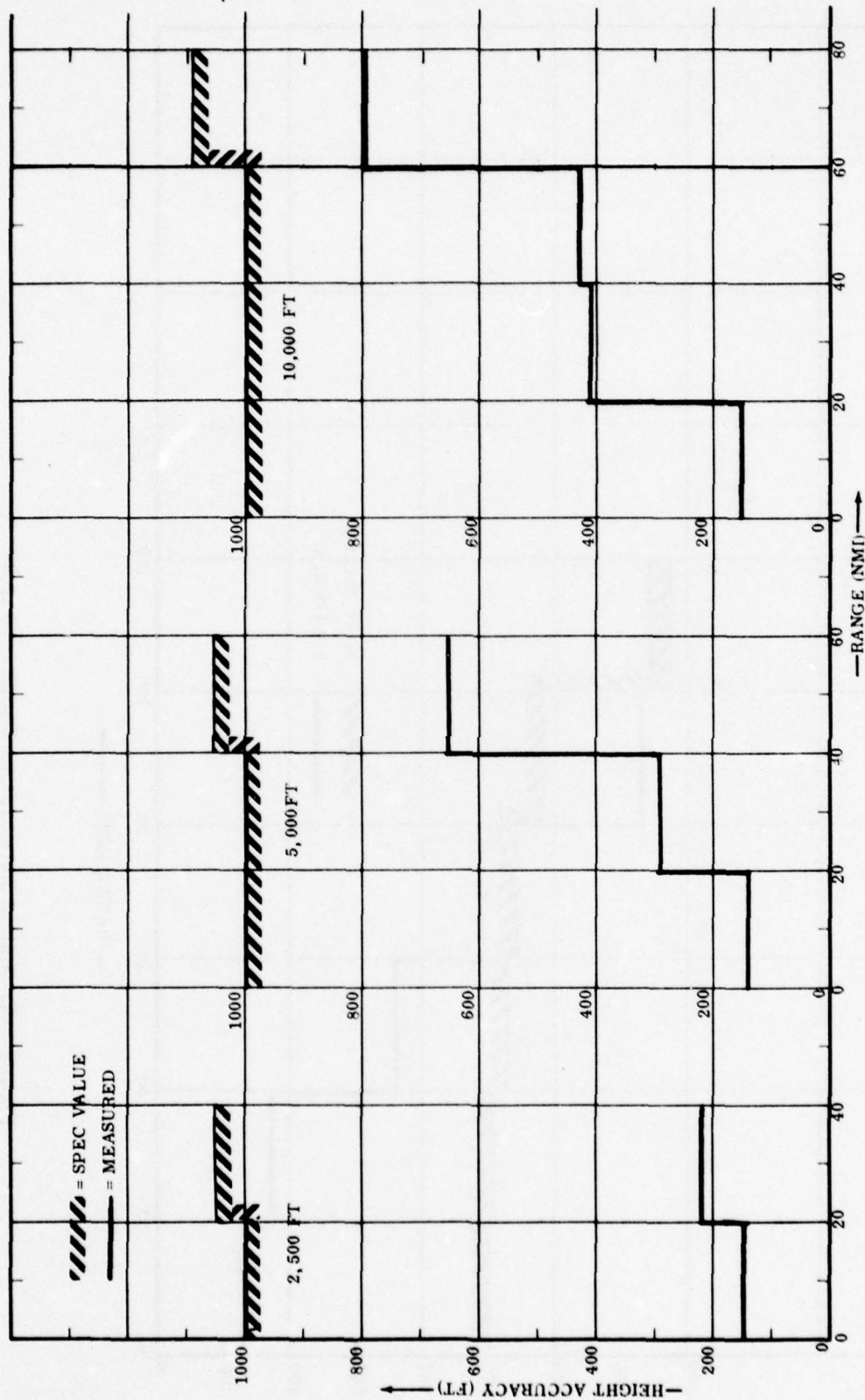
Figure 2-6. Height Accuracy vs Range 2.5, 5.0, and 10.0 K ft

2-35
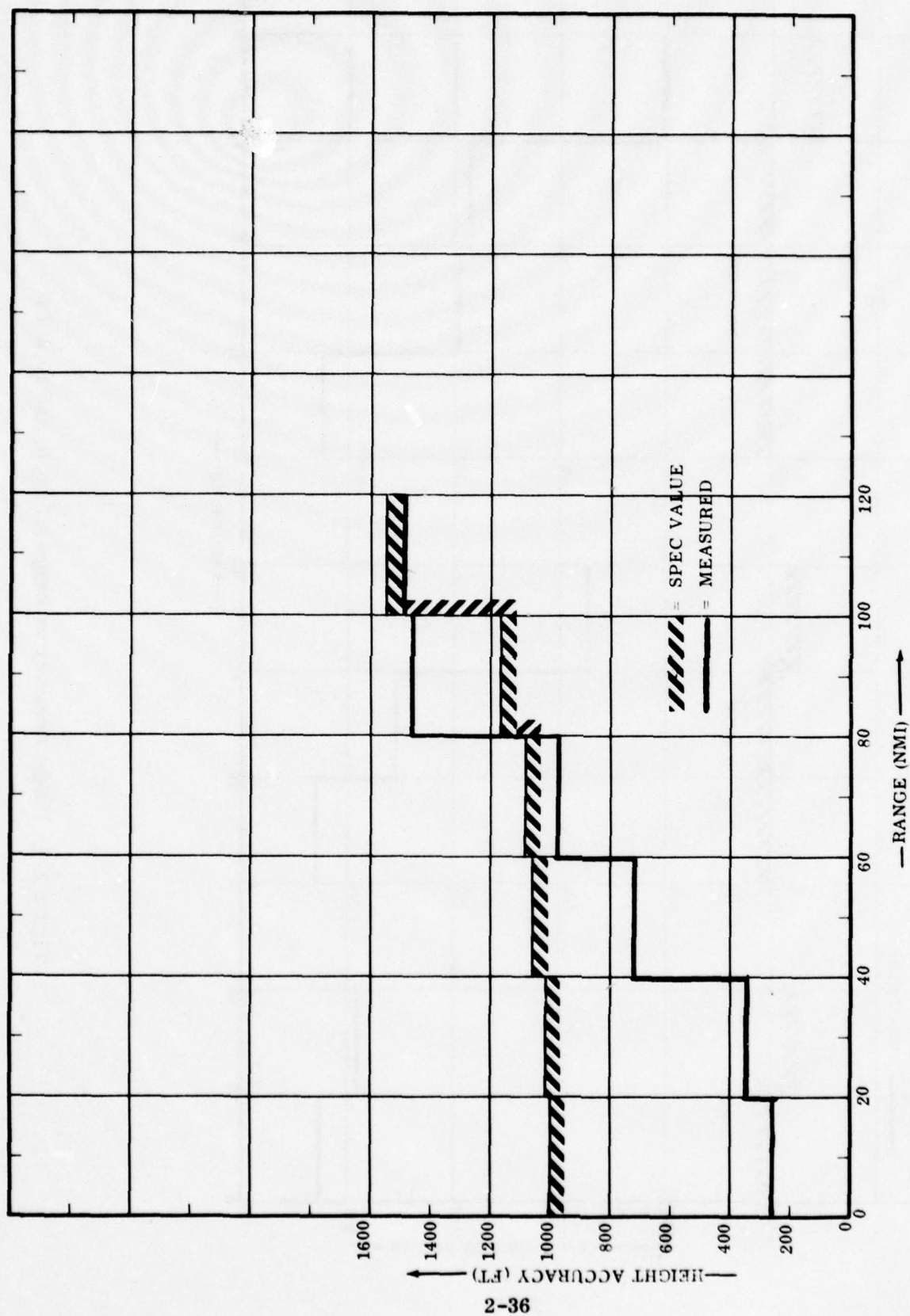
Figure 2-7. Height Accuracy vs Range - 20 K ft

2-36
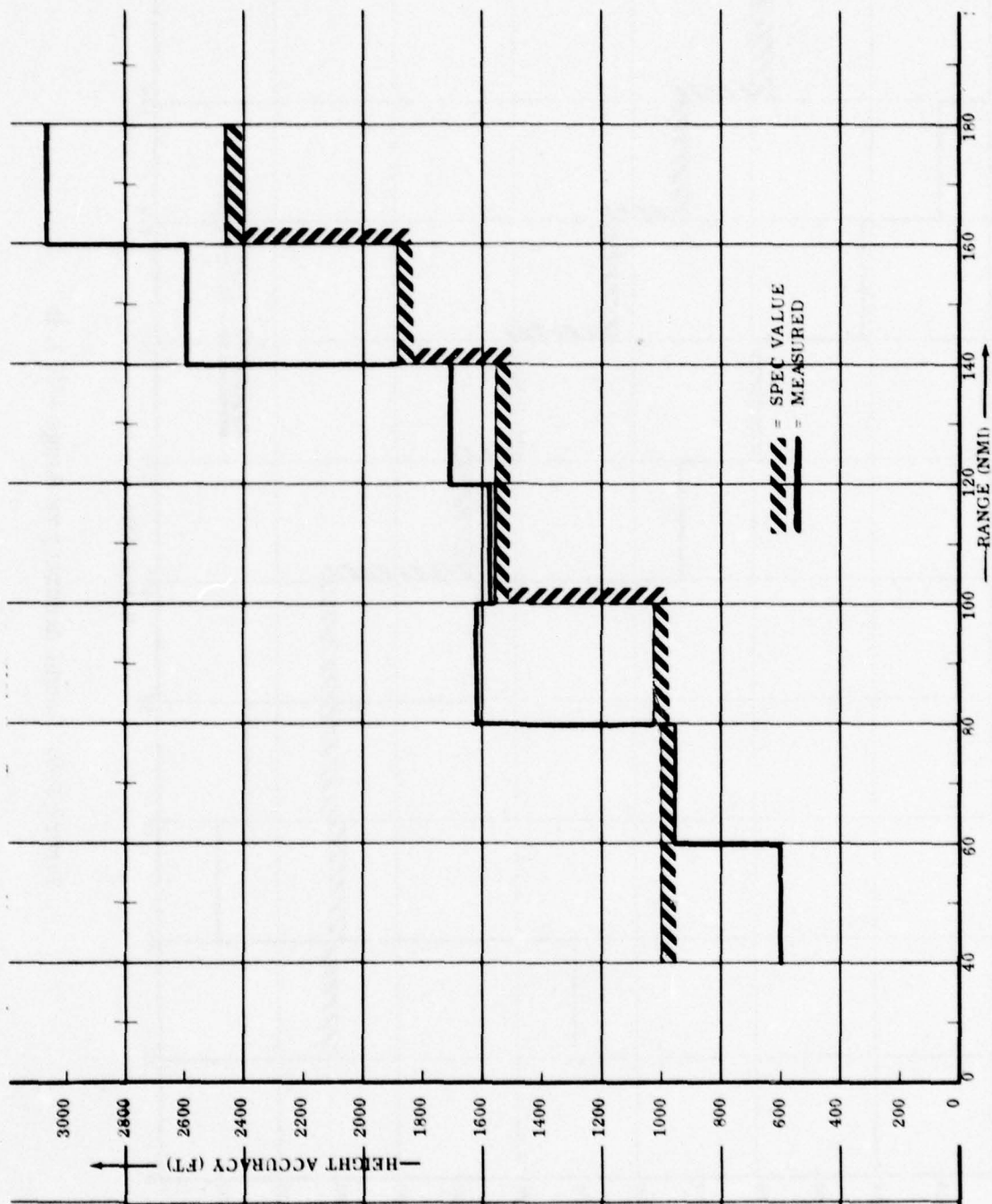
Figure 2-8. Height Accuracy vs Range – 30 K ft

2-37
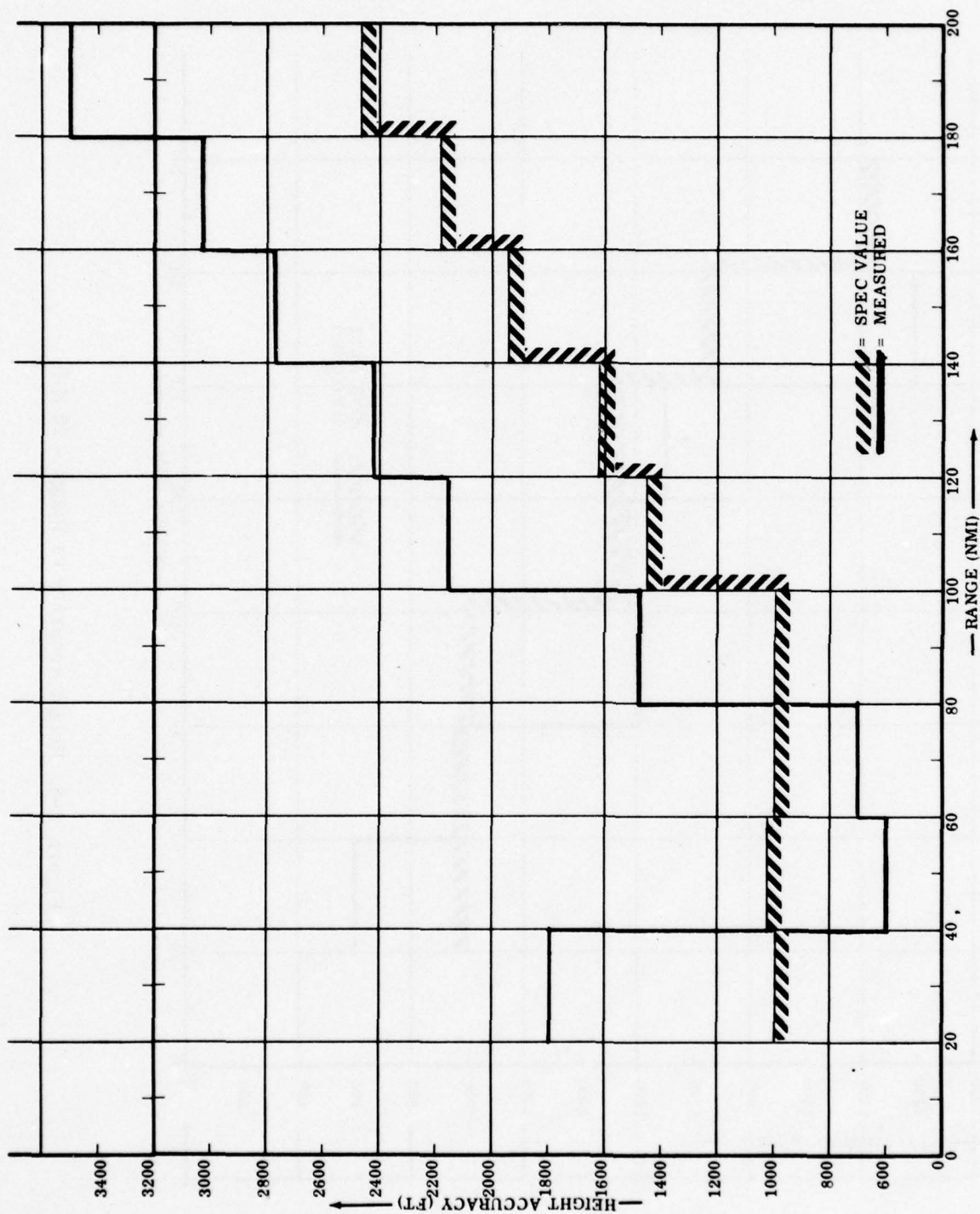
Figure 2-9. Height Accuracy vs Range - 40 K ft

In order to determine the height error of the AN/FPS-16 as a function of range and altitude for use in determining the AN/TPS-59(XN-1) height accuracy requirement, the mean height $(\overline{H_{16}})$ along with the standard deviation (σ_{16}) were computed for each leg of each flight. The standard deviation (σ_{16}) represents the AN/FPS-16 height error for each leg of each flight.

The height errors (σ_{16}) for different legs, but at the same altitude and within the same range interval were combined in a manner similar to that known in the range and azimuth accuracy subtests. This resulted in the total height error as a function of range and altitude for the AN/FPS-16 and is shown in Table 2-14.

2.6.3.3. Conclusions.

Solving the inequalities given in paragraph 2.6.3.1 using the AN/FPS-16 total height errors (σ_{16}) given in Table 2-14 yields the AN/TPS-59(XN-1) height accuracy requirement for each range interval and each altitude within each interval. The resultant requirement is shown in Table 2-13 and graphically in Figures 2-6 through 2-9.

Examination of Table 2-13 or Figures 2-6 through 2-9 shows that the AN/TPS-59(XN-1) is more accurate than required for all ranges and altitudes out to 80 nmi except for the 40,000 ft altitude in the 20-40 nmi range interval. As discussed in the aircraft detectability subtest, the multiple DTM's that appear to be caused by the spoiled elevation beams in the 40 K ft/20-40 nmi region are also affecting the height accuracy. Beyond 80 nmi, the AN/TPS-59(XN-1) height accuracy was degraded about 60% from the required height accuracy except for the 20,000 and 30,000 ft altitudes in the 100 to 120 nmi range interval where it meets the accuracy requirement.

In order to determine whether or not a residual elevation bias error existed, the average difference in height between the AN/TPS-59(XN-1) and the AN/FPS-16 were computed as a function of range. By dividing the average difference by the average range of a given range interval, the elevation angle was extracted. The results indicated an overall bias of about 1.5 mils. This error was not removed for flight testing because insufficient data were available at the time. However, it has been eliminated on the tactical tape shipped with the radar. After removing the bias term, the height accuracy of the AN/TPS-59(XN-1) is increased to the point where it only degraded about 30 to 40% from the required accuracy.

Table 2-14. AN/FPS-1

Range	0-20			20-40			40-60			60-80			80-100		
	N	$\overline{H_{16}}$	σ_{16}	N	$\overline{H_{16}}$	σ_{16}	H	$\overline{H_{16}}$	σ_{16}	N	$\overline{H_{16}}$	σ_{16}	N	$\overline{H_{16}}$	σ_{16}
1A & 2A (ATR 1-1)				17	41,946	73	23	41,898	117	22	41,971	87	21	42,193	217
1B & 2B (ATR 1-2)				16	41,837	47	18	41,779	94	17	41,813	84	17	41,807	198
1C & 2C (ATR 1-3)				17	41,818	252	24	41,797	404	24	41,937	158	24	42,067	96
2D (ATR 1-4)															
1D & 3B (ATR 1-7)				11	41,956	231	14	41,880	65	17	41,925	316	18	41,873	174
3A (ATR 3-8)															
3C (ATR 4-6)															
3D (ATR 3-3)															
4A (ATR 3-4)															
4B (ATR 3-5)															
4C (ATR 3-6)															
4D (ATR 3-7)															
Total 40,000 Ft Error				61		167	79		234	80		176	80		190
5A (ATR 3-9)										22	31,803	95	23	31,909	168
5B (ATR 4-1)							7	31,803	122	24	31,873	163	22	32,066	140
5C (ATR 4-2)										21	31,815	83	22	31,938	167
6A (ATR 4-3)										27	31,788	122	17	31,692	473
6B (ATR 4-4)										21	31,836	102	20	31,915	213
6C (ATR 4-5)										12	31,906	130	21	31,798	233
Total 30,000 Ft Error							7		122	127		120	125		248
7A (ATR 2-1)				21	20,471	119	26	20,563	385	27	20,832	623	26	21,054	1008
7B	11	20,336	31	24	20,407	54	25	20,505	100	24	20,616	164	24	20,948	242
7C				26	20,503	144	27	20,482	132	27	20,667	278	26	20,982	274
Total 20,000 Ft Error	11		31	71		111	78		239	78		406	76		617
8A	22	10,055	21	31	10,164	102	31	10,334	102	32	10,659	290			
8B	22	10,158	27	33	10,179	79	34	10,081	116	16	10,132	129			
8C	16	10,124	38	31	10,103	127	32	10,173	115	31	10,548	609			
Total 10,000 Ft Error	60		25	95		103	97		116	79		423			
9A	27	5,011	32	32	5,096	118	25	5,252	210						
9B	18	5,072	45	31	5,117	83	21	5,189	362						
9C	25	5,027	36	33	5,053	115	18	5,157	442						
Total 5,000 Ft Error	70		37	96		106	64		333						
10A	27	2,511	64	18	2,542	69									
10B	30	2,485	54	15	2,522	162									
10C	25	2,513	58	18	2,545	84									
10D	30	2,450	46	33	2,716	275									
10E	20	2,449	59	34	2,798	372									
Total 2,500 Ft Error	132		55	118		254									

1

-14. AN/FPS-16 Height Accuracy Data

	80-100			100-120			120-140			140-160			160-180			180-200	
N	$\overline{H_{16}}$	σ_{16}	N	$\overline{H_{16}}$	σ_{16}	N	$\overline{H_{16}}$	σ_{16}	N	$\overline{H_{16}}$	σ_{16}	N	$\overline{H_{16}}$	σ_{16}	N	$\overline{H_{16}}$	σ_{16}
21	42,193	217	20	42,309	569	20	42,078	483	21	42,259	1,028	19	43,183	1,156	16	43,545	1,594
17	41,807	198	17	41,773	172	17	42,201	682	13	42,714	807	17	43,140	943	15	42,624	1,121
24	42,067	96	23	42,075	293	23	42,123	574	23	41,581	979	20	42,471	941	15	42,292	680
						17	42,405	613	15	42,499	1,001	17	42,067	989	7	42,007	1,307
18	41,873	174	17	42,143	218	17	42,156	615	16	41,932	965	17	43,178	812	12	42,306	1,231
						22	40,366	334	22	42,402	472	17	42,839	541	11	43,182	646
						19	42,074	577	19	42,371	776	20	42,727	1,249	23	43,623	2,009
						18	42,572	886	19	42,756	1,152	16	42,698	1,232	8	41,959	3,821
						17	42,421	718	22	42,635	985						
						18	40,462	370	19	42,387	438	18	42,504	557	18	43,612	952
						22	42,263	687	23	42,520	578	21	42,603	407	22	42,693	952
						17	42,182	455	18	42,170	344	17	42,772	412	18	43,444	1,162
80		190	86		344	227		582	230		811	199		870	165		1,443
23	31,909	169	21	32,001	419	23	32,524	523	21	32,652	652	6	32,419	1,190			
22	32,066	140	23	32,261	275	24	32,462	454	24	32,801	559						
22	31,938	167	22	31,985	465	18	32,530	418	24	33,427	681	11	33,554	1,360			
17	31,692	473	23	32,117	494	23	32,258	353	23	32,711	719	5	33,875	530			
20	31,915	213	21	32,007	439	21	32,356	372	22	33,025	809	10	33,624	1,636			
21	31,798	233	23	31,937	501	22	32,124	518	22	32,430	754	17	32,658	1,689			
125		240	133		430	131		437	136		685	49		1,417			
26	21,054	1007	21	21,985	988												
24	20,948	242	19	21,214	432												
26	20,982	274	23	21,217	563												
76		617	63		694												

The gradual increase in degradation of the height accuracy with increasing range is low enough to suggest that it is not related to system sensitivity; i.e., increasing the signal-to-noise ratio will not substantially affect height accuracy.

It is believed that significant enhancement of the height accuracy can be achieved by making three relatively simple changes to the software associated with the monopulse signal processing and calibration.

2.6.3.4. Recommendations.

2.6.3.4.1. 20 to 40 nmi Range Interval.

To enhance height accuracy at 40,000 ft in this range interval, it is recommended that the two spoiled beams used at the upper elevation be replaced with three unspolied beams as discussed in the aircraft detectability subtest.

2.6.3.4.2. 80 to 200 nmi Range Interval.

Three relatively simple software changes are recommended to enhance height accuracy in this region. (See Figure 2-10.) These three changes will also enhance the azimuth accuracy.

1) Modify the position estimate averaging procedure employed in the event of multiple detections on the same target within a single scan.

2) Improve the accuracy of the monopulse calibration procedure.

3) Weight the long-range diversity channel angle estimates by the square of the sum signal magnitude.

The first change is important because of the sensitivity of the estimate error to arrival angle relative to boresight. The accuracy degrades significantly as the arrival angle moves off the boresight. As a result, when multiple detections are made on the same target in adjacent beams, the quality of the elevation (and azimuth) estimate may be very much better on one than the others. The present procedure, implemented in the computer, is to essentially randomly pick one of the estimates and discard the remainder. The recommended change is to perform a weighted average on the individual estimates, with the weighting in proportion to the squared magnitude of the sum signal.

2-41
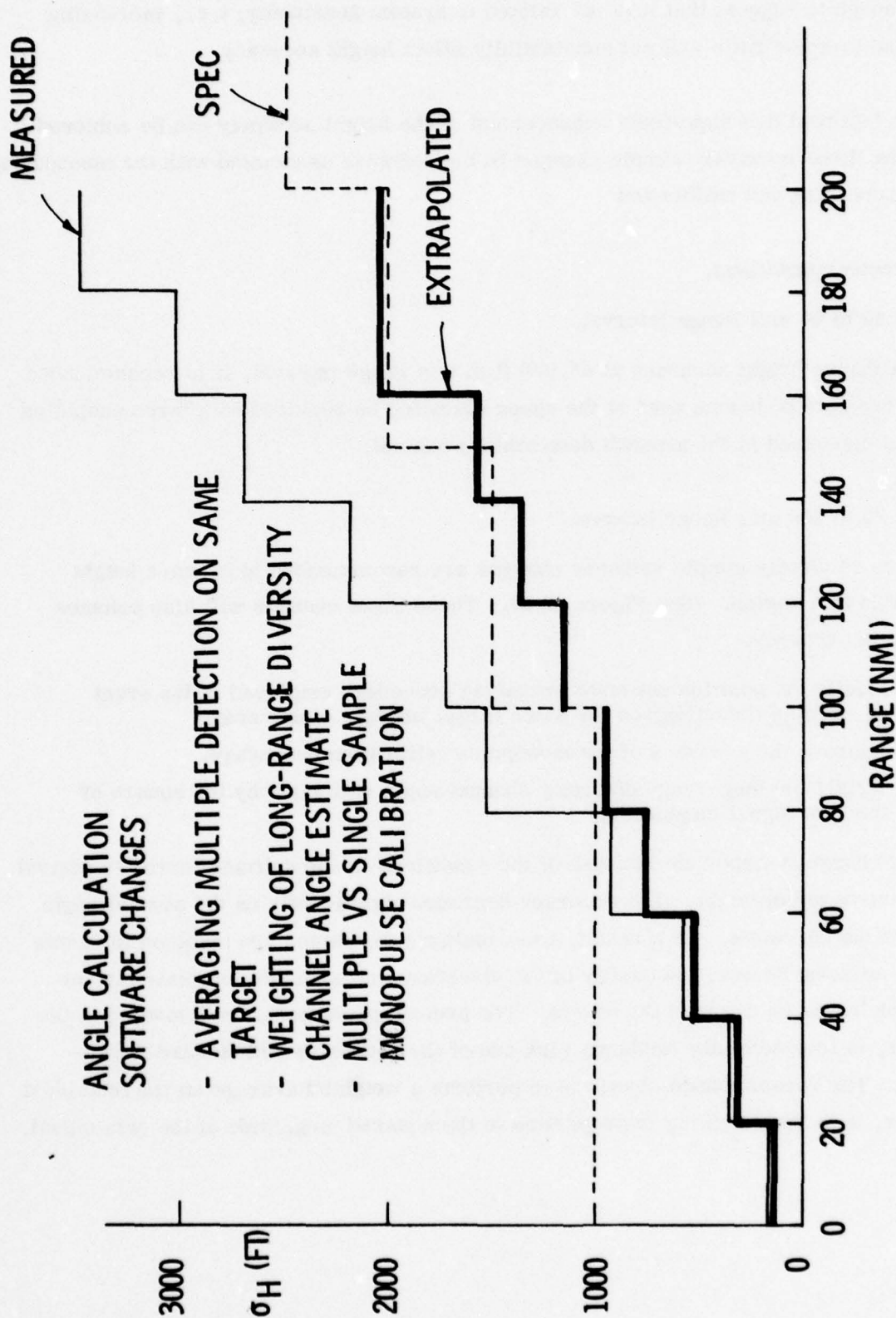
Figure 2-10. Height Accuracy Extrapolation

ANGLE CALCULATION
SOFTWARE CHANGES

 - AVERAGING MULTIPLE DETECTION ON SAME
   TARGET
 - WEIGHTING OF LONG-RANGE DIVERSITY
   CHANNEL ANGLE ESTIMATE
 - MULTIPLE VS SINGLE SAMPLE
   MONOPULSE CALIBRATION

The second change is important because of the extreme sensitivity of the angle estimate error on channel mismatch, especially the phase mismatch between the Σ and $\Sigma + i\Delta$ channels (i.e., after the hybrid in the preprocessor which converts Σ and Δ to Σ and $\Sigma + i\Delta$). The monopulse calibration process is designed to measure the pertinent channel amplitude and phase mismatches and properly compenstate the elevation and azimuth estimates for these mismatches. The present monopulse calibration procedure is probably not accurate enough. It can be improved by averaging the results of multiple calibration cycles and by allowing array noise to enter the preprocessor when performing the Loop B part of the monopulse calibration procedure. The array noise will reduce the quantization noise. The effect of the former can be reduced by averaging multiple cycles, the effect of the quantization cannot.

Weighting the estimates made on the individual pulses of the long range waveform by the square of the sum magnitude, instead of the present procedure of equally weighting them, will improve the overall estimate, particularly against a fluctuating target.

2.7. ANTI-CLUTTER DEMONSTRATION.

This demonstration consisted of the anti-ground clutter and anti-weather clutter subtests given below.

2.7.1. Anti-Ground Clutter Subtest.

2.7.1.1 Scope.

This subtest was conducted to determine the AN/TPS-59(XN-1) probability of detection for targets in the presence of ground clutter and the false alarm rate in the presence of ground clutter only over a specified number of range intervals. The subtest was performed in accordance with the procedures given in paragraph 4.1.4.4.3 of the Pre-Service Acceptance Test Procedures. Flights F12 and F13 were employed to collect data used in determining the detectability of the radar in clutter out to a range of 80 nmi. The false alarm rate data was collected during flights F12 and F13 out to a range of 300 nmi. No adjustments were made to the radar between the time when probability of detection data and false alarm data was taken.

The AN/TPS-59(XN-1) shall have passed this subtest if the averaged detection probabilities of a target in clutter (P_{DC}) (defined as the number of times at least one detection is made on a pair of successive scans divided by the number of scan pairs)

and false alarm rate (F_A) (defined as the total number of detections, less actual targets, divided by the number of scans in the test) satisfies the following inequalities:

Detection Probability ≥ 0.900 for each of the four range intervals from 0 to 80 nmi.

False Alarm Rate ≤ 10 per scan (5 for clutter, 5 for noise); however, no more than 5 are permitted outside clutter region (0–80 nmi, 0 to 4° in elevation)

2.7.1.2.   Results.

Processed detection data, collected from flights F12 and F13 along with applicable blip/scan data extracted from Appendix B were summarized and are shown in Table 2-15.   Dividing the number of detections by the number of scan pairs results in the probability-of-detection (P_{DC}) for the AN/TPS-59(XN-1) in the presence of ground clutter out to 80 nmi.

False alarm data were collected for 360 scans out to a range of 300 nmi after conclusion of flights F12 and F13.   Actual targets or returns that correlate over two scans or more were eliminated.   The remaining returns, representing false alarms as a result of clutter or noise, are shown in Table 2-15.   The distribution of false alarms is shown in Figure 2-11.

Table 2-15. Probability of Detection (In Clutter)

Range	No. of Scan Pairs	Detections	P_{DC}
0 – 20	168	143	0.851
20 – 40	247	245	0.992
40 – 60	215	215	1.000
60 – 80	85	85	1.000
80 – 100	24	24	1.000

AN/TPS 59
Flight Test
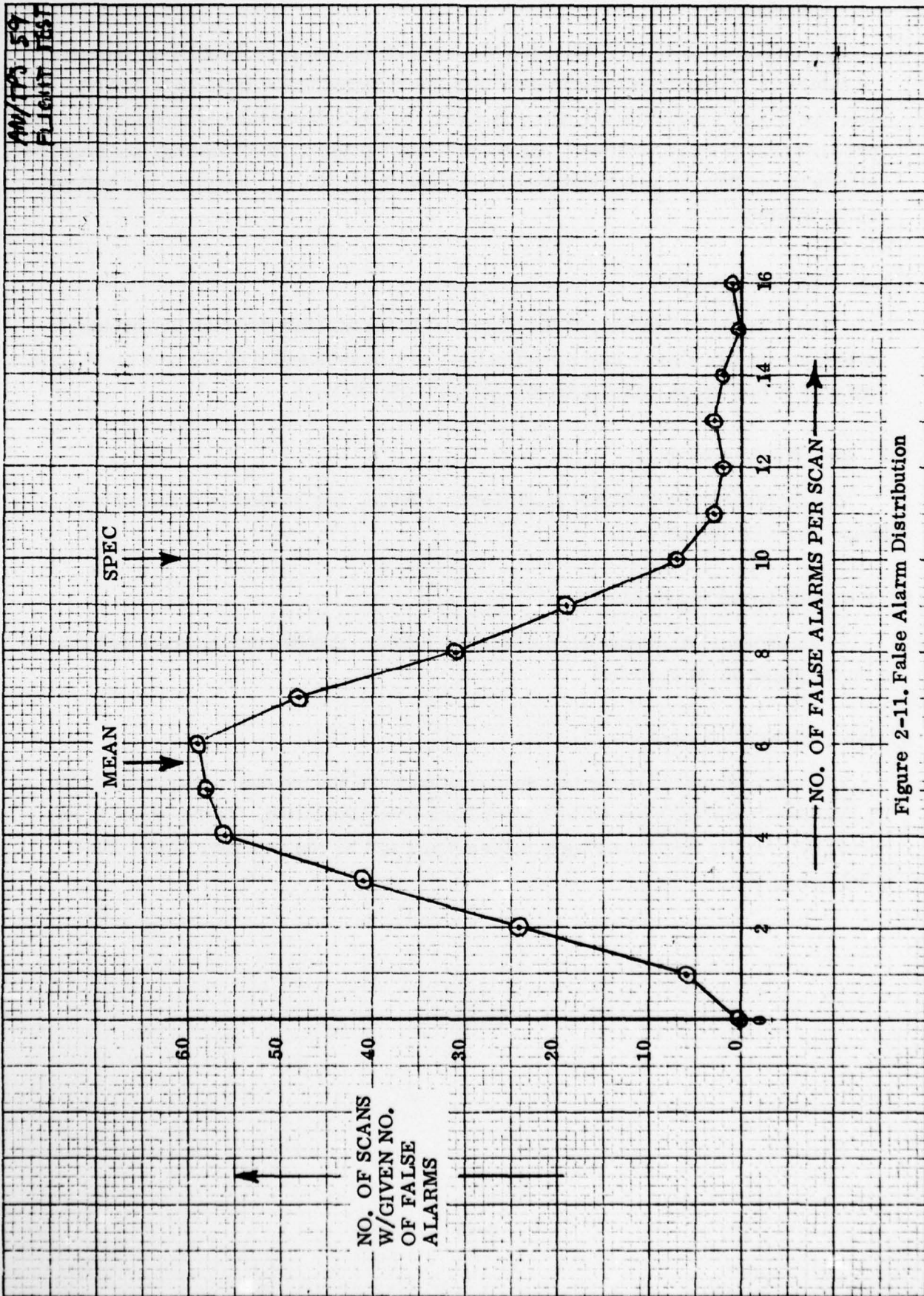
Figure 2-11. False Alarm Distribution

2.7.1.3. Conclusions.

Examination of Table 2-15 shows the AN/TPS-59 XN-1) probability-of-detection in clutter (P_{DC}) is significantly better than the required 0.900 from 20 to 100 nmi. In the 0 to 20 nmi range interval, the radar very nearly achieved the requirement. If the pre-driver turn on difficulties, (which were known prior to flight testing) are overcome, it is believed that the radar will meet or exceed the 0.900 P_{DC} requirement in this range interval.

2.7.1.4. Recommendations.

The changes recommended and discussed in the aircraft detectability subtest to overcome the pre-driver turn on difficulties are recommended to enhance the P_{DC} in the 0 to 20 nmi range interval for the AN/TPS-59(XN-1).

2.7.2. Anti-Weather Subtest.

In accordance with Contract Modification P00028, this subtest is deferred to a future phase of the contract.

2.8. ECCM DEMONSTRATION.

In accordance with Contract Modification P00028, this demonstration is deferred to a future phase of the contract.

2.9. IFF DEMONSTRATION.

IFF tests as defined in the test specification were not run due to inoperative IFF transmitters and interferences with other tests being conducted. At the recommendation of NAVALEX, these tests were deferred and will be run as a part of the USMC development tests.

2.10. CONTROL AND CONTROL CIRCUITS DEMONSTRATION.

This demonstration consisted of the GCI operation, TAOC-mated operation, and ancillary controls subtests given below.

2.10.1. GCI Operation Subtest.

2.10.1.1. Scope.

This subtest was conducted to determine if the AN/TPS-59(XN-1) controls are functional in the GCI (autonomous) mode. The subtest was performed in accordance with paragraph 4.1.4.7.2 of the Pre-Service Acceptance Test Procedures (See Appendix C). The AN/TPS-59(XN-1) shall have passed this subtest if all steps of the subtest are successfully completed as indicated on the specified data sheet.

2.10.1.2. Results.

The specified data sheet, completed at the time of the subtest, is shown in Figure 2-12.

2.10.1.3. Conclusions.

Examination of Figure 2-12 shows that the AN/TPS-59(XN-1) successfully passed this subtest and will operate in a GCI mode.

2.10.2. MTDS - Mated Operation Subtest.

2.10.2.1. Scope.

This subtest was conducted to determine if the AN/TPS-59(XN-1) controls are functional in MTDS (Sensor only) mode. The subtest was performed in accordance with paragraph 4.1.4.7.3 of the Pre-Service Acceptance Test Procedures. The AN/TPS-59(XN-1) shall have passed this subtest if all steps of the subtest are successfully computed as indicated on the specified data sheet.

2.10.2.2. Results.

The specified data sheet, completed at the time of the subtest, is shown in Figure 2-13.

Step #	Step Successfully Completed	
	Yes	No
1)	✓	—
2)	✓	—
3)	✓	—
4)	✓	—
5)	✓	—
6)	✓	—
7)	✓	—
8)	✓	—
9)	✓	—
10)	✓	—

GE TEST DIRECTOR _Ronald A Joseph_ 7/12/76

GOV'T WITNESS _R J LeVine_

Figure 2-12. Control and Control Circuit Tests, GCI Operation Subtest Data Sheet
(Figure 4.1-9 of ATP)

Step #	Step Successfully Completed	
	Yes	No
1)	✔	—
2)	✔	—
3)	✔	—
4)	✔	—

GE TEST DIRECTOR _Ronald A Joseph_ 7/12/76

GOV'T WITNESS _B. J. Kilian DFS_

Figure 2-13. Control and Control Circuits Test, MTDS Mated Operation Subtest
Data Sheet (Figure 4.1-10 of ATP)

2.10.2.3.   Conclusions.

Examination of Figure 2-13 shows that the AN/TPS-59(XN-1) successfully passed this subtest and will operate in the MTDS mode.

2.10.3.   Ancillary Controls Subtest.

2.10.3.1.   Scope.

This subtest was conducted to determine if the AN/TPS-59(XN-1) ancillary mode controls are functional. In accordance with Contract Modification P00028, the subtest was performed in accordance with paragraph 4.1.4.7.4 of the Pre-Service Acceptance Test Procedure except that steps 8, 9, 10 and 12 pertaining to weather and 2-D mode were deleted. Completion of the Alternate Modes Demonstration in a future phase of the contract shall constitute demonstration of the deleted steps.

The AN/TPS-59(XN-1) shall have passed this subtest if all steps of the subtest, as modified, are successfully completed as indicated on the specified data sheet.

2.10.3.2.   Results.

The specified data sheet, completed at the time of the subtest, is shown in Figure 2-14.

2.10.3.3.   Conclusions.

Examination of Figure 2-14 shows that the AN/TPS-59(XN-1) successfully passed this subtest except for a portion of step 2.

Clutter censor gate No. 3 was noted to be inoperative. Subsequent investigation conducted revealed a faulty circuit board in the equipment. Replacement of the board restored operation to clutter censor gate No. 3.

2.11.   ALTERNATE MODES DEMONSTRATION.

In accordance with Contract Modification P00028, this demonstration is deferred.

<u>Step #</u>   <u>Step Successfully Completed</u>

                              <u>Yes</u>   <u>No</u>

1)   ✓   —

2)   ✓   —   * CLUTTER CENSOR GATE #3
                                                   INOPERATIVE

3)   ✓   —

4)   ✓   —

5)   ✓   —

6)   ✓   —

7)   ✓   —

8)   —   —   ⎫ Those steps
                                                ⎬ deleted
9)   —   —   ⎭

10)   —   —

11)   ✓   —

12)   Deleted

13)   ✓   —

14)   ✓   —

GE TEST DIRECTOR _Ronald J. Joseph_ 7/12/76

GOV'T WITNESS _B. J. LaVine, QAS_

Figure 2-14. Control and Control Circuits Test, Ancillary Controls Subtest
Data Sheet (Figure 4.1-11 of ATP)

3.0. <u>RELIABILITY DEMONSTRATION TEST.</u>

3.1. SUMMARY.

3.1.1. <u>General</u>.

3.1.1.1. Purpose.

The AN/TPS-59(XN-1) Reliability Demonstration Test was conducted in accordance with the Pre-Service Acceptance Test procedures except as modified by Contract Modification P00028 to prove compliance with the requirements specified in Contract N00039-72-C-0356 and by Navalex Contract Specification ELEX-R-50, as amended.

This reliability demonstration test report was prepared in accordance with MIL-R-978, MIL-STD-781B, ELEX-R-0101A, and the outline specified in Table 4.2.11-1 of the Pre-Service Acceptance Test Procedures.

3.1.1.2. Test Team.

The test team was made up of representatives of the General Electric Company, United States Marine Corps (USMC) and Defense Contracts Administration Service Office (DCASO). We are very fortunate to have had three members of the USMC previously trained by the General Electric Company assigned to the AN/TPS-59(XN-1) test team during the reliability test. The three marines were trained in the fundamental operations of the radar and quickly adapted to operating the radar as a fully installed tactical system. Their duties encompassed the same tasks as were carried out by other members of the test team. Because of their previous training, their expertise in the maintenance of Government Furnished Equipment was greatly appreciated. The Marines, on occassions, were given on-the-job-training. This hands-on training would prove valuable in their future operation of the system. The Marines shared shifts with the other maintenance team members, rather than complement the teams.

DCASO representatives monitored all testing during the reliability test. They witnessed testing on a shift coverage basis from 0800-1600 hours Monday through Friday and 0800-1200 hours Saturday and Sunday. In the event DCASO coverage was required during hours other than those indicated above, DCASO was notified by phone. At most times during the tests, customer representatives were available to monitor all activities.

The following personnel were directly associated with the Test Team.

Name	Organization
Morton Fox	General Electric, Reliability and Quality Assurance Engr.
Howard Burris	General Electric, Radar Project Engr.
James Perry	General Electric, Signal Processing Engr.
Leo Gordona	General Electric, Display Engr.
Romand Joseph	General Electric, Test Evaluation Program Engr.
Leslie Bertz	General Electric, Lead Mechanical Engr.
Al Lentz, GYSGT	USMC
James Kehn, SSGT	USMC
Al Chesney, SSGT	USMC
Roger Lavine	DCASO
Stanley Blaszkow	DCASO

The assigned General Electric Test members were engineers associated with the radar design, evaluation and acceptance test phases. Only two members of this test team, H. Burris and J. Perry were familiar with all aspects of the design and test. The other four members were equivalent to technicians who had undergone on-the-job training. The twelve hour shifts were scheduled such that mixed crews operated the radar. For instance, a typical crew would consist of a USMC member with a General Electric test member such as M. Fox, L. Bertz etc. These teams adequately operated, maintained, and serviced the radar as required.

3.1.2. Test Result Summary.

Table 3-1 is a summary of the Reliability Demonstration Test results. Testing began at 2300 hours on June 21, 1976 and continued until 0805 hours on July 17, 1976. During this period, the system had undergone 546 hours of operation without a relevant failure. The system was down for maintenance actions as indicated by the test summary for 9.83 hours. This downtime was due in part to the incorporation of several design changes to correct certain hardware deficiencies. These deficiencies, for instance the L.O. amplifier in the exciter, were known to exist prior to the test. Because of certain contractual considerations, it was decided to test the equipment with these design deficiencies. The remaining downtime was associated with correction of several miscalculated threshold settings in the performance monitoring system or to tighten the drive motor/gear box mounting bolts.

Table 3-1. Reliability Demonstration Results Summary

Radar Mean Time Between Failure (MTBF)	(60% Confidence)	589 hours (1)
	(60% Confidence)	1000 hours (2)
	(53% Confidence)	1400 hours (2)
System Related Downtime (Due to hardware failure)		9. 83 hours
Radar Availability		.98

2 dB Degradation Time Interval
  (Due to power module failures only
    assuming Garrison operation)
		2. 7 years (3)

(1) Applicable when exciter improvement is completed; based on 546 hour test without a relevant failure

(2) Based on projected 900-hour test without relevant failure

(3) Successful demonstration of graceful degradation features

Table 3-2 is a hardware failure summary for the Reliability Demonstration Test.

The row power supplies had undergone a major modification just prior to the Reliability Demonstration Test. The associated row power supply failures were probably caused by extra handling during this major modification. Before the major modification these same power supplies had failed several times before. They had been opened and repaired frequently; many times above what should be expected during the life of any equipment or hardware.

The row transmitter failures occurring during these tests were due mainly to malfunctioning predrivers. The prediver was a recognized difficulty prior to the tests.

Another transmitter failure that occurred during the test was due to a shorted dc bus. The bus was shorted due to being crimped during installation of the transmitter just prior to the reliability test.

Table 3-2. 546 Hour Reliability Demonstration Hardware Failure Summary

Component	Failure Quantity	System Outage
Row Power Supplies	5	No (1)
Row Transmitter	4	No (1)
Digital Circuit Board	2	No (2) (3)
RF Circuits	1	Yes (4)
Blower Motor	1	No (5)
Loose Bolts	1	No (6)
Lamps	32	No (7)
Power Modules	15	No (8)

(1) Equivalent to 1.60 dB Sensitivity Degradation

(2) 5-Second Mode Board - Not Checked Out Prior to Demonstration - Corrected

(3) Intermittent Connection - Degraded MTI Performance

(4) Exciter Problem Identified Prior to Demonstration - Corrective Action In Process

(5) Motor Bearing Corroded - Snow Accumulated in Unit 11 When Door Was Left Open

(6) Drive Motor/Gear Box Mounting Bolts Will be Staked Priot to Shipment

(7) Function Switch Lighting - 1 Year Operation Without Replacement Prior to Demonstration

(8) Equivalent to 0.16 dB Sensitivity Degradation

The digital board failure, which did not cause a system failure, was caused by a temperature sensitive integrated circuit.

Edge lighting bulbs that failed during the test had accumulated more than a year of life without replacement. This was within the life limits for this device.

Eighteen (18) power modules had been replaced at the conclusion of the reliability test. Only fifteen had actually degraded/failed during this time. The other three had inadvertently been recorded as good prior to these tests.

The reliability test successfully demonstrated that the requirements of the tests were met. Given that the known design/hardware deficiencies could have been corrected prior to these tests, few faults would have been recorded.

The radar system operated during this period with:

- More than 25 days operation with no major problems.
- A wide range of environmental conditions with no noticeable degradation.
- Minimal downtime
- Only two system adjustments made due to readjusted threshold settings.
- No special test equipment usage.
- Accumulation of 500,000 power module hours.
- No analog board failures.
- No new problems identified.
- Significant increase in row power supply design confidence due to the major modification.

3.2. APPLICABLE DOCUMENTS.

The specifications and documents listed are applicable to the Reliability Demonstration Test Plan and Test Report. In case of conflict with test plan and NAVELEX specification ELEX-R-50, ELEX-R-50 shall have precedence.

Order of Priority

1	Acceptance Test Procedure, AN/TPS-59(XN-1) EDM as revised by contract mod P00028	Defines test activities, definitions, operational modes, and acceptance criteria
2	Naval Electronic Systems Command Contract Specification (ELEX-R-50) (4-8-70) as amended	Defines contractual tasks related to reliability test and and required achievement levels
3	MIL-STD-781-B Reliability Tests Exponential Distribution (11-15-67)	Requirements for overall reliability test
4	AN/TPS-59 Reliability Prediction Report (8-31-73)	Guide to test model definition (for information only)

<u>Order of Priority</u> (Cont)

5	MIL-STD-471 Maintainability Demonstration (2-15-66)	Guide for overall main-tainability test
6	AN/TPS-59 Maintainability Analysis & Prediction Report (8-31-73)	Guide to test model defi-nition (for information only)
7	Repair Parts Recommendations (9-27-73)	List of spare parts avail-able at the radar
8	MIL-R-978, Reports: Research & Development	Guide for submission of manufacturer's engineering data
9	ELEX-R-R0101A, Monthly Summary and Final Reliability Test Reports	Guide for submission of manufacturers engineer-ing data

3.3 ACCEPTANCE CRITERIA.

The technical task associated with the contractual test requirement was to measure reliability (MTBF) by operating the system for 540 hours without the occurrence of a relevant failure.

Customer acceptance criteria for the Reliability Demonstration test is according to the requirement of ELEX-R-50, MIL-STD-781B, Reliability Demonstration Test Plan (as modified) and changes to the contract as modified by P00028 dated 4 Mar 1976.

For the purpose of applying acceptance criteria, failures were classified as either relevant or non-relevant. Only relevant failures are used in establishing the demonstra-tion test results.

3.4. TEST CONFIGURATION.

3.4.1. <u>Equipment Complement</u>.

Shown in Table 3-3 were the equipments operated during the Reliability Test. Although, Government Furnished Equipment was used during these tests, it was not the intent in any way to evaluate these equipments. At one time or another, during these tests, all five generators furnished to the General Electric Company for their tests were used.

3-6

Table 3-3. Equipment Compliment

Group No.	Unit No.	Equipment Nomenclature
1		Antenna Transmitter
1	1	Antenna Transmitter
	2	Trailer Ancillary
	3	Final Receiver
	4	Exciter
	5	Power Supply
2		Signal Processor
	6	Preprocessor/Waveform Generator
	7	Digital Processor
	9	IFF Subsystem
3		Radar Control
	8	Radar Set Console
	10	Computer Set
	14	Interface Controller (IFF/TAOC/Array)
	11	MTDS Interconnection Box
		Generator Set
		Cable Set

Although all equipments were operated during the demonstration tests, not all were used to evaluate the reliability requirements.

3.4.2. Test Site.

The Reliability Test Demonstration for the AN/TPS-59(XN-1) was conducted at facilities located at the USAF RADC Verona Test Annex, Verona, New York. The Reliability Test Site chosen had a low screening angle around the site. Azimuth blanking was limited. However, potential interference with an FAA radar at Star Hill, New York necessitated azimuth blanking from 270° to 90° (180° coverage east of the test site).

The system was powered by two 400 Hz generators. Five such generators were available for the test. Two air conditioners per shelter were used. Figure 3-1 shows an approximate system layout at the test site.
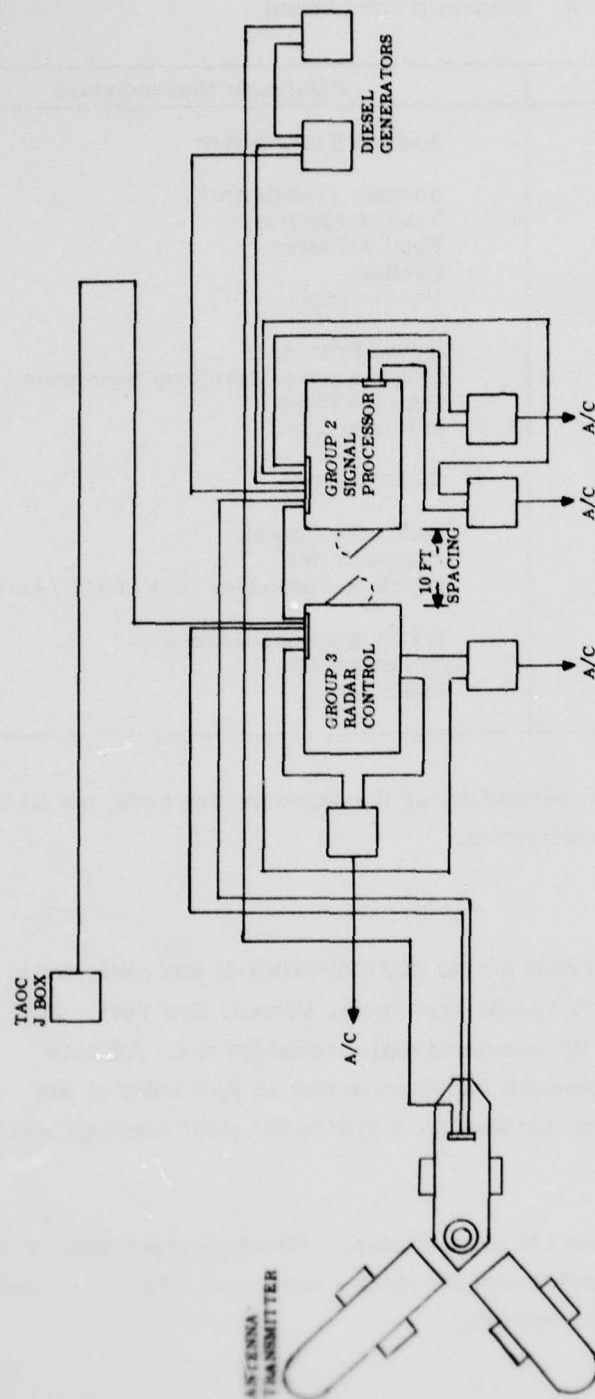
Figure 3-1. AN/TPS-59(XN-1) System Arrangement

3-8

3.4.2.1. Primary Power System.

The GFE generators supplied 3 phases, 208 volt ± 10%, 400 Hertz ± 5% power. Three backup power generators were available for these tests. The generators were alternately operated during the test. System power was monitored continuously. The built-in system power meters provided in the Radar Control Group Shelter and with each power generator were visually checked at least once during each shift and the data recorded in the system log. Phase-to-phase voltage, transient voltages and frequency variations of the prime generator set were monitored for out-of-limit conditions. These out-of-limit conditions were noted and entered into the system log. During the test the STE 408 power test monitor designed to monitor out-of-limit power conditions became quite erratic. It would continually indicate erroneous power conditions, when all other conditions of the site indicated normal operation. Often, STE 408 had to be disabled bacause of these inconsistencies. It appeared at times that as the generators would heat-up, the STE 408 would report continuous error signals. Observations on the oscilloscope, indicated that because the generators did not put out a clean waveshape (trapezoidal at times - rather than a sine wave) - the monitoring system could not evaluate the preset out-of-limit conditions. Other than drop out due to load unbalance, the diesels generators were probably not responsible for failures with the radar set.

3.4.2.2. Air Conditioning.

The Reliability Demonstration Test was conducted under normal external ambient temperatures and atmospheric conditions. The MAC4V20 air conditioners were controlled to maintain a typical nominal ambient temperature of 72° to 76°F within the shelters. Normal ducting of conditioned air was provided for the shelter electronics group. Air temperatures within the shelter and shelter equipment areas were monitored and recorded on a shift schedule.

Separate temperature sensors were used at the inlet and outlet to each air conditioner. These readings were monitored and recorded every twelve (12) hours. This data was recorded in the system log.

Test site ambient conditions including temperature, humidity and barometric pressure were read and recorded daily in the system log. On June 26, 1976, air conditioner #4 (Radar Control Group - console) experienced a failure. The failure was observed just prior to the over temperature light coming on for the console power supply system. The inlet for the A/C #3 duct was attached to the duct for #4 A/C and the console was noted to cool down. The radar was operated with the one air conditioner for two hours and forty-four minutes. Air conditioner #4 failed due to a faulty bearing. The bearing was replaced, and the air conditioner resumed its normal operation.

Appendix D shows the temperature extremes for the following during the test phase:

1) Ambient outdoor temperatures
2) Each air conditioner inlet and outlet temperature
3) Shelter #1 and #2 room temperature

This data was taken during each shift (twice a day, approximately at 0800 and 2000 hours).

Also recorded for the test period was the local humidity (relative) and barometric pressure. (See Appendix E.)

3.4.2.3. Time Keeping.

A clock for recording times associated with significant events throughout the test period was provided. Appendix F shows the initial and final elapsed times in addition to the accumulated operating times for:

1) Generators
2) TPX-28
3) Shelters
4) Trailer

3.4.2.4. Access to Test Area.

Personnel authorized by NAVELEX had complete access to the test area during these
tests. These personnel were allowed to take and obtain additional data during the entire
test period. The acquisition of this data did not disrupt normal system operation.
Manipulation of console controls, and taking of additional data from the TTY was a
daily routine.

3.4.2.5. Access to the Units on Test.

Access to the inside of an equipment enclosure during test was controlled by the
use of serial numbered seals. The seals had to be broken if entry to an enclosure was
made. All units were sealed prior to the test; dated and stamped by the DCASO repre-
sentative. A new serialized, dated, and DCASO stamped seal was required each time
a unit was opened. A history of entry, exit, replacements, inspections, adjustments,
troubleshooting and repairs were recorded in a maintenance equipment log. Appendix G
is a record for all maintenance actions requiring entry to equipment areas resulting
in broken seals.

3.4.3. Test Equipment.

All tools and test equipment necessary to maintain or service the AN/TPS-59(XN-1)
during this test were available at the test site. No other tools or test equipment were
required other than those supplied as part of the contract and/or loaned for continuing
support at Camp Pendelton, California. (Refer to Appendix 4.2.1 of the Pre-Service
Acceptance Test Procedure for a listing of available tools and test equipment at the
test site.)

All test equipment used for test purposes during this test was calibrated and/or
inspected as verified by DCASO representatives.

3.5. TEST PROCEDURE.

The duration of the Reliability Demonstration Test was 540 hours of operation.
During this operation, the system was capable of tracking and monitoring targets of
opportunity. The demonstration was conducted with the AN/TPS-59(XN-1) operating
under normal external ambient temperatures and atmospheric conditions existing at
the time of the tests.

The only times the radar was taken off the air was when:

1) A system failure occurred.
2) Scheduled one-hour shutdown period per day.
3) Diesel generator outage.
4) Air conditioner outage.
5) Troubleshooting abnormalities in the system due to suspect failures.
6) AN/UYK-7 malfunctions.

In general during the one-hour period each day that the radar was shutdown, power to all equipments was turned off. However, the shelter equipment was enabled so that fault location programs could be operated during this time.

3.5.1. System Operating Test.

The scheduled daily/weekly tests performed during the reliability test are depicted in Table 3-4. The table shows a typical daily test cycle, that was repeated throughout the test until completion. The only deviations allowed from these tests during the test period were the following:

1) The 12 RPM mode (5 sec mode) was run during the final 24 hours of the test. This was a continuous 12 RPM operation test for one day, 24 hours.

2) TAOC was exercised for approximately eight hours every other day, except when thunderstorms were prevalent in the area. TAOC remained on during the test, throughout the system test, but was disabled by the AN/UYK-7 except as noted above.

3.5.2. Reliability Test.

In accordance with contract modification P00028, the following changes were made to the Reliability Demonstration Tests.

1) The duration of the test was changed to 540 hours of operation.
2) Total PM/FL system was not in place.
3) ECCM system had not been checked out due to lack of necessary performance monitoring capability. ECCM was therefore not evaluated during the test.

In addition several areas of equipment that were recognized as deficient existed in the AN/TPS-59(XN-1) during the test:

1) Predrivers - 725016A0262P1, P2.
2) LO Amplifiers 725016A0265 located within the exciter unit.

Table 3-4. Operational Mode Duty Cycle[4]

___

Time Period

0800 - 0900 SSC

System completely shutdown. All power off for 45 minutes. The remaining 15 minutes shall be used to run the SSC to determine satisfactory system operation. [1] [3]

0900 - 1600 Perform SPC

The following modes are exercised: [2] [3]
- (a) MTI - disabled for 5 minutes
- (b) Weather - enabled in inclement weather
- (c) SET 1 - disabled for 5 minutes
- (d) Normalizer - disabled for 5 minutes
- (e) Preview/postview display alternated for equal time (both displays normally on)
- (f) Control settings for target/display intensity, trackball tag settings, censor gate initiation, target height correlation, etc., exercised at least once during this period.
- X(g) SET 2 enabled periodically during the day - deleted
- X(h) SET 3 enabled periodically during the day - deleted
- (i) At least once during this period the visual check part of the SPC shall be run.

1600 - 2400 Perform SPC

Same as 0900-1600 except for (e) and (f). No manual activity or control settings allowed during this period unless requested by DCAS/NAVELEX [2] [3]

2400 - 0800

Same as 0900-1545 except for (e) and (f). No manual activity or control settings allowed during this period unless requested by DCAS/NAVELEX.
Once/week for 8 hours - 5 second mode

NOTES:
(1) The complete SSC test is operated at this time including fault location program.
(2) Does not include fault location program.
(3) Obtain system performance data from 1538 with printout and record in daily log. RHI data may be used to supplement the 1538.
(4) This operational cycle is relevant to operation Mondays - Fridays. Saturday and Sunday operational cycle (0900 hrs Sat. to 0800 hrs on Mon.) shall duplicate the 1600-0800 operation.

All references to FD&L shall be changed to "available FOL-SSC and those appropriate portions of loop tests as agreed by the Government necessary to establish system status".

___

3) Row Power Supplies - 725016A0592.

4) Main Drive Bearing

5) Suspect Duplexer - 725016A0320

6) Suspect Phase Shifter - 725016A3319P1, P2

7) Minimal Exciter Performance

Procedural revisions allowed during this test included:

1) Failed row power supplies were allowed to be removed from the array during scheduled down periods to prevent additional component damage in the power supply. After repair, the failed power supplies were allowed to be replaced on the same rows from which they were removed.

2) Limits on PM164 were allowed to be changed from 13_{10} to 26_{10}. The cause of this PM message problem would be determined at the conclusion of the reliability test and corrective action taken.

If a new or repaired exciter X8 multiplier board was installed prior to the conclusion of the test, the limits would be returned to 13_{10} for PM164.

3.5.2.1. Maintenance Team Tasks.

The maintenance team tasks required during this test is shown by Appendix H. The maintenance procedure followed in the event of failure is shown by Table 3-5.

Table 3-6 is the daily schedule followed by the maintenance team during the demonstration tests.

A detailed description for each standard operation procedure (SOP) that was performed by a member of the test team is given in Appendix J.

3-14

Table 3-5. Procedure in the Event of Fault

1) Record time on 1538 immediately

2) Type R carriage return (clears PM Msg.)

3) Wait for two minutes. If Msg. does not reoccur, continue test.

4) Enter time of Msg. and time of reset in test log sheet.

5) If Msg. does repeat in two minutes, repeat steps 1, 2, 3 and 4.

6) If Msg. repeats third time, observe PPI, RHI and transmit power for ab-
    normal indication. If all indications normal, wait five minutes and repeat
    steps 1, 2, 3, and 4.

7) If Msg. repeats again, terminate tactical operation, log time immediately
    and inform DCAS of action taken. DCAS will inform us of go-ahead
    condition for repair.

8) Run F1 and F1 supplemental programs.

9) If F1 defines a specific documented fault area, pull boards in fault area
    from spares, break seal on cabinet (if DCAS authorized same) replace
    boards one at a time running F1 for each board. (See instructions for
    running F1.) If replacing a board does not repair equipment, take care to
    replace original board in original location.

10) If F1 defines a hard frequency fault, load tactical program and detect
    failed unit.

Table 3-6. Daily Schedule

0800	Shut Down System		SOP 1
0800 – 0845	Diesel Maint of Change Over		
0845	Power On		SOP 2
0845 – 0900	System SSC		
	I.	a. Load supplemental F1 tape	SOP 3
		b. Run Receiver Test	
		c. Run Monopulse Test (Receiver's off)	
	II.	a. Load tactical F1 SOP 4 at all enabled frequencies.	SOP 4
0900		a. Load "T" Tape	SOP 5
		b. Collect system performance data	SOP 6
0900 – 1230	Operate per		SOP 7
0900 – 0935	Normalizer Test		SOP 8
0935 – 0940	SET 1 Test		SOP 9
0940 – 0945	MTI Test		SOP 10
0945 – 1000	Controls Test		SOP 11
1000	Return controls to normal Conf.		SOP 12
1000 – 2000	Operate System		
2000 – 2035	Normalizer Test		SOP 8
2035 – 2040	SET 1 Test		SOP 9
2040 – 2045	MTI Test		SOP 10
2045 – 0800	Operate System		
	Collect System Perf. Data		SOP 6
As Required:			
	Weather Mode		SOP 13
	Mounting Magnetic Tape		SOP 14
	Magnetic Tape Rewire and Dismount		SOP 15

3.6. FAULT/FAILURE EVALUATION.

3.6.1. Ground Rules and Assumptions.

There were two distinct fault/failure types that occurred during the test.

The first was easily identified and categorized. This type of fault/failure we will refer to as a hard fault/failure. An example of this type of failure is:

1) Row Power Supply.
2) Predriver.
3) Printed Circuit Board.
4) Power Module.

This type failure was isolated to a components' failure to function due to a catastrophic failure. This fault/failure could have caused a system or degraded failure. In any event, the performance monitor and/or fault location system did identify this malfunction. The failure to these units may have been classified as a relevant or nonrelevant failure depending on the accepted definitions spelled out by the Pre-Service Acceptance Test Procedures (see Table 3-7).

The second type of fault/failure definition is somewhat more subtle. During the test we evidenced PM messages that occurred temporarily. They could be cleared by resetting the software (clearing data from storage). At times the PM message would clear for days and then would reappear unexpectedly. Other PM messages would clear for minutes on end, continuing for several hours, and then, just as un-expectedly, disappear. Several PM messages faults have been diagnosed and their failure cause resolved. Others, due to the unavailability of the radar at 100% of its capacity, have not been resolved.

Since PM messages were cleared immediately and as long as the radar was meeting its performance requirements set forth by the Pre-Service Acceptance Test Procedures, these temporary fault indications were considered nonrelevant.

As mentioned in paragraph 3.5.2, the AN/TPS-59(XN-1) entered the demonstration phase with known deficiencies in its design as a result of contractual considerations. Table 3-8 is a summary of the known deficiencies of equipments during these tests. In evaluating "What is a relevant failure?", the criticality of these components was taken into account.

Table 3-7. Relevant/Nonrelevant Failure Definitions

<u>Relevant failures are thosed caused by:</u>

1) Equipment designs, manufacturing or parts defect.

2) Internal transients or performance degradation which requires diagnostic time, repair time or repetitive operator attention.

3) Unknown or other causes not specifically listed as nonrelevant in paragraph 4.2.13.2.

<u>Nonrelevant failures are:</u>

1) Those caused by accidental mishandling, improper storage, improper operation, external test equipment, input power transients or improper maintenance.

2) Failures occurring because the equipment does not reflect the drawings, maintenance manual, or other documentation to be identified on a list and approved by the government prior to testing, providing prompt correction is made to these documents and the correction is shown to eliminate future similar faults and then only when approved by the government in writing.

3) Failures resulting from failures of any Government Furnished Equipment. A failure attributable to failure of GFE is specifically excluded from relevant failure definition regardless of effect on system functions.

4) Other than the initial failure in cases where failure of multiple, simultaneous or immediate sequential nature occurs. (These failures are dependent as specified by MIL-STD-781B.)

5) A failure attributable to human error or defective workmanship, regardless of effect on system function.

Table 3-8. Previously Identified Deficiencies in Equipment Prior to Reliability Test

Equipment	Comment
Row Power Supplies	The Row Power Supplies had recently undergone major modification prior to Reliability Test. Schedule necessitated a tight modification schedule which could have attributed to a less than desired power supply quality. Many of the supplies had a failure history requiring opening/closing the supplies beyond normal expected frequency.
Predrivers	Recognized as an inadequate design. New designs being evaluated. An overstressed first stage amplifier transistor. Transistor ratings misquoted in specifications.
Exciter Multiplier/Amplifier	Corrective action was being implemented prior to test.
Power Modules	Recognized potential problems included aluminum migration (MSC modules), metallization lifting and low breakdown voltage (PAI module).
Exciter	Over temperature problem.
Duplexer	Questionable high power band pass filter
Phase Shifter	Mechanically failure prone interconnection strap

3.6.2. **Summary of Faults and Failures.**

Several items entered the reliability test in a failed state. Table 3-9 shows the pretest failures identified.

Table 3-2 is a hardware failure summary for the Reliability Test Phase. Based on our definitions for relevant failures as defined by the Reliability Demonstration Test Procedure and further explained here, there were no relevant failures during this test phase.

Table 3-10 is a summary of the performance monitor messages obtained during these tests. Additional data can be found in Appendix K.

3.7. PERFORMANCE ANALYSIS.

3.7.1. **Introduction.**

This section of this report contains a data summary (test performance and failure) collected during the reliability test, assumptions used to define a relevant failure, conclusions of the recorded test, and conclusions showing compliance with a 1,000 hour MTBF (60% LCL).

3.7.2. **Ground Rules and Assumptions.**

The reliability demonstration test procedure clearly states the conditions whereby a relevant failure is determined. It also states tolerable system losses (failures, faults, degradation, etc.) permitted during these tests. Table 3-11 summarizes functions or equipments pertinent to the acceptance criteria (pass/fail criteria) of paragraph 3.3.

Relevant/nonrelevant failure definition has been defined earlier in paragraph 3.6, Fault/Failure Evaluation (Table 3-7).

Further comments in paragraph 3.7.4 will address the relevancy of faults and failures which occurred during these tests.

Table 3-9. Pretest Failures

Equipment	Comments
Radar Receiver Transmitter S/N 17 (725016A0961)	The Reliability Test was started with RRT S/N17 transmitter out. (as indicated by Supplemental Test Data).
Radar Receiver Transmitter S/N 55 (725016A0961)	The sum (Σ) receiver was out. S/N was located on Row 3.
Radar Receiver Transmitter S/N 41 (725016A0961)	The sum (Σ) receiver had a low amplitude indication which was a fault in the monitor path and not the receiver. This had no effect on the tactical path.
Row Fans (725016A1176)	Blower fans were out on rows 19-20 and 5-6.

Table 3-10. Performance Monitor Message Summary
(Reliability Demonstration)

Functional Area	No. of Message Types	Potential Cause
Signal Processor (MTI)	1	Exciter Problem
Final Receiver (STC)	15	Exciter Problem
Final Receiver ($\triangle$ Azimuth)	1	Exciter Problem Receiver Intermittent
Array Receiver (Gain and Noise)	8	Exciter Problem Array Output Test Signal Path
Computer/Sync - Signal Processor Data Controller (Parity Error)	4	Computer Cabling Temperature Problem
IFF (Parity Error/Target Overload)	5	TPX-28 Spurious Output
TAOC	7	Test Equipment Drift
Miscellaneous	~ 100	Noise Spurious Self-Clearing

1.0

1.1

1.25   1.4   1.6

2.8   2.5
3.2   2.2
3.6   2.0
4.0   1.8

MICROCOPY RESOLUTION TEST CHART
NATIONAL BUREAU OF STANDARDS-1963-A

Table 3-11. Tolerable System Losses for the Automatic Mode

Function/Equipment	Acceptable Pass Condition [3]
Sensitivity	Less than or equal to 2 dB degradation
Plan Position Indicator Display (PPI)	One PPI operational
Range Height Indicator Display (RHI)	Not relevant
Electronic Counter-Counter Measures (ECCM)	Not relevant [4]
Transmitter Frequency Source	More than half the available frequencies [5]
Row Receiver/Transmitter	Loss acceptable as long as system performance does not degrade more than 2 dB
Logic Chassis Blower Motors	Loss acceptable as long as system performance does not degrade more than 2 dB
Performance Monitor Equipment	Note (1)
Fault Location Equipment	Note (2)
Government Furnished Equipment	Not relevant
IFF (GFE) and Identor	Not relevant
Σ, $\Delta e\ell$, $\Delta az\ell$, Set 1 Processor Channel	Three of four channels are operable and height accuracies are within tolerances

NOTES: (1) Performance monitor hardware failures are only relevant when their failure prevents determination of degradation system performance by the PMSD.

(2) Fault isolation or local hardware equipment that fails and has no adverse operational affect on system performance is considered an acceptable loss.

(3) This table applies only to the reliability test and not to any other acceptance test.

(4) Excluded from test criteria with change in contract.

(5) Exciter problems identified prior to test.

Previous to the reliability demonstration tests, the radar had been aligned, calibrated, and tested to establish its capabilities using the System Status Check (SSC) tests. The reliability test began only after the radar had undergone baseline tests using the SSC. Further daily checks using the SSC were used as the pass/fail criterion during these tests.

The SSC is a built-in function of the radar capable of providing system performance checks (SPC) and fault location data. The SPC included both automatic and manual performance monitoring. The automatic and continuous performance monitoring (PM) of the AN/TPS-59(XN-1) is executed under control of the AN/UYK-7. The primary PM objective is the detection of system degradation and communication of the nature and severity of the degradation.

The complete PM system was not in place at the time the reliability testing began. Therefore, degradation monitoring testing using a supplemental test program tape was made at the beginning of each morning shift. This included row transmitter and receiver status which provided:

1) Transmitter power output status
2) Receiver amplitude and phase status (Σ, $\triangle e \ell$, and $\triangle a z$)
3) Monopulse calibration status

During normal operation (tactical operation) system failures were indicated by the performance monitor status display (PMSD). The PMSD was the primary indicator of system failure. In the absence of failure, all lights shown green.

Fault location testing was accomplished at least daily. This testing was conducted off-line due to the nature of the computer program design. Summaries of the daily results of these tests are shown in Appendix N. Further fault location testing was accomplished by audio, visual, as well as normal operation of the display console. Potential relevant failures were classified based on these failure indications derived by the SSC.

3.7.3. Analytical Techniques.

The system radar reliability demonstration test is a fixed-time test. The radar was to operate for 540 hours without a relevant failure. According to the poison distribution for zero failures, this would approximate a system mean-time-between failure of a 1000 hours to a 42 percent lower confidence level based on Equation (1).

$$\text{CUSTOMER CONFIDENCE LEVEL} = 1 - e^{-T/MTBF} \qquad (1)$$

where

    T = duration of the test
    MTBF = specified MTBF by contract

This assumes no relevant failures based on catastrophic or degration failure definitions.

The confidence factor achieved is directly related to the test duration time. The high reliability of the AN/TPS-59(XN-1) radar, and certain contractual limitations precluded any additional test time to further increase the confidence factor of passing this test.

3.7.4. Test Results.

3.7.4.1. Random Catastrophic Failures.

Based on the failure/faults that occurred during the test (reference paragraph 3.6.2), the conditions preceding the test, and the definitions for a nonrelevant/relevant failure presented in this report, no relevant system failures occurred during this test. The tests further proved:

1) Random array failures (row power supplies, receivers, transmitter) although minimally affecting overall performance limits, allowed for successful tactical operation none the less.

2) Digital and analog designs using high reliability components and derating practices were extremely reliable.

3) Diesel generator outages would not adversely affect equipment reliability. No hardware failure was ever attributed to a diesel generator failure. Although the diesel generator output was less than desirable, no adverse radar operation was recorded.

4) Equipment was capable of operation without air conditioned air for limited times.

5) Daily adjustments to the equipment were not necessary. Adjustments at times (2) were required to adjust threshold settings.

Appendix L contains a further failure analysis for components which failed during the test.

Appendix M is a summary of failure frequency and maintenance actions as they occurred during the test.

3.7.4.2.   Performance Monitoring Summary.

The performance monitor data in Appendix N summarizes the performance monitoring (PM) messages that occurred during the Reliability Test. Of those, PM messages 9, 10, 61, 164, 178, 257, 258 and 995 will be discussed. The rest of the messages occurred so infrequently that they cannot be considered to be failures. Almost all PM tests involve test targets plus noise being compared to a threshold. Even when there is no equipment failure, occasional PM messages occur when the noise reduces the signal amplitude below the PM test threshold. The meaning of the various PM messages is discussed below.

PM 9	Checks parity of data received at input to Signal
PM 10	Processing Data Buffer (SPDC) from AN/UYK-7.
	These messages occurred periodically. At one time when they came up repeatedly, the AN/UYK-7 was turned off for 30 minutes and the messages no longer occurred after resuming the test.
PM 61	Indicates too much data from Identor into IFF Data Controller. This message occurred when high noise level was measured at TPX-28 receiver output.
PM 164	Insufficient Cancellation.
	The Exciter design was marginal at the beginning of the test. After an improved Exciter is implemented this PM test will be evaluated.
PM 178	ΔAZ Final Receiver Gain Low
	The attenuation in the ΔAZ Final Receiver was reduced in order to correct this problem.

PM 257   Low Σ Receiver and △AZ
PM 258   Receiver array gain

         Exciter test output level was lower than pretest
         levels. After installing improved Exciter components,
         these tests must be evaluated; no system performance
         resulted.

PM 995   Too many detections into AN/UYK-7

         Most of the time this occurred when both MTI and normalizer
         were turned off on postview PPI. This is an abnormal
         condition that will not exist in a normal tactical environment.

3.7.4.3. Fault Location Summary.

  Fault location data in Appendix N summarized the Fault Location (FL) messages that
occurred each day of the Reliability Test. The meaning of each of the FL messages
is listed below.

FL 361   FL 361 indicates one or more row power supply failures and
 Row X   the rows that have failed (i.e., Row X, Row Y, etc.) follow
 Row Y, etc.   the message.

FL 998   Undefined FL message. From observation of the fault
         location list 5 that was taken during the test, it was de-
         terminated that flag 170 was set. This indicates that the
         $\triangle AZ_4$ channel gain was low. It was determined after the
         Reliability Test that FL in Unit 6 had an intermittent con-
         nection that caused the low gain condition. Even though the
         $\triangle AZ_4$ channel gain was below the FL program limits, there
         was minimal affect on monopulse accuracy during tactical
         operation.

FL 42   Refer to comments on FL 998

FL 47   Refer to comments on FL 998

FL 155   Undefined FL messages. From observation of the fault
FL 153   location list 5 that was was taken during the test, it was
         determined that the following flags were set: 124, 170, 160,
         157, 151, 152, and 168. These flags indicate the $\triangle AZ_4$
         channel gain and the SET 1 gain were both low. As previously
         discussed, the $\triangle AZ_4$ gain has minimal affect on system per-
         formance. The low SET 1 gain has no affect on detection or
         monopulse accuracy during tactical operation. It may allow
         some increase in false alarms from large aircraft or clutter
         received through the antenna sidelobes. In tactical operation,
         a failure in the SET 1 channel is not considered a system
         failure.

3.7.5. Tabulation Summary of Test Data.

A summary of data taken during the reliability test is contained in Appendix N. This data consists of:

1) Row transmitter power output status per day.

2) Row receiver amplitude and phase data taken per day.

3) Fault location status data taken per day.

4) Performance monitor data taken during the test period.

5) Monopulse estimation data taken per day.

6) Summary of daily activities. Complete daily activities are included as Appendix P of this report.

3.7.6. Conclusion Showing Compliance with 1000 Hours MTBF (60% LCL) Minimum.

There were no relevant failures that occurred during the reliability demonstration test. There were, however, several component failures that resulted in degradation to overall performance such as:

1) Row power supplies   5

2) Row transmitters   4

3) Power modules   15

On the basis of degradation for the 546 hours of operation, the signal-to-noise ratio S/NR would have degraded by:

1) Row power supply   0.84 dB

2) Row transmitter   0.67 dB

3) Power module (note 1)   <u>0.16</u> dB

                           1.67 dB

NOTE 1

Row 17 was not in an operating condition at the start of the test.

If all of these failures had been relevant faults (which they were not); then at the end of 900 hours, if the same failure trends continued uniformly, we would expect, at most, the following failures to exist:

	Failures	Degradation
Power supplies	8	1.39 dB
Transmitters	6	1.02
Power modules	24	0.25
		2.66 dB

All of the transmitter failures that occurred during the test were the result of failed predrivers (a known design deficiency prior to the test). Definitely two, if not all five power supplies, were nonrelevant failures (known design deficiencies). Therefore, discounting the known design deficiencies, the system would have had a projected degradation of only about 1.09 at the end of 900 hours.

	Failures	Degradation
Power supply	5	0.84 dB
Power modules	24	0.25
		1.09 dB

Since an allowed 2.0 dB degradation was permitted during these tests, a relevant system failure would not have occurred for the projected 900 hour test.

A system mean-time-between-failure of 1000 hours at a confidence level of 60% would then have occurred for the 900 hours. Stated another way, a system MTBF of 1400 hours at a 56% confidence level exists for the 900 hour test.

4.0. MAINTAINABILITY AND INTERCHANGEABILITY DEMONSTRATION TEST.

4.1. PURPOSE.

The purpose of the test was to demonstrate the off-line Fault Detection and Location software developed for the AN/TPS-59(XN-1) EDM Radar. The demonstration was modified in accordance with Contract Modification P00028.

4.2. SCOPE.

In accordance with Contract Modification P00028, a test method that was mutually agreeable between NAVELEX and General Electric was developed. The test was divided into two parts. Part A tested the FL program that detects failures in the S/SPDC, ACU, FET, MTI, Input Distribution and Target Detection, Preprocessor/Waveform Generator, Final Receivers and the Exciter equipment. Part B tested those Loop Tests that supplement the portions of the FL program that were not completed.

4.3. TEST METHOD.

The test was conducted in accordance with the test procedure dated 6/9/76 (see Appendix Q). In Part A, a selected list of fault conditions were inserted into the system in a sequential manner, and the FL program was run. The FL message was compared with expected messages to verify proper operation. In Part B, failures were inserted in the array and monopulse equipment, and the appropriate Loop Test was run to verify that the failure had been correctly identified. Appendix R contains the data as recorded on the teletypewriter (TTY) for the test.

4.4. RESULTS.

Loading the FL program into the computer caused the following output to appear on the TTY:

SET JUMP SWITCH NO. 1 UP FOR POWER MODULE TEST OPTION DOWN FOR FAULT LOCATION FUNCTION

PRESS START SWITCH AFTER MAKING SELECTION

For this test, the Fault Location function was selected. After depressing the start switch, the following four-line message appeared on the TTY:

FAULT LOCATION OPTION
DEFINE DESIRED FREQUENCIES IN BITS 1 THRU 20 OF CMR 100

4-1

SET JUMP SWITCH 3 UP TO TERMINATE AFTER 64 FL CYCLES

SET JUMP SWITCH 2 UP TO FORCE -FL- INTO DIAGNOSTICS

Frequency F2 was selected and JUMP SWITCH 3 was set up in order to terminate after 64 cycles. The message FLSTOP then appeared on the TTY, indicating that no fault was detected in 64 cycles. Depressing the start switch caused the same four-line message to reappear.

At this point, the first fault was inserted in the system, (see Table 1, Appendix Q) and FL was started. The proper FL message was obtained (see Appendix R). The fault was removed and FL rerun with JUMP SWITCH 2 up to force FL into diagnostics. The message FL 000 indicated that the fault had cleared.

The next fifteen faults were inserted and the proper response obtained. One message, "NO FREQUENCIES SELECTED", is self-explanatory.

When the 17th fault was inserted, the reply was FL 357 instead of FL 357 AL. It was determined that for this particular fault, either message is correct. The program was rerun several times to demonstrate that either message can occur.

The 20th and 41st fault were incorrectly inserted (wrong pin). This was noted on the TTY data.

The faults listed in the procedure with a NOTE 1 required a software patch in order to simulate the fault. For these cases, the program had to be reloaded each time. After the proper response was obtained, the program was rerun with the patch removed to verify that the patch had indeed been properly removed. In the case of the 55th fault (FL 402), the patch had not been removed, thereby causing two consecutive FL 402 messages.

The last fault that was inserted was supposed to indicate that the low end of the frequency band was bad (FL 562). However, since only f2 was selected, and F2 fault was declared (FL 572). Enabling f2 and f3 resulted in f2 and f3 being declared bad (FL 572, FL 573). Then a frequency in the upper band was enabled, along with f2. Again, f2 reported bad (FL 572). Finally, the diagnostic logic was checked, and it

4-2

was found that all ten of the low frequencies have to be bad in order to get a Low Frequency band fault. Frequencies f1 through f10 were enabled, and the proper FL message was obtained.

The first and second tests of Part B check the status of the Σ and ΔAZ receivers and the transmitters. The data sheets are self-explanatory.

The third test simulates an off-boresight signal into the azimuth and elevation monopulse equipment. The test was run initially to establish the mean values of AZ and EL, and then a 6 dB attenuator was inserted first in the elevation channel and then in the azimuth channel. Proper operation was observed in each case.

The ability of this Loop D test to detect changes in phase was demonstrated in Test #4. Ninety degrees of phase was inserted first in the Σ channel and then in the ΔAZ channel. The proper response is indicated on the data sheets.

4.5. CONCLUSIONS.

All aspects of the FL system performed as expected.

5.0. POWER TEST.

In accordance with Contract Modification P00028, two years of AN/TPS-59(XN-1) operation utilizing standard Marine Corps engine generators are considered as a substitute for these tests and as an adequate demonstration that the AN/TPS-59(XN-1) meets the requirement that maximum power required to operate the system is less than 94.4 KW. Experience to date indicates satisfactory operation as achievable with standard power equipment.

6.0. SUPPLY LINE VOLTAGE AND FREQUENCY TESTS.

In accordance with Contract Modification P00028, two years of AN/TPX-59(XN-1) operation utilizing standard Marine Corps motor generators are considered as a substitute for these tests and as an adequate demonstration that the AN/TPS-59(XN-1) operates over the steady state range of voltage and frequency for which it was designed. Experience to date has shown that satisfactory operation is achievable with standard power equipment.

7.0. PRELIMINARY HEAT TEST.

7.1. PURPOSE.

The purpose of this test was to demonstrate that the AN/TPS-59(XN-1) could operate in the 50° C ± 5° environment with a selected portion of the array. The test was also run to determine how long the shelter equipment could run on just one air conditioner.

7.2. SCOPE.

In accordance with Contract Modification P00028, the test consisted of sealing off four rows of the array which was operational, making periodic temperature measurements and reviewing equipment status. The shelter equipment was operated at the same time with one of the two A/Cs off in each shelter. Periodic temperature measurements were made and equipment status was monitored.

7.3. TEST METHOD.

The heat test was conducted in accordance with contract modification P00028. The heat test was performed on a selected summer day to satisfy the requirements of the preliminary heat test. It was conducted on each of the shelters with one air conditioner off, and on the array by sealing off four complete rows. A copy of the Test Procedure along with the data sheets is included in Appendix S.

7.4. RESULTS.

7.4.1. Shelter Equipment.

The heat test was conducted on a clear sunny day. Temperatures measured in the shade were 20.5°C at beginning and 27.3°C maximum in the afternoon. Winds were 0 to 8 mph in the morning and 10 to 20 mph in the afternoon. The temperature measured with a thermometer in the sun on top of shelter at 1330 was 48°C.

The Signal Processor Shelter had the room aid conditioner (A/C) shut off, and the remaining A/C was used to cool Unit 7 (Signal Processor) with the cabinet doors closed. The vent fans were used to remove the heat from the room and remaining equipment. The shelter door was closed.

7-1

The Radar Control Shelter also had the room A/C shut off. The remaining A/C cools the Radar Control Console and provides some cooling to the room. Vent fans could not be turned on in this shelter because of their close proximity to the A/C input.

Both shelter doors were closed. Thermometers were located as shown in Figure 7-1. The average temperatures for the Signal Processor Shelter went from 30°C to 34°C and 32.3°C to 39°C for the Radar Control Shelter. The external ambient went from 22°C to 27°C. Detailed readings are shown in Table 7-1.

Temperature indicators were mounted on specific components and assemblies. The location and the temperatures are as shown below and in Figure 7-2. The only apparent over temperature problem was as indicated on the console power supply.

Shelter Temperature Sensor Readings (Summary)

8A8A6	Greater than 40.6°C Less than 49°C
8A8A10	Greater than 49°C Less than 60°C
8A13PS1 +5V	71°C
7A1A1A416	Less than 40.6°C
7A3A1A412	Less than 40.6°C
7PS3	Greater than 60°C Less than 71°C
6A3A4	Greater than 49°C Less than 60°C

The performance of the shelter equipment was monitored by measuring the signal processor outputs in both long range and short range modes. The results are shown below at the beginning and the end of the heat test.

Processor Response

	Limits	Beginning of Test	End of Test
LR-LFM	145 Min	200	190
SR-SP	47 Min	102	96
SR-LFM	47 Min	78	69
MTI-LFM	13 Max	3	11

7-2

SIGNAL PROCESSOR

SHELTER
● 1

● 2

WALL
THERM. }

WALL THERM.

● 3

PIZZA HUT

● 7

● 4

● 8

RADAR CONTROL SHELTER

● 5

THERMOMETERS
1. ON BENCH
2. 12" FROM CEILING
3. PIZZA HUT
4. NEXT TO 1538
5. OVER CONSOLE
6. UNDER TRAILER
7. WALL OF PIZZA HUT
8. OUTSIDE OF PIZZA HUT, IN SHADE
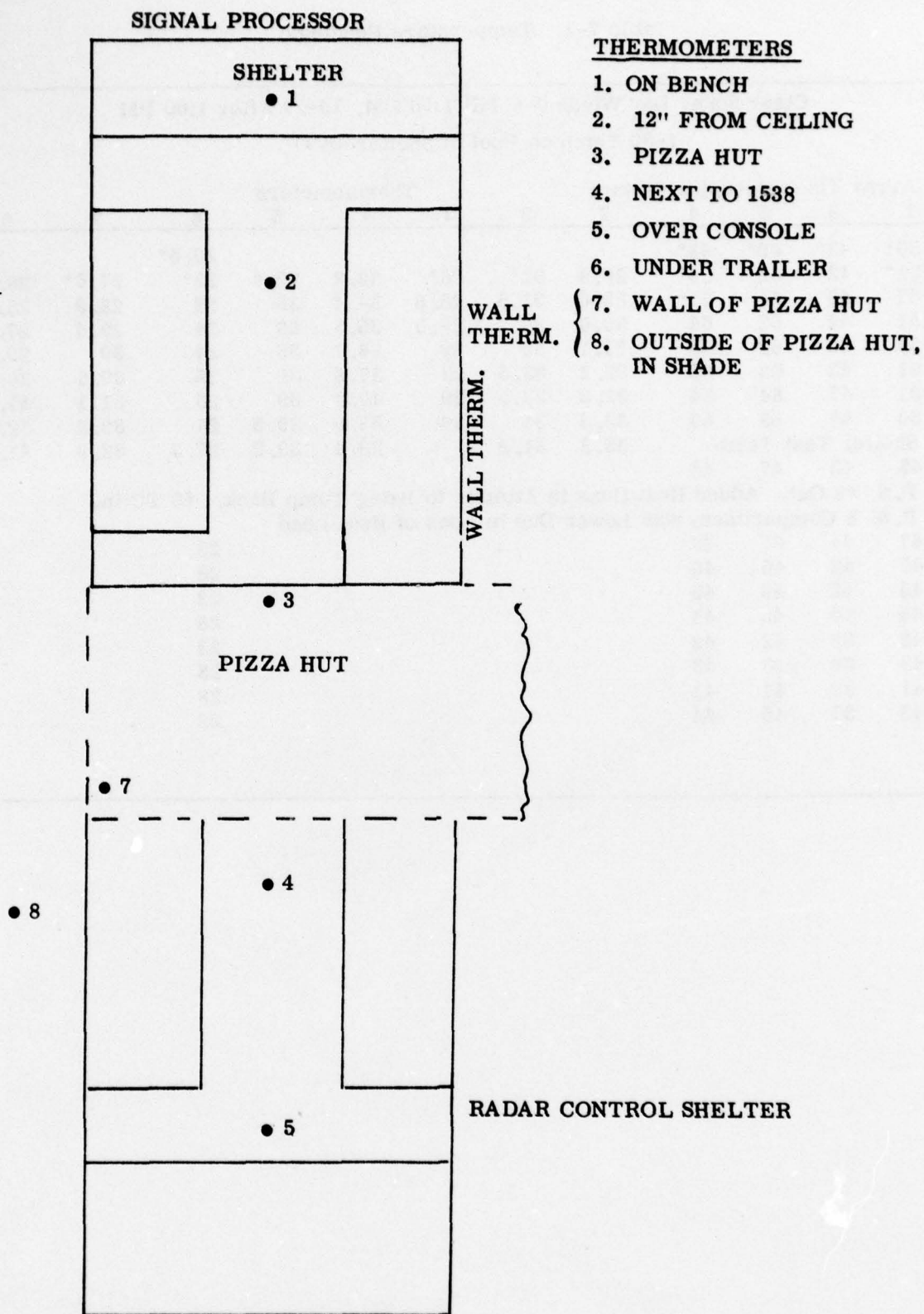
Figure 7-1. Thermometer Locations

7-3

Table 7-1. Temperature Readings

	Clear Sunny Day Winds 0-8 Till 1:00 PM, 10-20 After 1:00 PM											
	1:30 Temp on Roof of Shelter 48°C											
Time	Array Thermocouples (Temp)				Thermometers							
	1	2	3	4	1	2	3	4	5	6	7	8
0930	50°	43°	62°	63°						20.5°		
1000	51°	42°	62°	65°	28.9	31°	26°	32.2	32.4	22°	27.0°	26.7
1030	52	40	64	67°	30.0	31.5	26.5	34.4	35	22	28.9	26.7
1100	51	44	62	64	30.6	32	27.5	35.5	36	24	29.4	27.8
1130	53	40	62	63	31.1	33	29	36.1	36	24	30	29.4
1200	51	42	62	65	32.2	33.5	29	37.8	38	25	30.6	30.6
1230	51	47	64	64	32.2	33.5	29	40.6	39	26	31.1	31.1
1300	50	47	53	50	33.3	34	30	38.9	39.5	27	32.2	32.2
1320	Shelter Test Term				33.3	34.5		38.4	39.2	27.3	32.8	31.7
1330	45	43	47	45								
P.S. #8 Out. Added Heat Guns in Attempt to Bring Temp Back. #2 TC in.												
P.S. 8 Compartment was Lower Due to Loss of Heat Load												
1400	47	44	47	46						28		
1430	47	42	46	46						28		
1500	45	42	45	45						28		
1530	45	40	45	44						28		
1600	42	38	42	42						28		
1650	43	38	43	43						28		
1700	41	38	41	41						28		
1750	45	37	45	44						28		

+5 VOLT P.S.
(8A13 PS1)

Power Supply Regulator   PWB
(8A8A6)

Arithmetic Unit, PWB
(7A3A1A412)

+5V Power Supply
(7PS3)
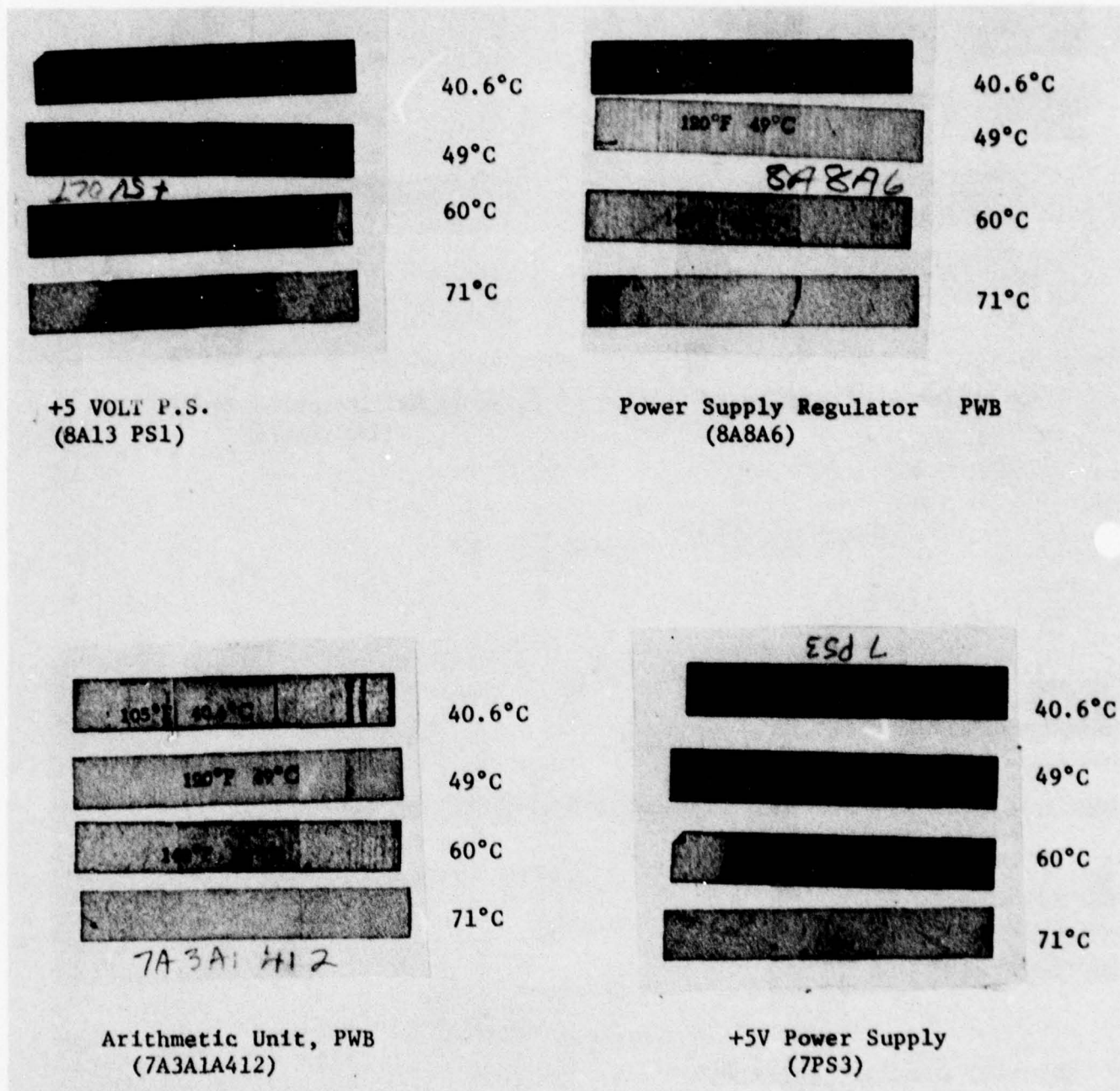
Figure 7-2. Shelter Temperature Sensor Readings (Sheet 1 of 2)

Amplifier - Filter Board
(6A3A4)
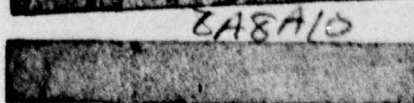
Arithmetic Unit, PWB
(7A1A1A416)

Digital Display Indicator
(8A9A10)

Figure 7-2. Shelter Temperature Sensor Readings (Sheet 2 of 2)

where

LR-LFM	=	Processor Output in Long Range Mode
SR-SP	=	Processor Output in Short Range Simple Pulse Mode
SR-LFM	=	Processor Output in Short Range Linear Frequency Modulation Mode
MTI-LFM	=	MTI Output in Linear Frequency Modulation Mode

As seen from this data, none of the processor outputs fell outside the specified limits at the end of the heat run.

7.4.2. Four Sealed Rows on Array.

The array temperature test was performed on four rows which were enclosed with plastic and insulating materials. This is shown in the photos in Figure 7-3. The location of the thermocouples were:

#1   Transmitter/Receiver Compartment   Compartments connected through
#2   Power Supply Compartment   Row Board Spacing at front
#3   P.S. #8, center of heat sink
#4   Transmitter/Receiver #8, heat sink,
       center of AR1-AR8

The test commenced when the average of locations #1 and #2 reached 50 ± 5°C (see Table 7-1). The lower readings of #2 were attributed to being near a crack where the wind affected the thermocouple. This was subsequently sealed. After P.S. #8 failed, it was difficult to maintain the desired ambient. The loss of heat load in conjunction with an increased wind velocity made this impossible even with two heat guns which were used all afternoon.

The array performance was monitored by measuring the transmitter, sum receiver, and delta azimuth receiver outputs. The results are shown below at the beginning and the end of the heat test.

Transmitter Output

Row	Limit	Beginning of Test	End of Test
7	3.5	12.69	7.08
8	6.5	13.99	0.32
9	4.3	14.82	11.95
10	10.0	16.97	14.40

7-8
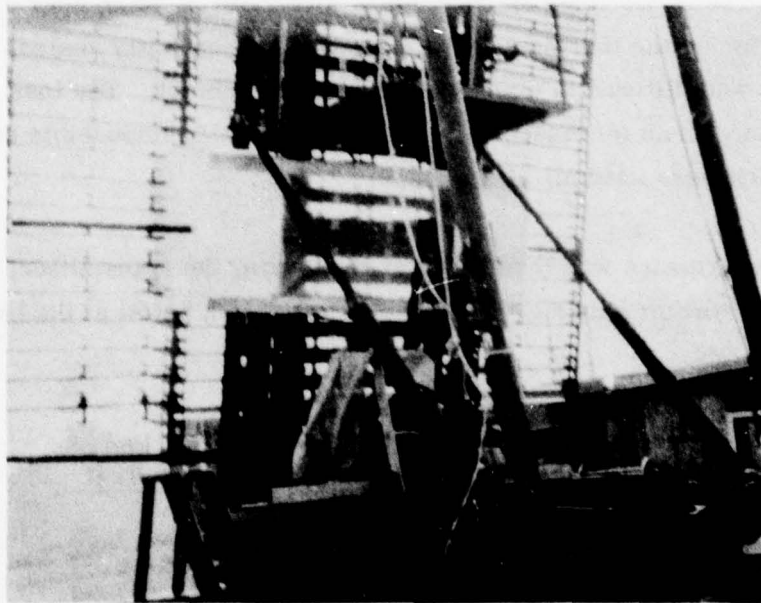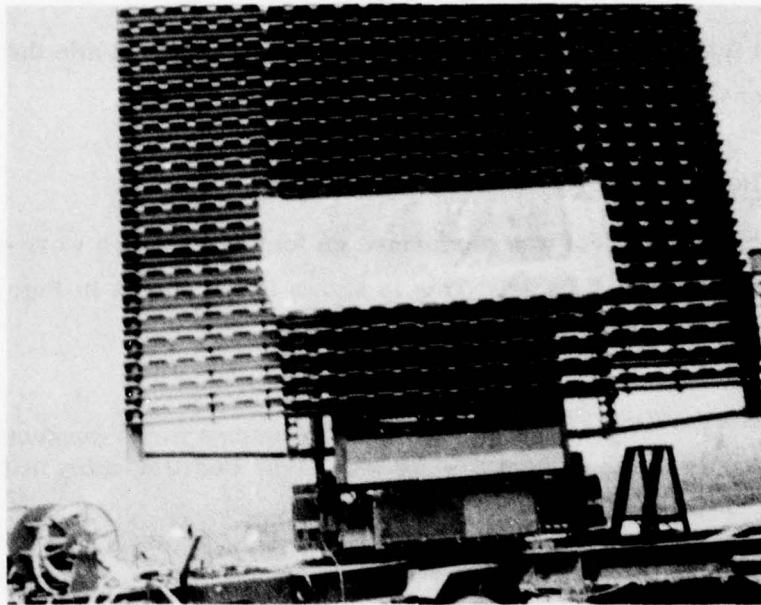
Figure 7-3.   Four Row Temperature Enclosure

7-8

Sum Receiver Output

Row	Limit	Beginning of Test	End of Test
7	6	19	18
8	6	17	15
9	6	20	19
10	6	24	20

Delta Azimuth Receiver Output

Row	Limit	Beginning of Test	End of Test
7	6	19	14
8	6	12	14
9	6	23	13
10	6	21	12

As can be seen from the results, Row 8 transmitter output was the only measurement below the specified limits at the conclusion of the heat test. Further tests indicated that the row power supply (serial number 45) feeding Row 8 had failed.

Power Supply Serial No. 45 failed due to a shorted HIC inverter driver module. The module failed due to a poor thermal path to the heat sink. When the module was built inearly 1974, a poor solder bond was made between the module substrate and its moly carrier. In fact, only 50% of the substrate was in a good thermal contact to the moly carrier. The excess heat during the heat test was sufficient to overheat the transistors, resulting in a catastrophic failure.

7.4.3. Performance Monitoring.

The Performance Monitoring Program was active continuously during the test period and is described in the test procedure. Performance data that was collected every hour is included in Appendix S.

7.5. CONCLUSIONS.

Shelter Equipment - All shelter equipment operated satisfactorily for 3.5 hours with only one air conditioner on before a fault occurred. The performance monitoring program was active continuously and after 3.5 hours, the over-temperature light came on. The PM message indicated a problem in the Radar Control Console. This turned out to be a power supply over heating. The power supply did not fail. Since the test was being performed for information only related to operation with one air conditioner, the shelter temperature test was terminated.

Array Electronics Temperature Test - Four rows of electronics operated satisfactorily for 4 to 4.5 hours in a sealed temperature environment. A fault indicated on the E-15 program (run each hour) was verified to be a Row 8 power supply failure. Subsequent failure analysis on the supply showed a failed HIC inverter.

The test was continued for a total of eight hours. All four row receivers operated satisfactorily throughout the test along with the remaining three transmitters. Row 8 transmitter operated satisfactorily when attached to a new power supply.

7.6. RECOMMENDATIONS.

1) Temporary baffeling was added after the test to the radar control console for more efficient use of the cooling air. These changes will be implemented during preship and should preclude a similar fault in the console P.S. area.

2) Additional testing should be accomplished to determine temperature effects of:

   a) Leave room air conditioner on and console air conditioner off in conjunction with vent fans on.

   b) Disconnect the fan at the air conditioner input side, go to vent with remianing fan, and run with console air conditioner on.

   c) Repeat previous test reported herein with final changes (1) implemented.

3) The power supply fault appeared to be temperature related. However, the failure analysis indicated a HIC inverter process problem.

8.0. ENCLOSURE TEST.

In accordance with Contract Modification P00028, eighteen months exposure of the AN/TPS-59(XN-1) equipment to the Central New York area environment are considered as a substitute for this test and as an adequate demonstration that the AN/TPS-59(XN-1) meets the requirement to withstand any practical set of weather conditions including gale rainstorms. It has withstood conditions which exceeds those required by the Enclosure Test by a factor of 2.

9.0. ASSEMBLY/DISASSEMBLY.

In accordance with Contract Modification P00028, assembly and disassembly procedures that have been developed and demonstrated in this and prior phases of the contract shall be considered as an adequate demonstration that the AN/TPS-59(XN-1) meets the requirement for the ability to be assembled and disassembled. An actual time-trail demonstration of assembly and disassembly is deferred to a future phase of the contract (USMC DT/IOT&E Tests).

10.0. WEIGHTS AND DIMENSIONS.

10.1. PURPOSE.

The purpose of this test was to demonstrate that the AN/TPS-59(XN-1) Radar Set meets the requirements for total system transport weight, individual package transport weights, and size of each transport package.

10.2. SCOPE.

The test consisted of weighing and measuring each transport package, and calculating the system weight.

10.3. TEST METHOD.

The test was conducted in accordance with Section 4.9.7 of the Pre-Service Acceptance Test Procedure except as modified for the tests to be performed at the Verona Test Site. The weighings and measurements were performed as part of the move from Verona to Griffiss AFB. As a result, only an uncalibrated commercial sling scale (dynometer) was available. The reported accuracy from the scale rental vendor was ±2%. The accuracy of reading the scale was ±1%.

The center of gravity for each of the packages was determined from weighing and calculations.

10.4. RESULTS.

Results are shown on the data sheets reflected in Figures 10-1 through 10-6. There are no specific dimensions specified in ELEX-R50 but the following criteria has been met. The shelters are a basic S-280 and must be transportable in an M-35 truck. This has been demonstrated on each move the equipment has made. The trailers were designed to be towed by an M-35 truck and meet the ICC requirements of 96" maximum width and less than 35' long. This has been demonstrated. The maximum height requirement resulted from the air transport limitations of 108". This also had been demonstrated on the move from Rome, New York to California.

SLING WEIGHT 200 lbs.

1. Radar Control Shelter Gross Weight   5900 lbs.

    Deduct Sling Weight   200 lbs.

    Radar Control Shelter Transport Package Wgt. 5700 lbs. (5000 lbs. max.)

        Computer Set Weight   1325 lbs.

        TAOC Cables & Reels   220 lbs.

        TAOC Junction Box   155 lbs.

            Total Excludable Weight   1700 lbs.

    Radar Control Shelter System Weight   4200 lbs.

2. Signal Processor Shelter Gross Weight   5800 lbs.

    Deduct Sling Weight   200 lbs.

    Signal Processor Shelter Transport Pkg. Wgt. 5600 lbs. (5000 lbs. max.)

        TAOC Cables & Reels   420 lbs.

    * Shelter Cables & Cases   1087 lbs.

            Total Excludable Weight   1507 lbs.

    Signal Processor Shelter System Weight   4093 lbs.

    * Now Includes: 2 25' Lengths of Intergenerator CBLS
                 8 A/C Ducts
                 8 A/C Cables
                 5 Slings
                 8 Shelter Truck Tie Down Turn Buckle Assmys.

Figure 10-1.   Weight Data Sheet AN/TPS-59(XN-1) Radar Transport Condition
(Sheet 1 of 3)

3. Trailer A Gross Weight   7500 lbs.

                                              Pounds

        Sling Weight   200

        Net Transport Weight   7300

        Maximum Allowable Weight   5000 lbs

4. Trailer B Lower Gross Weight   7250 lbs.

                                              Pounds

        Sling Weight   200

        Net Transport Weight   7050

        Maximum Allowable Weight   5000 lbs

5. Trailer B Upper Gross Weight   6850 lbs.

                                              Pounds

        Sling Weight   200

        Net Transport Weight   6650

    GFE Equipment Separately Crated

    Generator Set

        PU-711/G (Quantity 3) Crated Weight 13,020 lbs.

    Air Conditioner

        MAC 4V - 20 (Quantity 4) Crated Weight 1,980 lbs.

Figure 10-1. Weight Data Sheet AN/TPS-59(XN-1) Radar Transport Condition
(Sheet 2 of 3)

AN/TPS-59 Radar System Weight General Electric Only

1. Radar Control Shelter System Weight   4200

2. Signal Process or Shelter System Weight   4093

3. Trailer A Net Weight   7300

4. Trailer B (Lower) Net Weight   7050

5. Trailer B (Upper) Net Weight   6650

        TOTAL SYSTEM WEIGHT   29,293 lbs.

Maximum Allowable System Weight   20,000 lbs.

Figure 10-1. Weight Data Sheet AN/TPS-59(XN-1) Radar Transport Condition
(Sheet 3 of 3)

10-4

Height

	Measured	Maximum
Left Front	83	108"
Left Rear	83	108"
Right Front	83	108"
Right Rear	83	108"

Length

	Measured	Maximum
Left Top	147	None
Left Bottom	147	None
Right Top	147	None
Right Bottom	147	None

Width

	Measured	Maximum
Front Top	87	89"
Front Bottom	87	89"
Rear Top	87	89"
Rear Bottom	87	89"

Tested by _L. E. Best_ Date _8-10-76_

Verified _____ Date _____

Figure 10-2. Radar Control Shelter Data Sheet

10-5

HEIGHT

	Measured	Maximum
Left Front	83	108"
Left Rear	83	108"
Right Front	83	108"
Right Rear	83	108"

Length

	Measured	Maximum
Left Top	147	none
Left Bottom	147	none
Right Top	147	none
Right Bottom	147	none

Width

	Measured	Maximum
Front Top	87	96"
Front Bottom	87	96"
Rear Top	87	96"
Rear Bottom	87	96"

Tested by _L E Bell_ Date _8-10-76_

Figure 10-3. Signal Processor Shelter Data Sheet

	Measured	Limit
Trailer A		
Length	207	240" max.
Width (front)	96	96" max.
(center)	96	96" max.
(rear)	96	96" max.
Height left side	68	108" max.
Height right side	68	108" max.
Trailer B Lower		
Length	240	240" max.
Width (front)	96	96" max.
(center)	96	96" max.
(rear)	96	96" max.
Height left side	78	108" max.
Height right side	78	108" max.
Trailer B Upper		
Length	240	240" max.
Width (front)	96	96" max.
(center)	96	96" max.
(rear)	96	96" max.
Height left side	78	108" max.
Height right side	78	108" max.

DATE _8/10/76_   *H. K. Gardner*

Figure 10-4. Trailer Data Sheet

10-7

W = 87   W = 87

```
     .52W⌐ .48W                    .49W⌐ .51W
    ┌─────┬──────┐                ┌─────┬──────┐
    │  ●= 46"│    │                │  ●= 43"│    │
.51L│     │      │            .52L│     │      │
    │     │      │                │     │      │
L = 147├ ─ ─ ●─ ─ ─ ─          ├ ─ ─ ●─ ─ ─ ─
    │     │      │                │     │      │
    │     │      │                │     │      │
H = 83.49L│ = 72"│                .48L│ = 71"│
    └─────┴──────┘                └─────┴──────┘
```

SHELTER 2   SHELTER 3

SIGNAL PROCESSOR   RADAR CONTROL
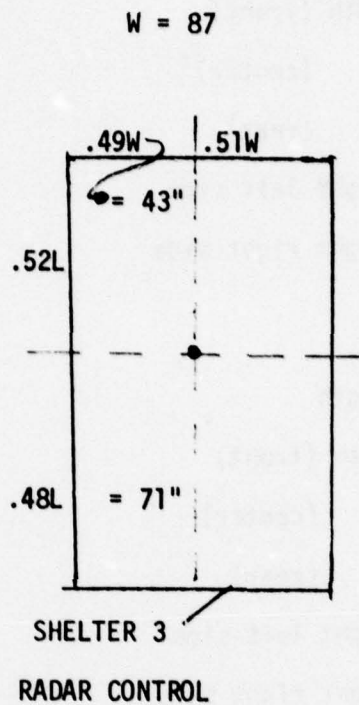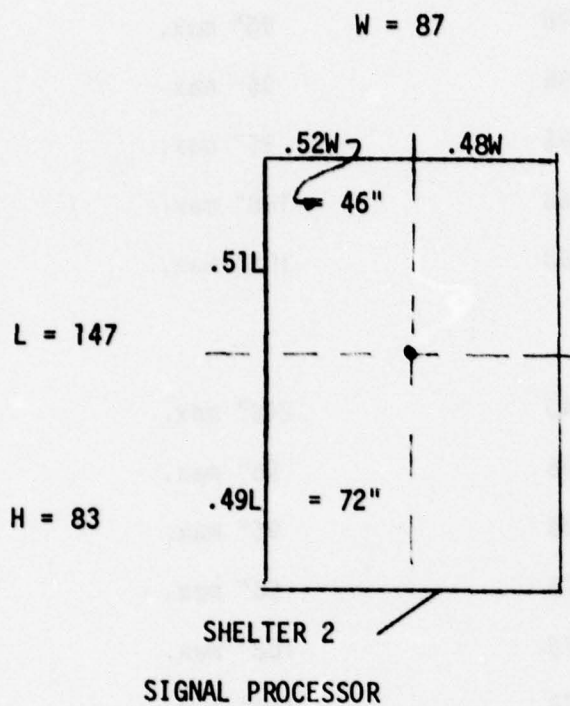
CG of H =   .33 (83) = 28

Figure 10-5.   AN/TPS-59 Shelter CG's and Dimensions
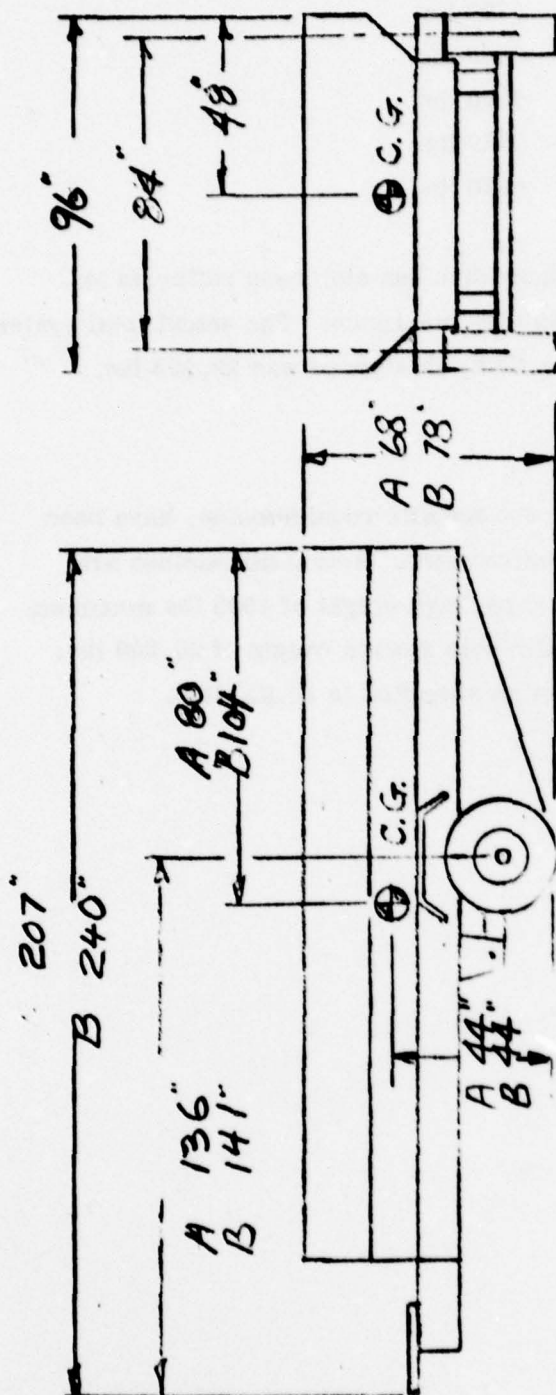
10-8

	TRAILER A	TRAILER B LOWER	TRAILER B UPPER
TOTAL	7300	7050	6650
LUNETTE	400	400	300
WHEELS	6900	6750	6350

Figure 10-6. AN/TPS-59(XN-1) Trailer CG's and Dimensions

Weight measurements show that each of the transport packages (with GFE) exceed the ELEX-R50 requirement of 5000 pounds maximum.

Radar Control Shelter	5700 lbs
Signal Processor Shelter	5800 lbs
Trailer A	7300 lbs
Trailer B lower	7959 lbs
Trailer B upper	6650 lbs

The result of the growth in transport package size has also been reflected in exceeding the allowable system weight of 20,000 lbs maximum. The actual total system weight of the General Electric Equipment (less GFE) as shipped was 29,293 lbs.

10.5. CONCLUSIONS.

The dimensional measurements, although not specific requirements, have been demonstrated satisfactorily in the transport environment. Actual dimensions are shown in Figures 10-5 and 10-6. The transport package weight of 5000 lbs maximum was exceeded on all packages along with the allowable system weight of 20,000 lbs; therefore, the equipment does not meet weights as specified in ELEX-R50.

11.0. PRELIMINARY ROAD TEST.

In accordance with Contract Modification P00028, satisfactory transport of the AN/TPS-59(XN-1) without damage on primary, secondary, and lesser roads for a distance in excess of 100 miles using military tow vehicles is considered as a substitute for this test and as an adequate demonstration that the AN/TPS-59(XN-1) meets the requirement for undamaged transport on similar roads.

12.0. RF ANTENNA MEASUREMENTS.

12.1. PURPOSE.

RF Antenna measurements tests were conducted as part of the Pre-Service Acceptance Test Procedures to verify the radiation patterns of the AN/TPS-59(XN-1) Radar Set.

12.2. SCOPE.

All tests were made at the HMED Antenna Test Site near Cazenovia, New York using standard antenna pattern recording techniques to determine antenna sidelobe levels, beam widths, and angular sensitivity factors. The AN/TPS-59(XN-1) shall have passed this test if the requirements specified in paragraph 4.11 of the Pre-Service Acceptance Test Procedure are satisfied.

12.3. TEST METHOD.

The tests were conducted in accordance with paragraph 4.11 of the Pre-Service Acceptance Test Procedures. A detailed test procedure for receive patterns is given in Appendix T, and for transmit patterns in Appendix U.

12.4. RESULTS.

12.4.1. Introduction.

This paragraph describes the antenna pattern measurement results for the tests made at the HMED Antenna Test Site near Cazenovia, New York. All of the receive pattern measurements are reproduced in Figure 12-1 and all of the transmit pattern measurements are reproduced in Figure 12-2. At the beginning (sheet 1) of each figure is an index listing each antenna pattern by number and a description of the type of each pattern. In these figures, the array tilt angle (θ_T) is the angle of the array face with respect to vertical. It should be noted that angle scale for all the antenna patterns in Figures 12-1 and 12-2 is 1/3 degree per small division. Also, in these figures, the following frequency designation is used:

F1 = 1222.32 MHz
F2 = 1231.28 MHz
F8 = 1285.04 MHz
F15 = 1347.76 MHz

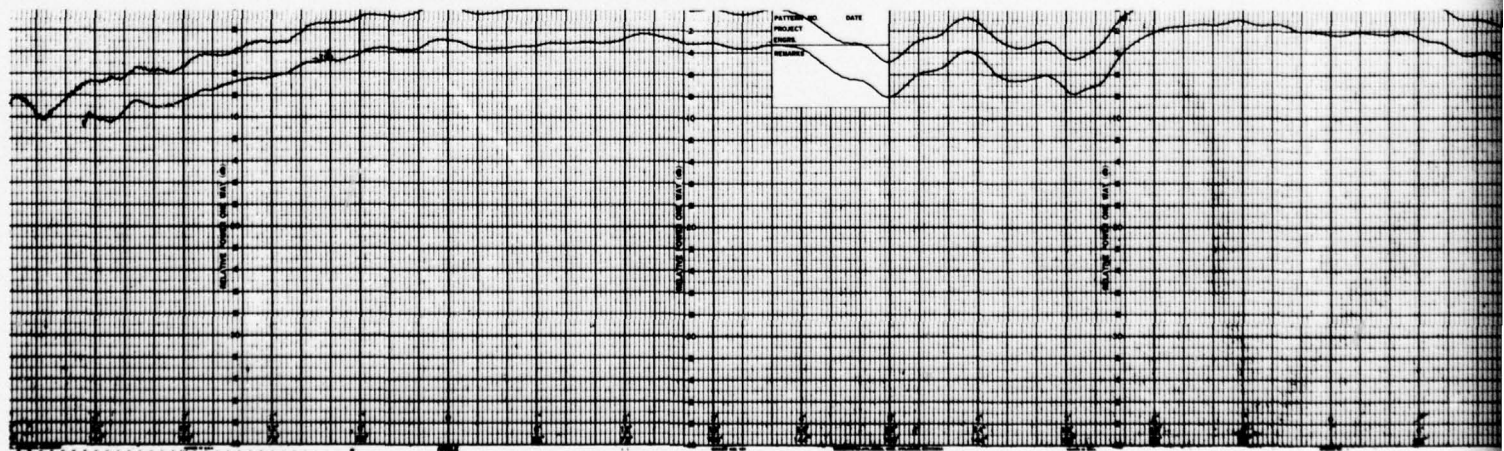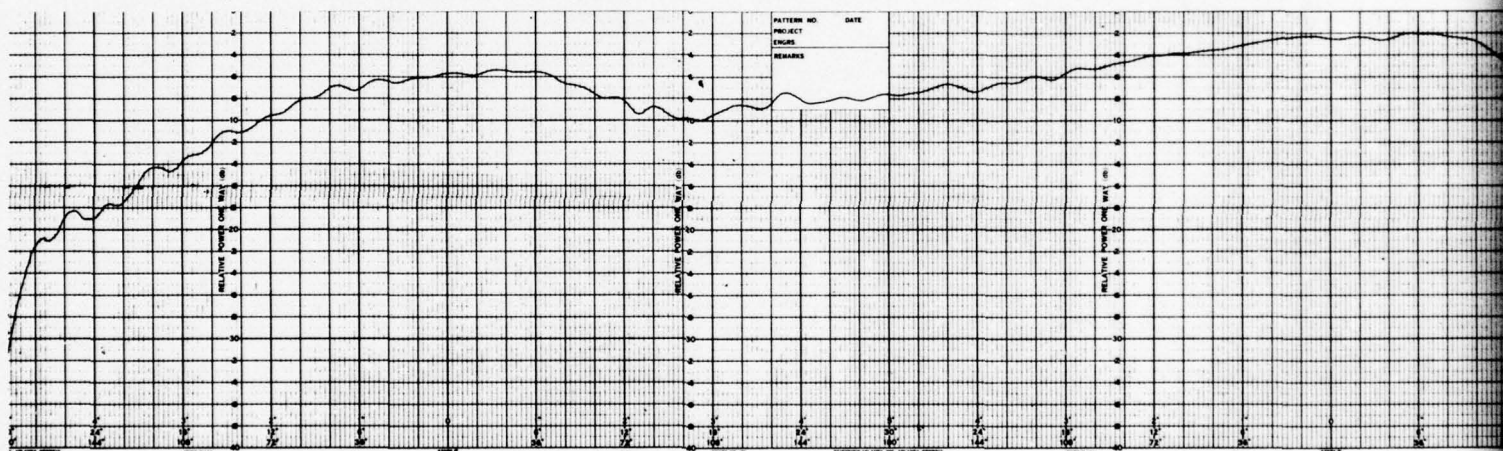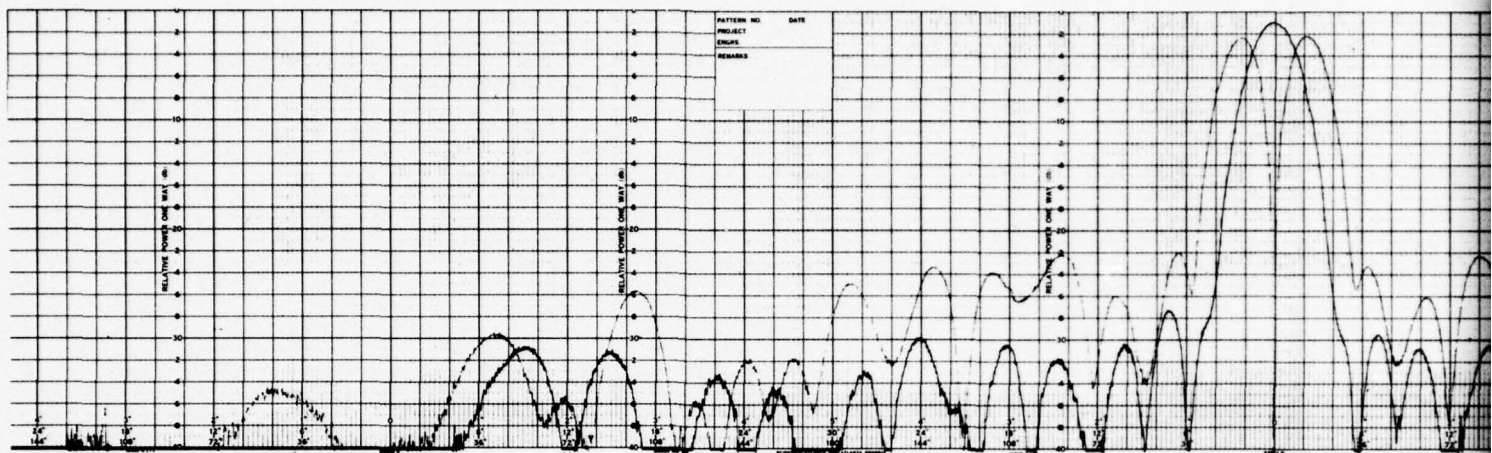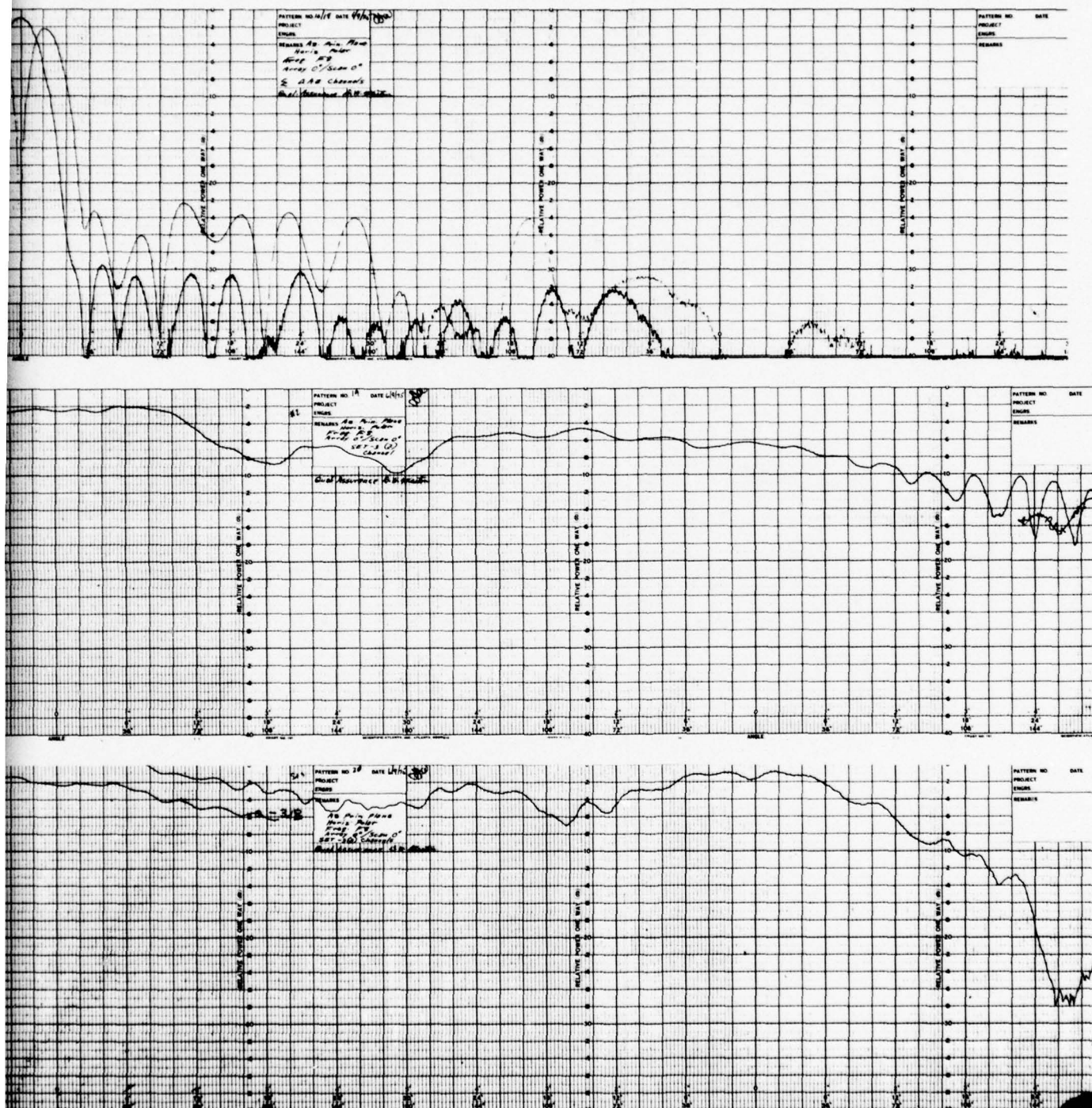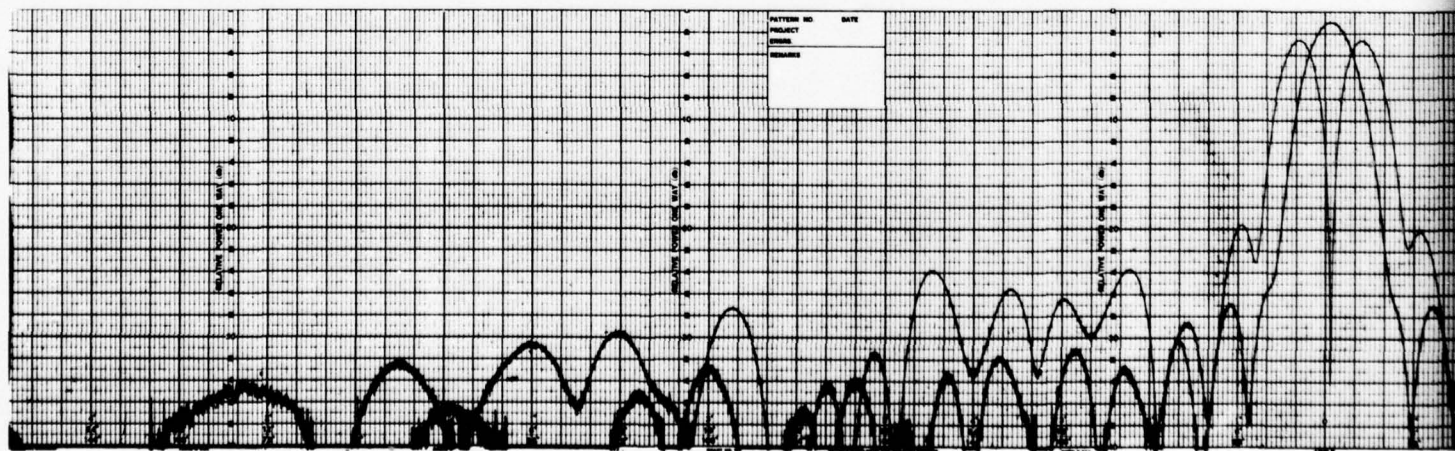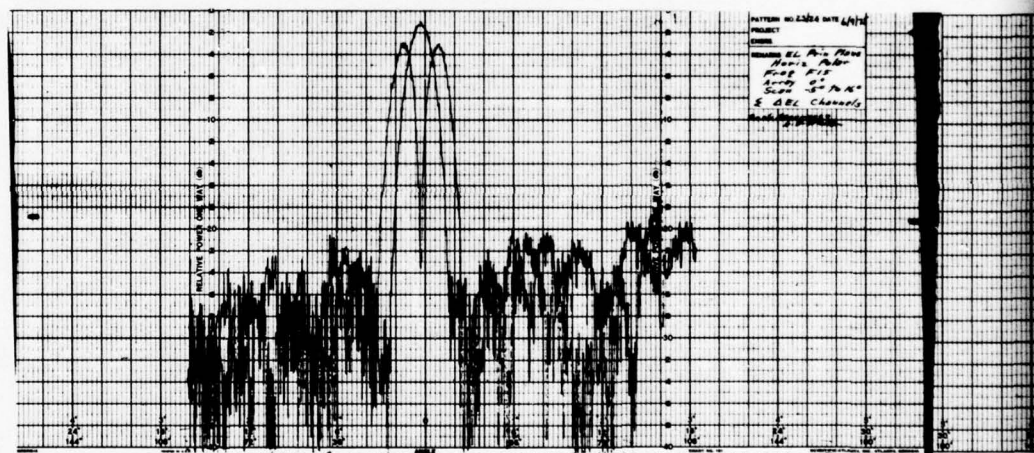| Pattern Number	Beam Type	Frequency	Polarization	Array Tilt Angle (θ_T)	Scan Angle Relative to Broadside	Pattern Type
1	Normal Sum	F1	Horizontal	0°	−5 to +16°	Elevation Principal Plane (Dynamic)
2	Elevation Difference	F1	Horizontal	0°	−5 to +16°	Elevation Principal Plane (Dynamic)
3	Broaden Sum (1.5:1)	F1	Horizontal	0°	−5 to +16°	Elevation Principal Plane (Dynamic)
4	Broaden Elevation Difference (1.5:1)	F1	Horizontal	0°	−5 to +16°	Elevation Principal Plane (Dynamic)
5	Normal Sum	F1	Horizontal	0°	0°	Azimuth Principal Plane (Static)
6	Azimuth Difference	F1	Horizontal	0°	0°	Azimuth Principal Plane (Static)
7	Normal Sum	F1	Vertical	0°	0°	Azimuth Principal Plane (Static)
8	Azimuth Difference	F1	Vertical	0°	0°	Azimuth Principal Plane (Static)
9	Normal Sum	F8	Horizontal	0°	−5 to +16°	Elevation Principal Plane (Dynamic)
10	Elevation Difference	F8	Horizontal	0°	−5 to +16°	Elevation Principal Plane (Dynamic)
11	Broaded Sum (1.5:1)	F8	Horizontal	0°	−5 to +16°	Elevation Principal Plane (Dynamic)
12	Broaden Elevation Difference (1.5:1)	F8	Horizontal	0°	−5 to +16°	Elevation Principal Plane (Dynamic)
13	Weather Beam I	F8	Horizontal	0°	−5 to +16°	Elevation Principal Plane (Dynamic)

Figure 12-1. Receive Antenna Patterns (Sheet 1 of 21)

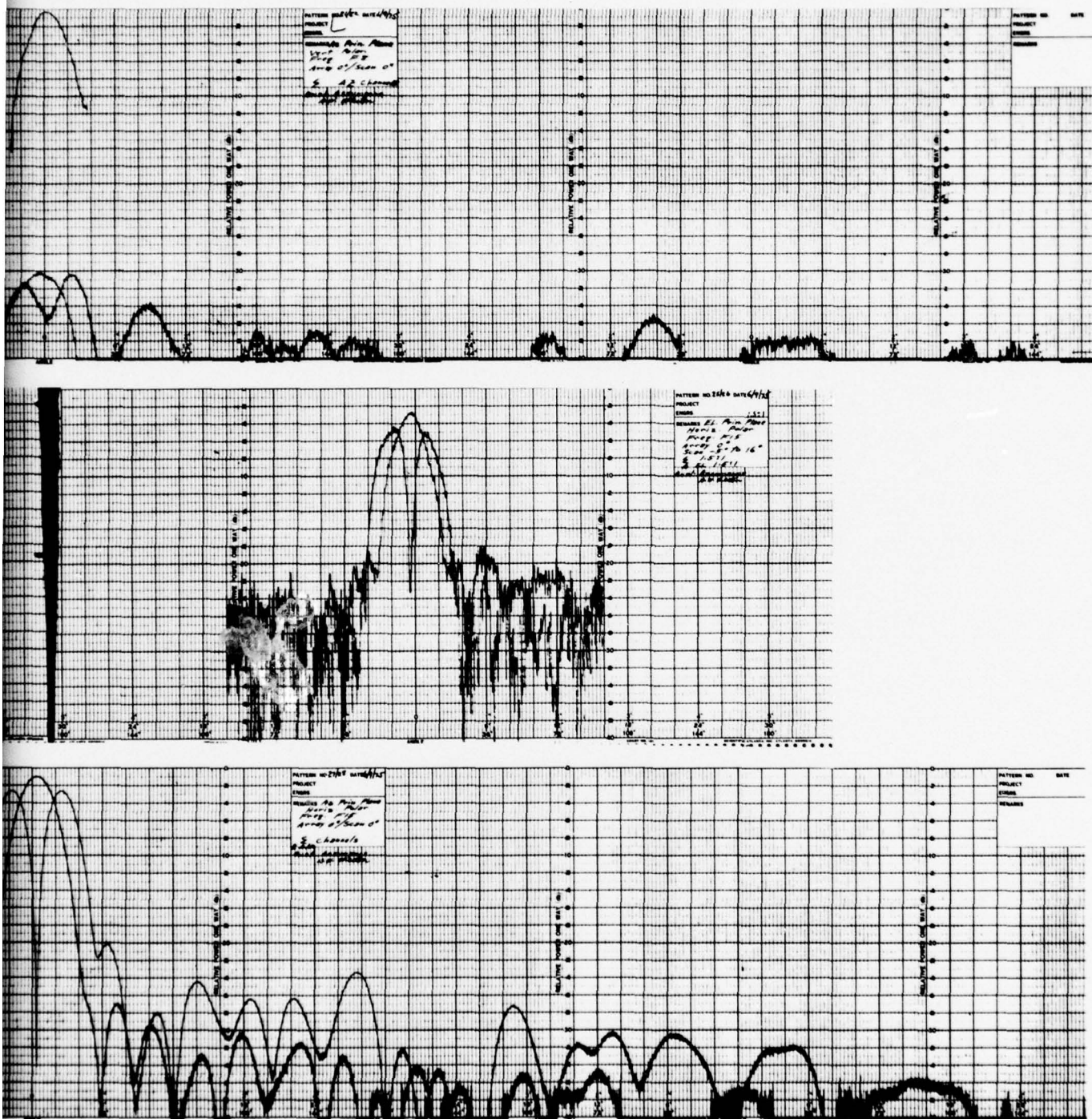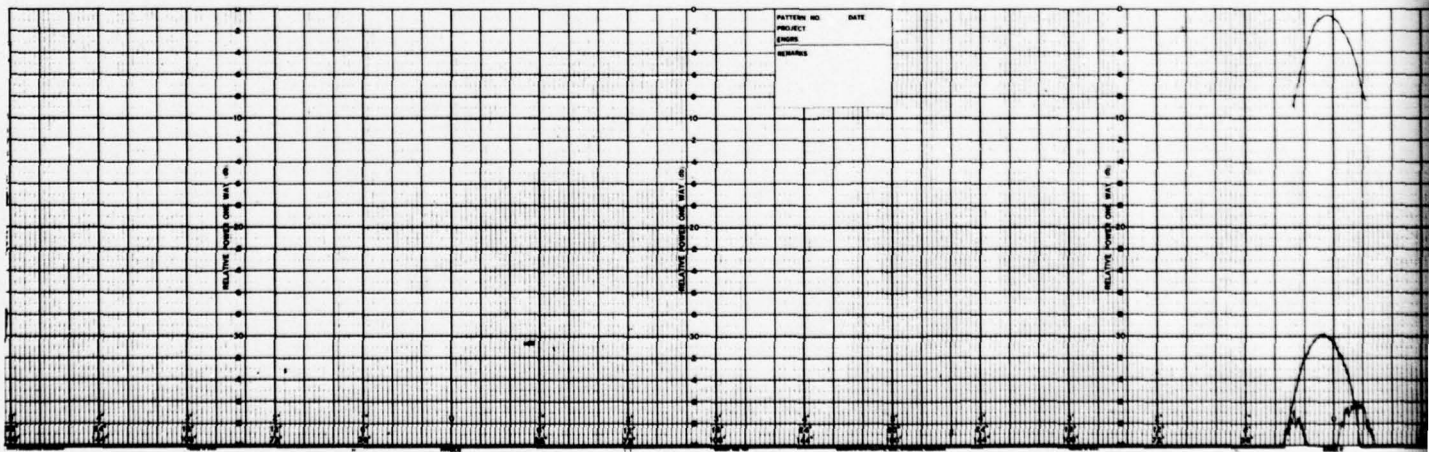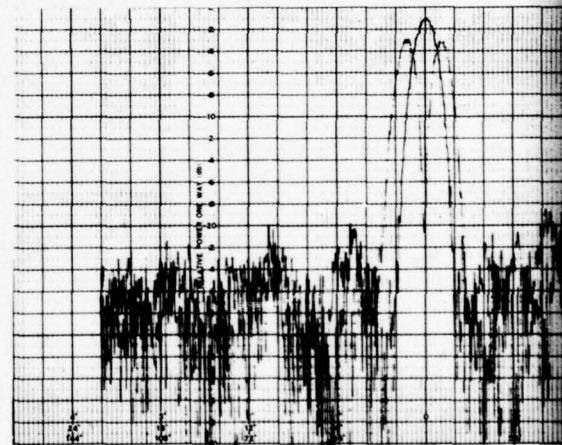| Number	Type	Frequency	Polarization	Array Tilt Angle (θ_T)	Scan Angle Relative to Broadside	Pattern Type
14	Weather Beam II	F8	Horizontal	0°	−5 to +16°	Elevation Principal Plane (Dynamic)
15	Cosecant Beam	F8	Horizontal	0°	−5 to +16°	Elevation Principal Plane (Dynamic)
16	Normal Sum	F8	Horizontal	0°	0°	Azimuth Principal Plane (Static)
17	Set-3 Serial No. 1	F8	Horizontal	0°	0°	Azimuth Principal Plane (Static)
18	Azimuth Difference	F8	Horizontal	0°	0°	Azimuth Principal Plane (Static)
19	Set-3 Serial No. 2	F8	Horizontal	0°	0°	Azimuth Principal Plane (Static)
20	Set-3 Serial No. 3	F8	Horizontal	0°	0°	Azimuth Principal Plane (Static)
21	Normal Sum	F8	Vertical	0°	0°	Azimuth Principal Plane (Static)
22	Azimuth Difference	F8	Vertical	0°	0°	Azimuth Principal Plane (Static)
23	Normal Sum	F15	Horizontal	0°	−5 to +16°	Elevation Principal Plane (Dynamic)
24	Elevation Difference	F15	Horizontal	0°	−5 to +16°	Elevation Principal Plane (Dynamic)
25	Broaden Sum (1.5:1)	F15	Horizontal	0°	−5 to +16°	Elevation Principal Plane (Dynamic)
26	Broaden Elevation Difference (1.5:1)	F15	Horizontal	0°	−5 to +16°	Elevation Principal Plane (Dynamic)
27	Normal Sum	F15	Horizontal	0°	0°	Azimuth Principal Plane (Static)

Figure 12-1. Receive Antenna Patterns (Sheet 2 of 21)

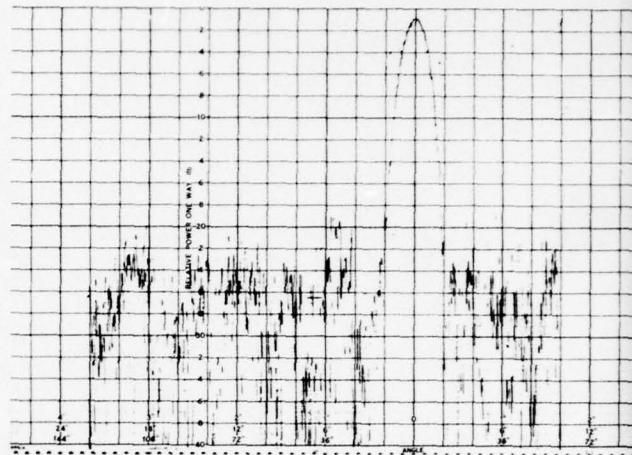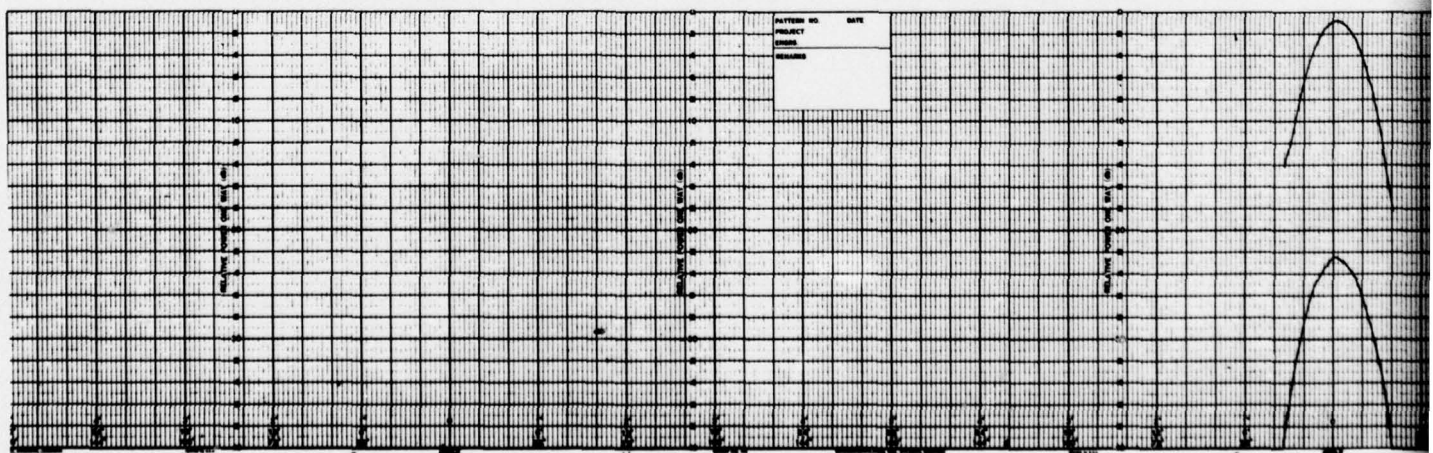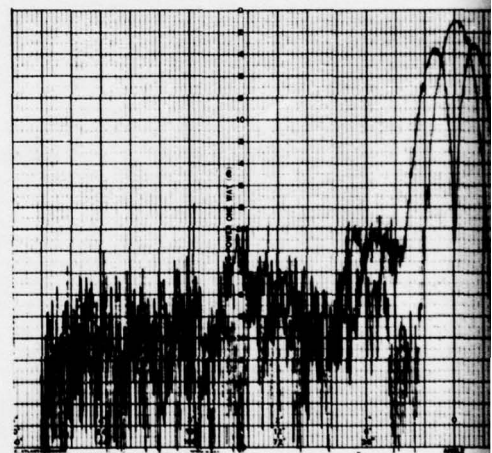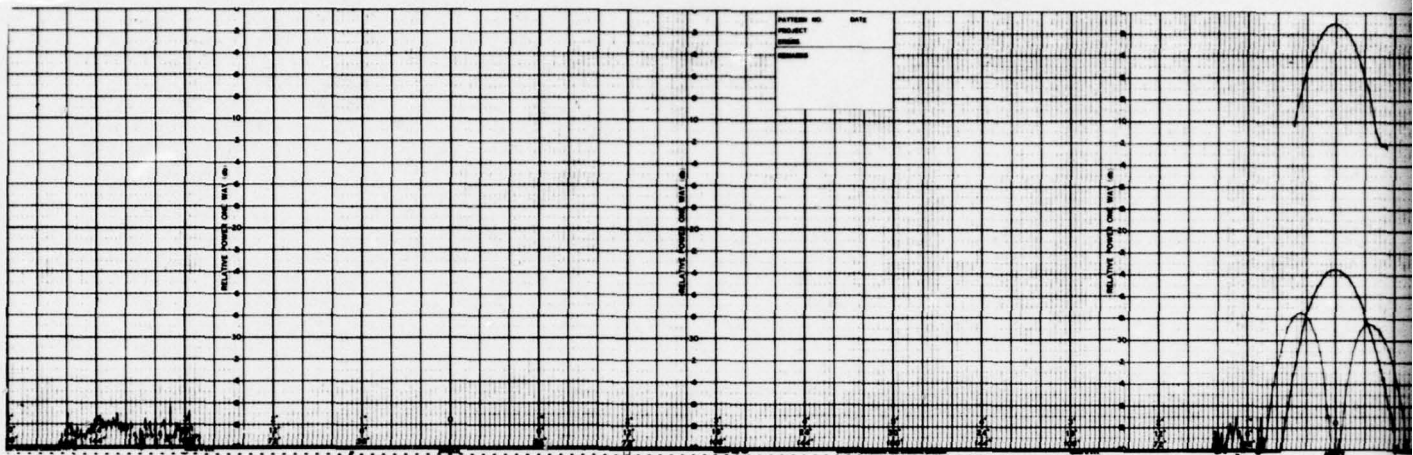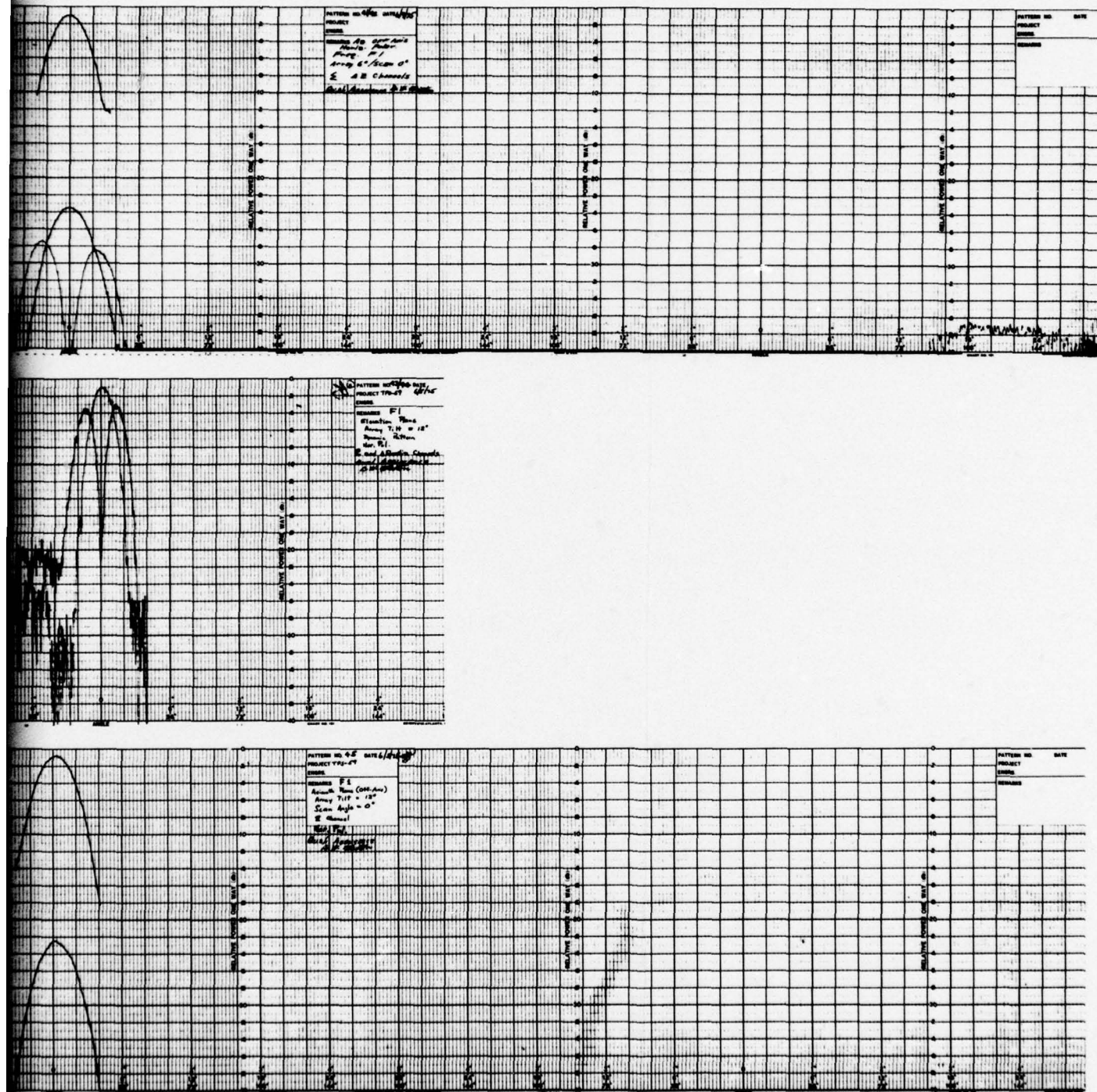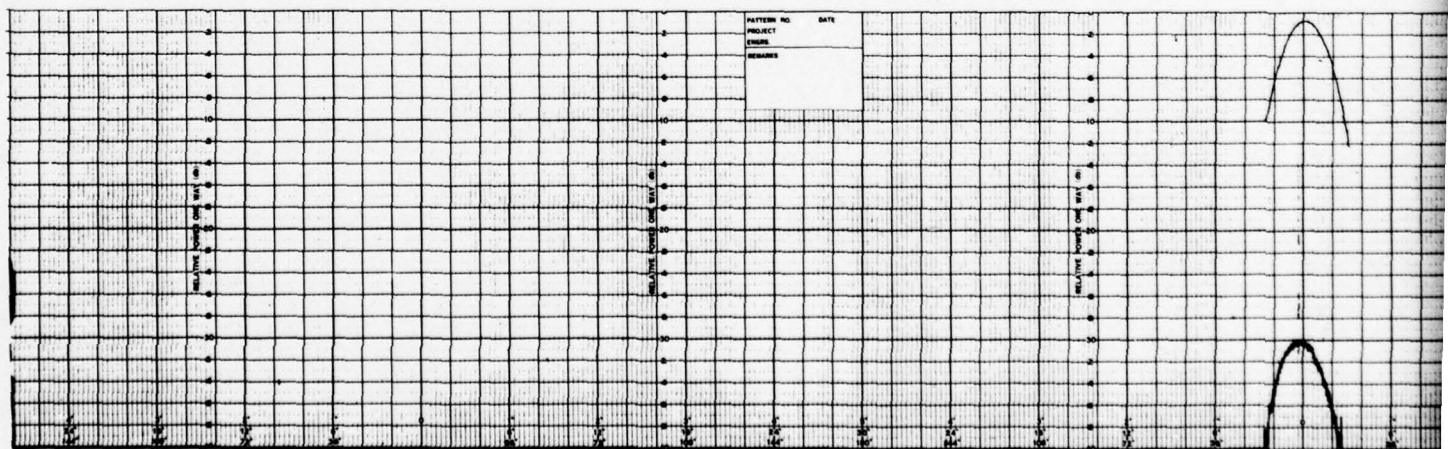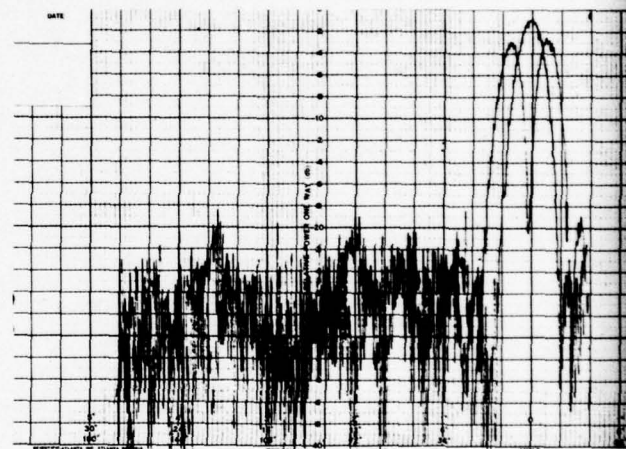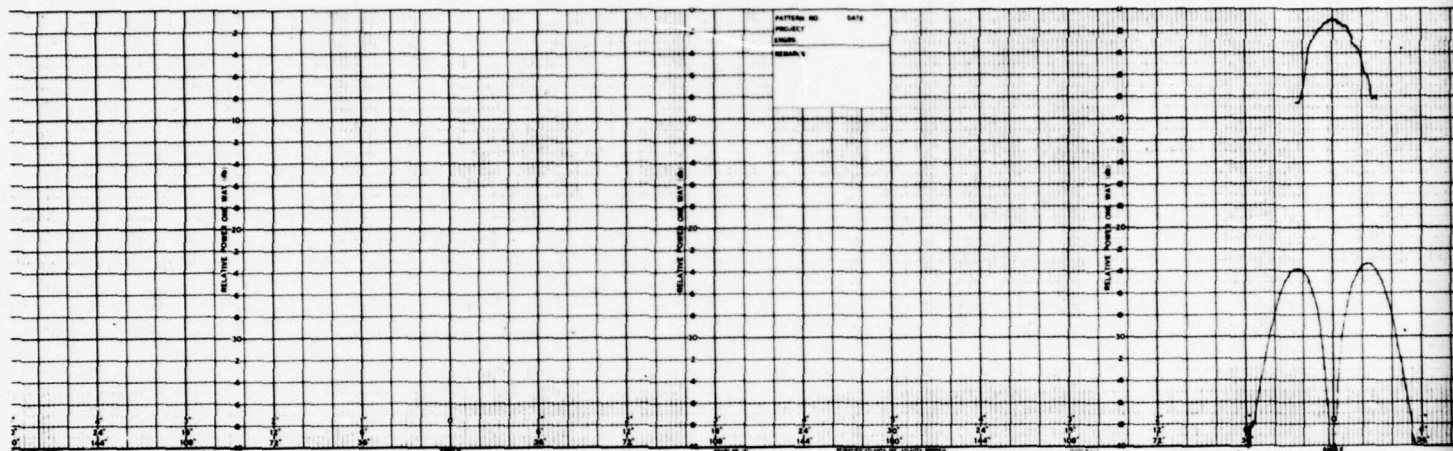| Number	Beam Type	Frequency	Polarization	Array Tilt Angle (θ_T)	Scan Angle Relative to Broadside	Pattern Type
28	Azimuth Difference	F15	Horizontal	0°	0°	Azimuth Principal Plane (Static)
29	Normal Sum	F15	Vertical	0°	0°	Azimuth Principal Plane (Static)
30	Azimuth Difference	F15	Vertical	0°	0°	Azimuth Principal Plane (Static)
31	Normal Sum	F15	Horizontal	6°	−11 to +16°	Elevation Principal Plane (Dynamic)
32	Elevation Difference	F15	Horizontal	6°	−11 to +16°	Elevation Principal Plane (Dynamic)
33	Normal Sum	F15	Horizontal	6°	0°	Azimuth Off–Axis (Static)
34	Azimuth Difference	F15	Horizontal	6°	0°	Azimuth Off–Axis (Static)
35	Normal Sum	F8	Horizontal	6°	−11 to +16°	Elevation Principal Plane (Dynamic)
36	Elevation Difference	F8	Horizontal	6°	−11 to +16°	Elevation Principal Plane (Dynamic)
37	Normal Sum	F8	Horizontal	6°	0°	Azimuth Off–Axis (Static)
38	Azimuth Difference	F8	Horizontal	6°	0°	Azimuth Off–Axis (Static)
39	Normal Sum	F1	Horizontal	6°	−11 to +16°	Elevation Principal Plane (Dynamic)
40	Elevation Difference	F1	Horizontal	6°	−11 to +16°	Elevation Principal Plane (Dynamic)
41	Normal Sum	F1	Horizontal	6°	0°	Azimuth Off–Axis (Static)

Figure 12-1. Receive Antenna Patterns (Sheet 3 of 21)

Number	Beam Type	Frequency	Polarization	Array Tilt Angle (θ_T)	Scan Angle Relative to Broadside	Pattern Type
42	Azimuth Difference	F1	Horizontal	6°	0°	Azimuth Off-Axis (Static)
43	Normal Sum	F1	Horizontal	12°	-16 to +16°	Elevation Principal Plane (Dynamic)
44	Elevation Difference	F1	Horizontal	12°	-16 to +16°	Elevation Principal Plane (Dynamic)
45	Normal Sum	F1	Horizontal	12°	0°	Azimuth Off-Axis (Static)
46	Azimuth Difference	F1	Horizontal	12°	0°	Azimuth Off-Axis (Static)
47	Normal Sum	F8	Horizontal	12°	-16 to +16°	Elevation Principal Plane (Dynamic)
48	Elevation Difference	F8	Horizontal	12°	-16 to +16°	Elevation Principal Plane (Dynamic)
49	Normal Sum	F8	Horizontal	12°	0°	Azimuth Off-Axis (Static)
50	Azimuth Difference	F8	Horizontal	12°	0°	Azimuth Off-Axis (Static)
51	Normal Sum	F15	Horizontal	12°	-16 to +16°	Elevation Principal Plane (Dynamic)
52	Elevation Difference	F15	Horizontal	12°	-16 to +16°	Elevation Principal Plane (Dynamic)
53	Normal Sum	F15	Horizontal	12°	0°	Azimuth Off-Axis (Static)
54	Azimuth Difference	F15	Horizontal	12°	0°	Azimuth Off-Axis (Static)

Figure 12-1. Receive Antenna Patterns (Sheet 4 of 21)

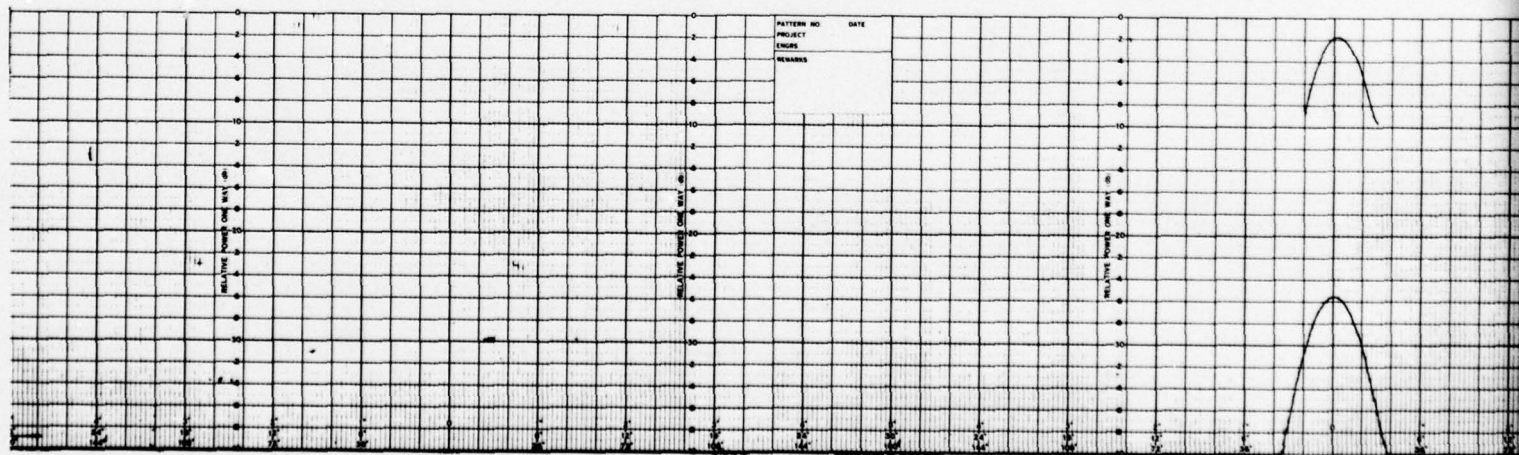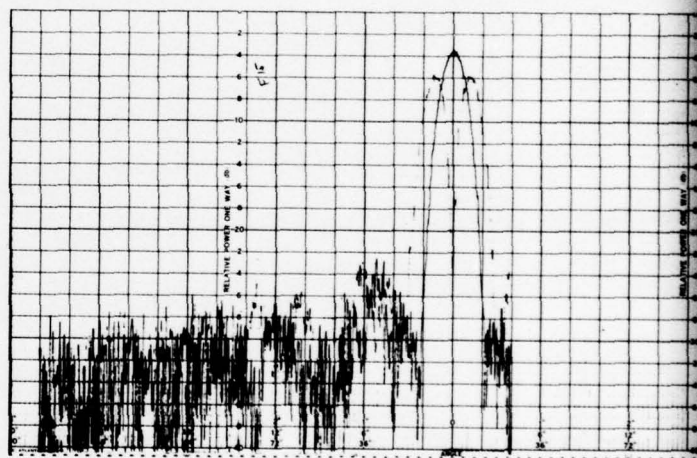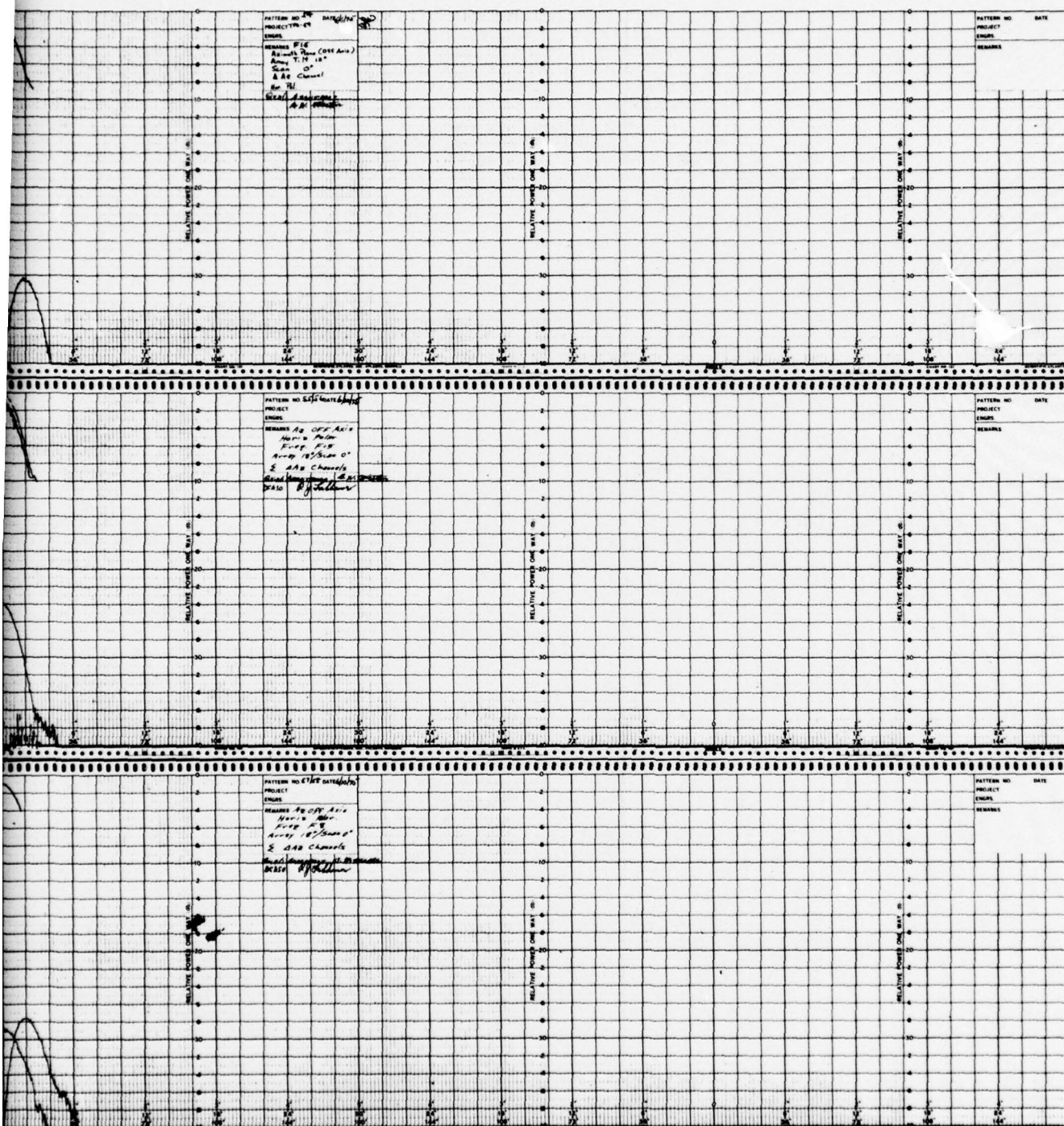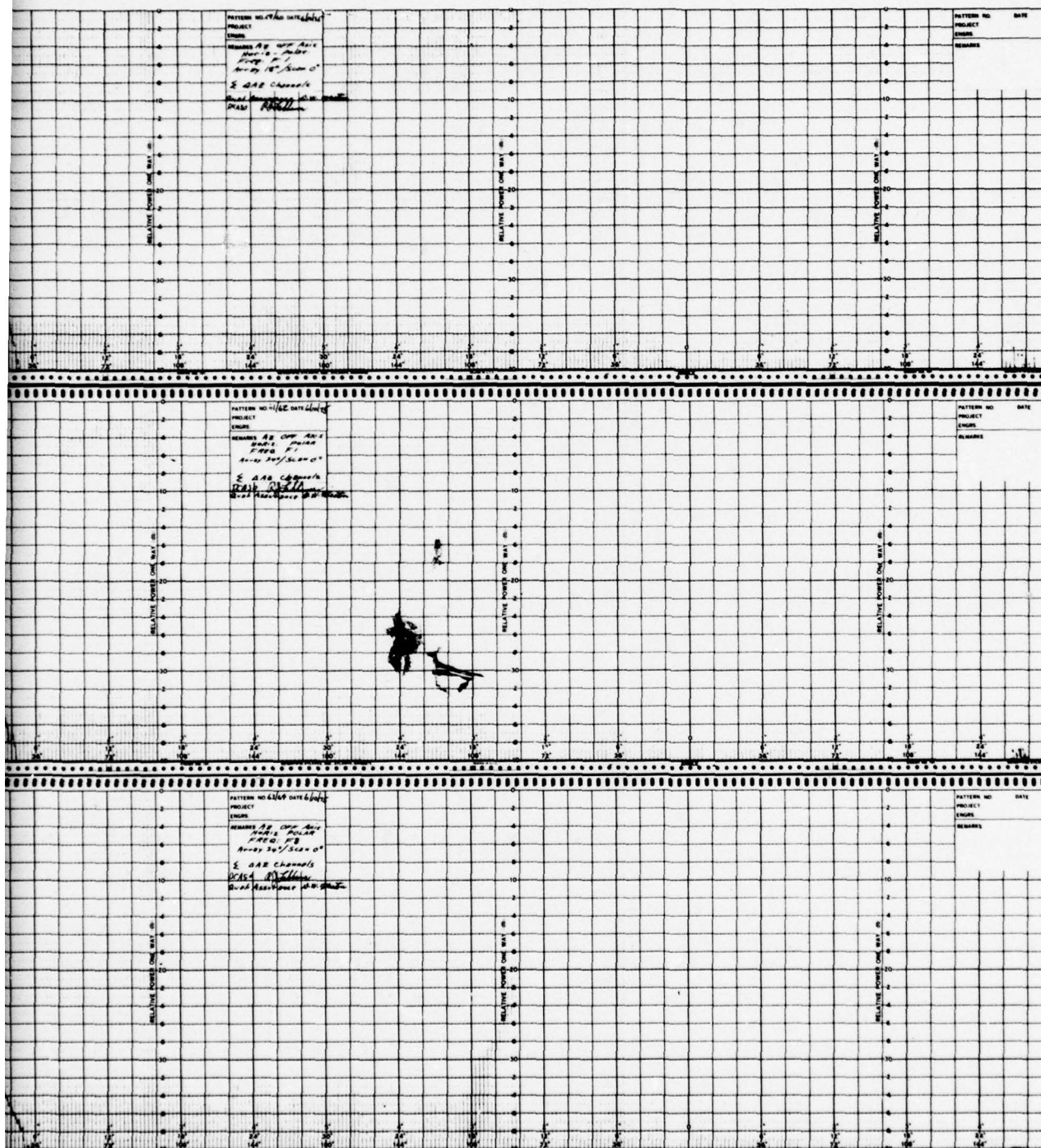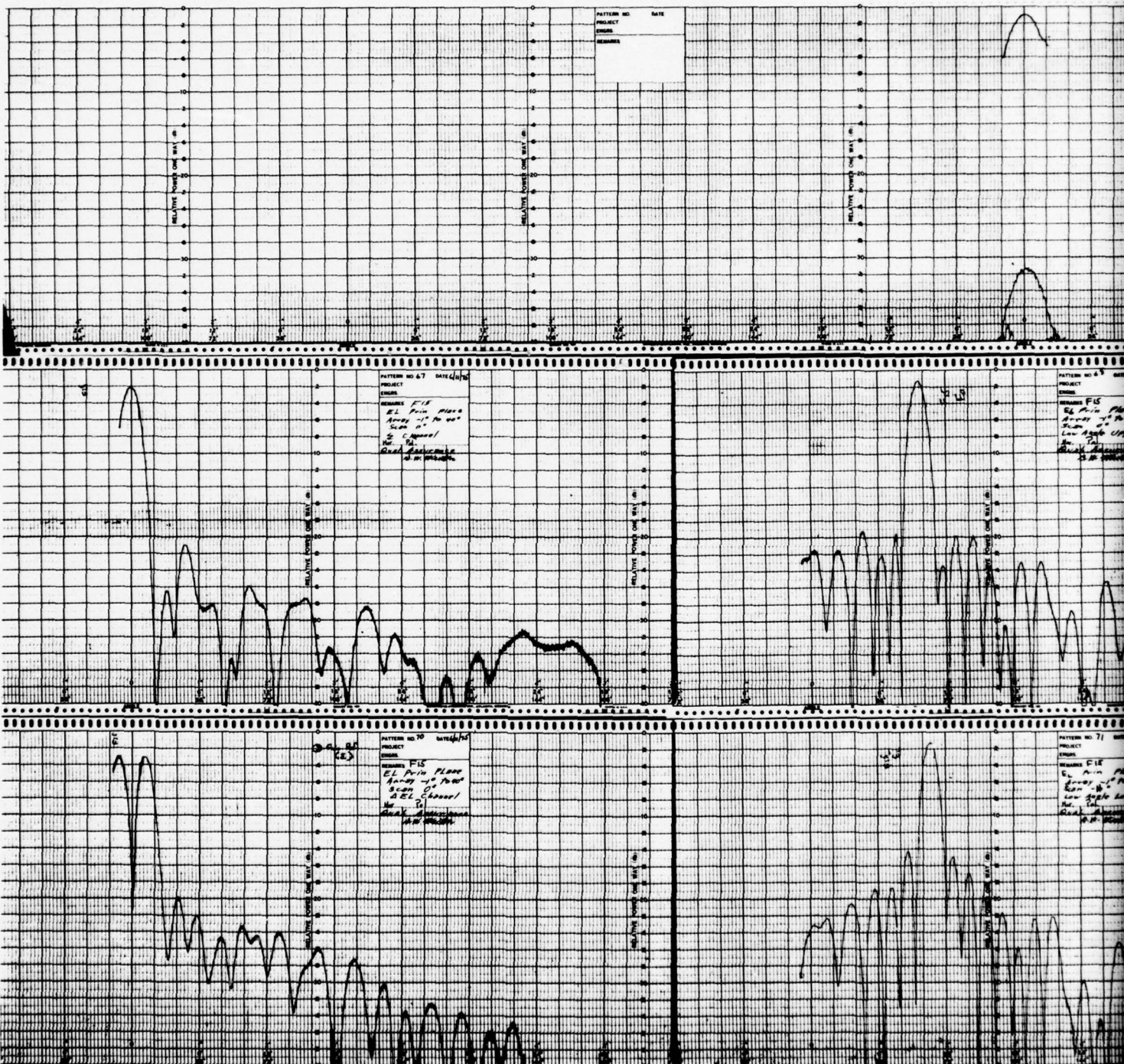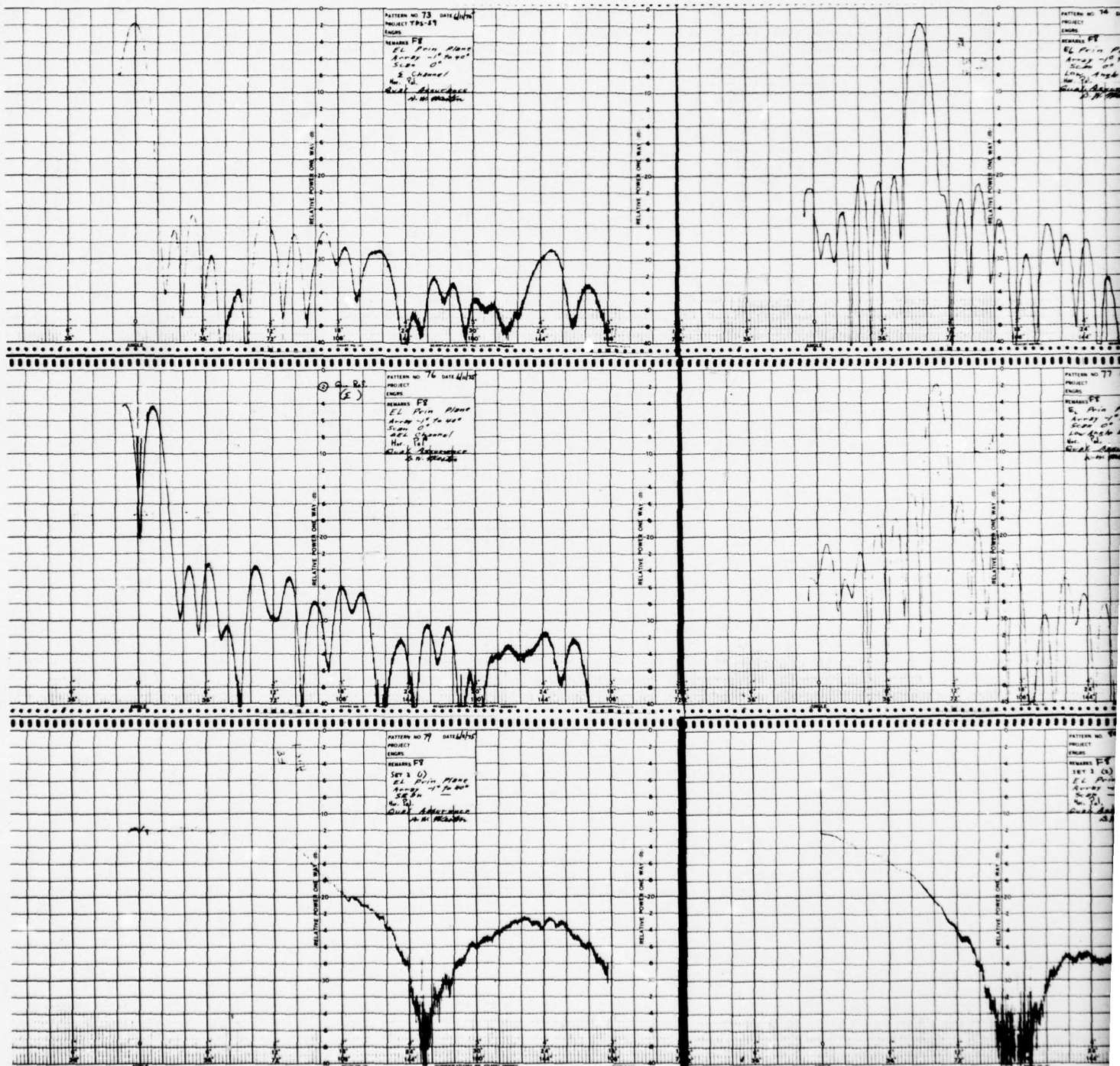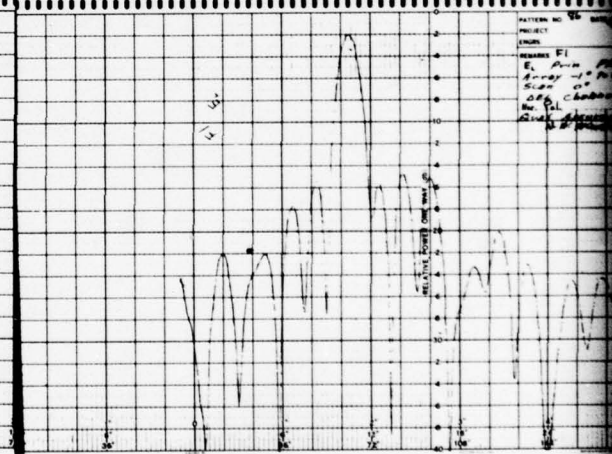| Number	Beam Type	Frequency	Polarization	Array Tilt Angle (θ_T)	Scan Angle Relative to Broadside	Pattern Type
55	Normal Sum	F15	Horizontal	18°	0°	Azimuth Off–Axis (Static)
56	Azimuth Difference	F15	Horizontal	18°	0°	Azimuth Off–Axis (Static)
57	Normal Sum	F8	Horizontal	18°	0°	Azimuth Off–Axis (Static)
58	Azimuth Difference	F8	Horizontal	18°	0°	Azimuth Off–Axis (Static)
59	Normal Sum	F1	Horizontal	18°	0°	Azimuth Off–Axis (Static)
60	Azimuth Difference	F1	Horizontal	18°	0°	Azimuth Off–Axis (Static)
61	Normal Sum	F1	Horizontal	24°	0°	Azimuth Off–Axis (Static)
62	Azimuth Difference	F1	Horizontal	24°	0°	Azimuth Off–Axis (Static)
63	Normal Sum	F8	Horizontal	24°	0°	Azimuth Off–Axis (Static)
64	Azimuth Difference	F8	Horizontal	24°	0°	Azimuth Off–Axis (Static)
65	Normal Sum	F15	Horizontal	24°	0°	Azimuth Off–Axis (Static)
66	Azimuth Difference	F15	Horizontal	24°	0°	Azimuth Off–Axis (Static)
67	Normal Sum	F15	Horizontal	–1 to +40	0°	Elevation Principal Plane (Static)

Figure 12–1. Receive Antenna Patterns (Sheet 5 of 21)

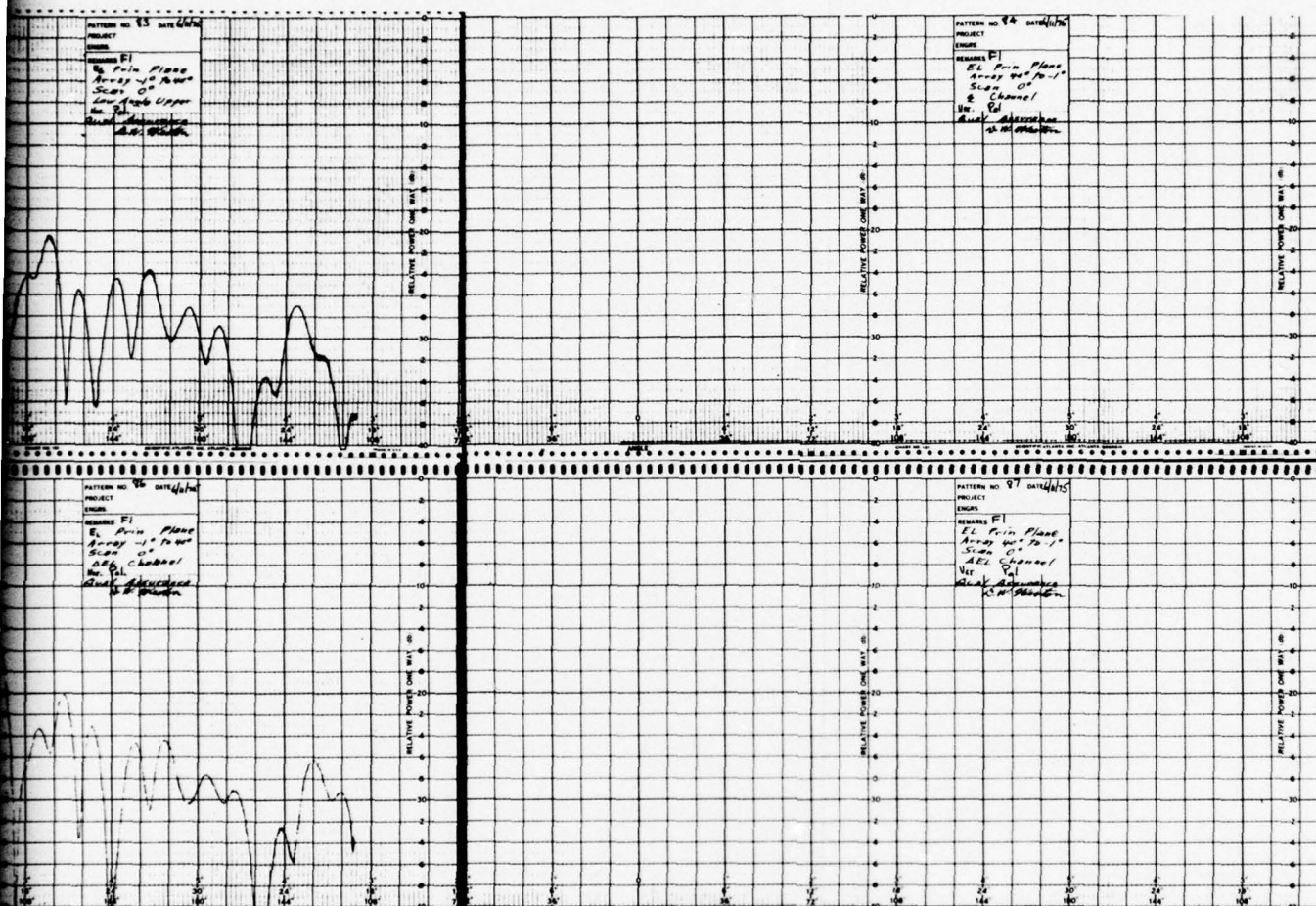| Number	Beam Type	Frequency	Polarization	Array Tilt Angle (θ_T)	Scan Angle Relative to Broadside	Pattern Type
68	Low Angle Upper Beam	F15	Horizontal	-1 to +40°	0°	
69	Normal Sum	F15	Vertical	+40 to -1	0°	
70	Elevation Difference	F15	Horizontal	-1 to +40°	0°	
71	Low Angle Lower Beam	F15	Horizontal	-1 to +40°	0°	
72	Elevation Difference	F15	Vertical	+40 to -1°	0°	
73	Normal Sum	F8	Horizontal	-1 to +40°	0°	
74	Low Angle Upper Beam	F8	Horizontal	-1 to +40°	0°	
75	Normal Sum	F8	Vertical	+40 to -1	0°	
76	Elevation Difference	F8	Horizontal	-1 to +40°	0°	
77	Low Angle Lower Beam	F8	Horizontal	-1 to +40°	0°	
78	Elevation Difference	F8	Vertical	+40 to -1°	0°	
79	Set-3 Serial No. 1	F8	Horizontal	-1 to +40°	0°	
80	Set-3 Serial No. 2	F8	Horizontal	-1 to +40°	0°	
81	Set-3 Serial No. 3	F8	Horizontal	+40 to -1°	0°	Elevation Principal Plane (Static)
82	Normal Sum	F1	Horizontal	-1 to +40°	0°	

Figure 12-1. Receive Antenna Patterns (Sheet 6 of 21)

Number	Beam Type	Frequency	Polarization	Angle (θ_τ)	Scan Angle Relative to Broadside	Pattern Type
83	Low Angle Upper Beam	F1	Horizontal	-1 to +40°	0°	
84	Normal Sum	F1	Vertical	+40 to -1°	0°	
85	Elevation Difference	F1	Horizontal	-1 to +40°	0°	
86	Low Angle Lower Beam	F1	Horizontal	-1 to +40°	0°	
87	Elevation Difference	F1	Vertical	+40 to -1°	0°	

Figure 12-1. Receive Antenna Patterns (Sheet 7 of 21)
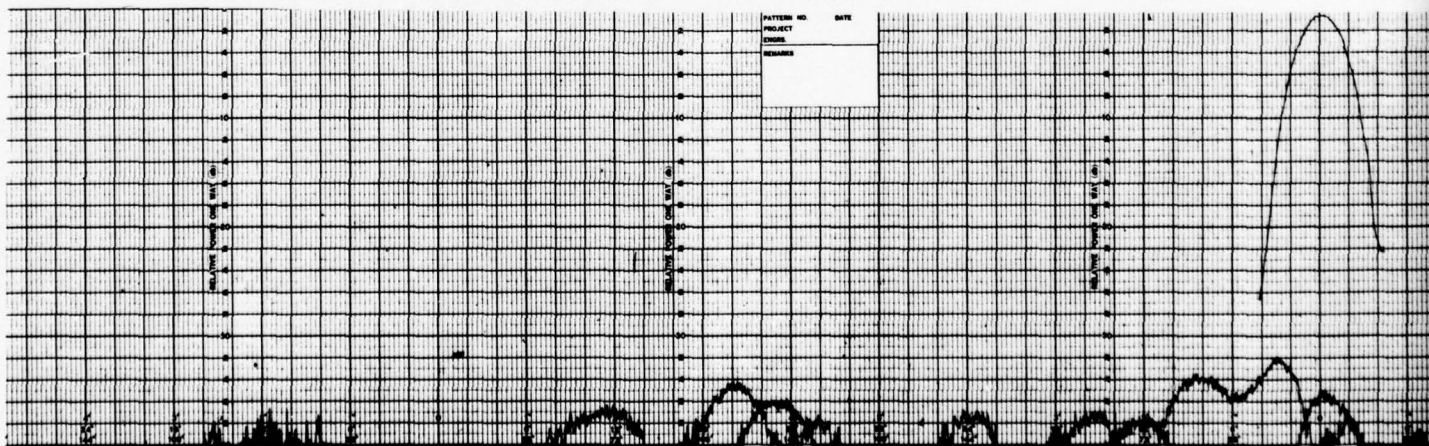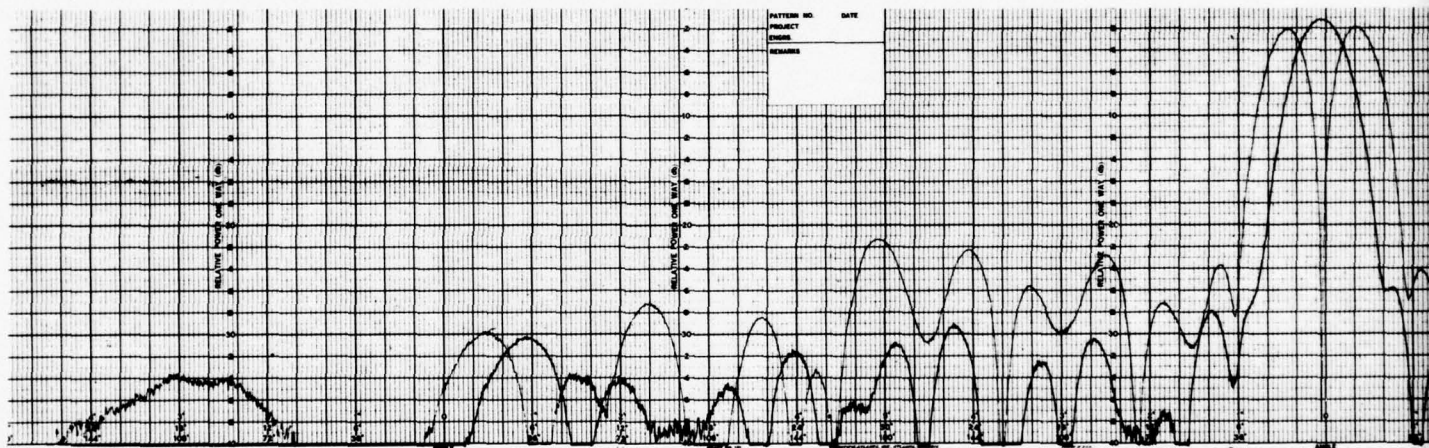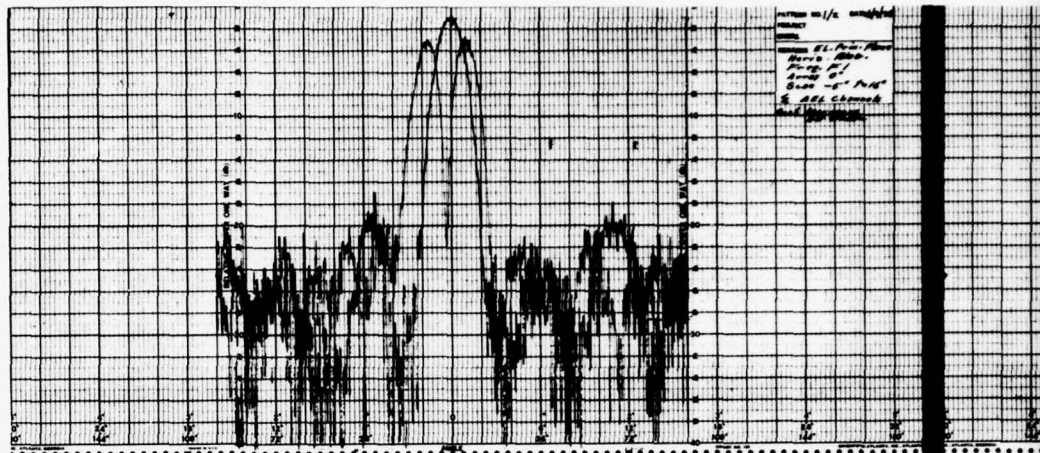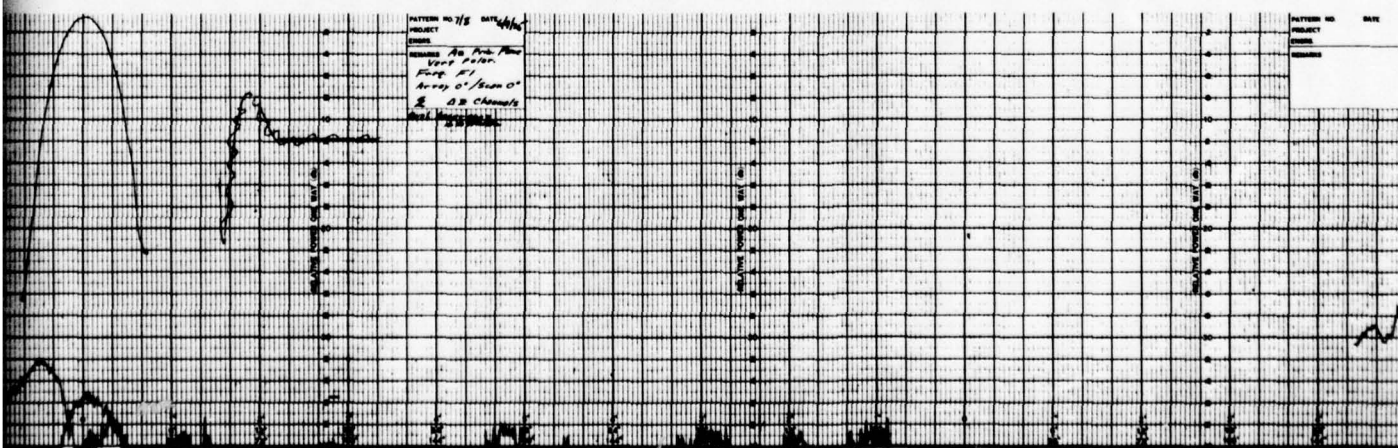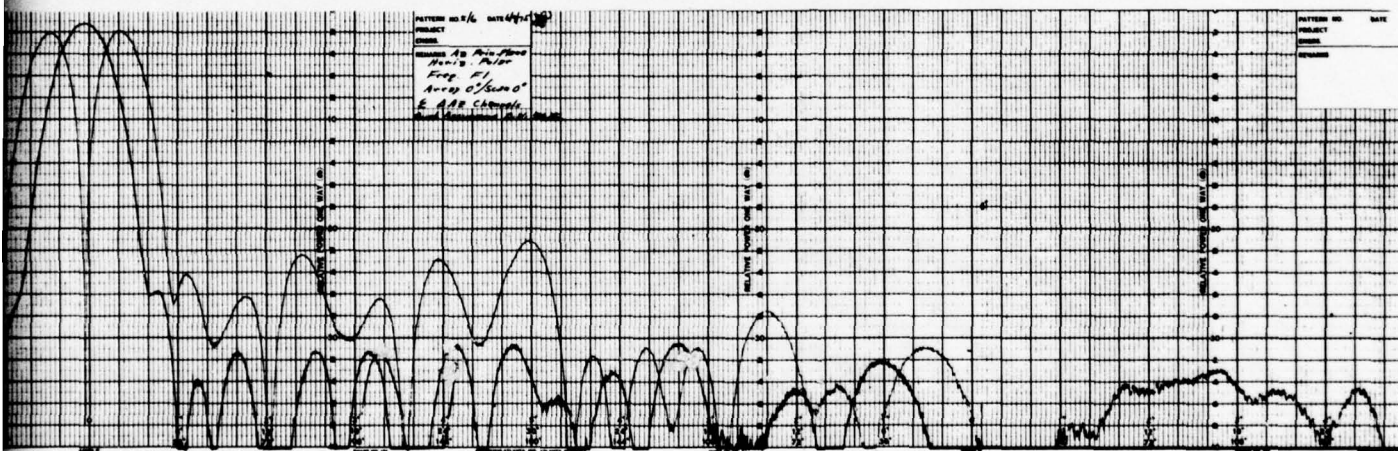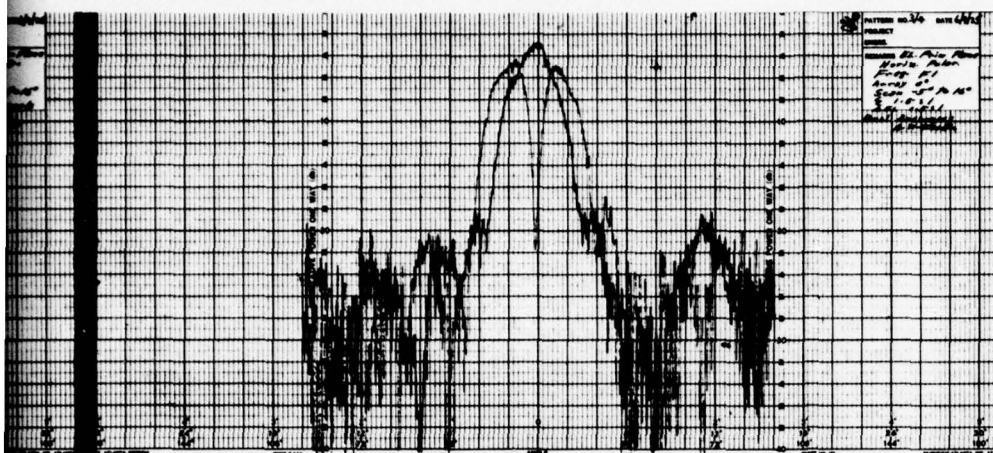
Figure 12-1. Receive Antenna Patterns (Sheet 8 of 21)
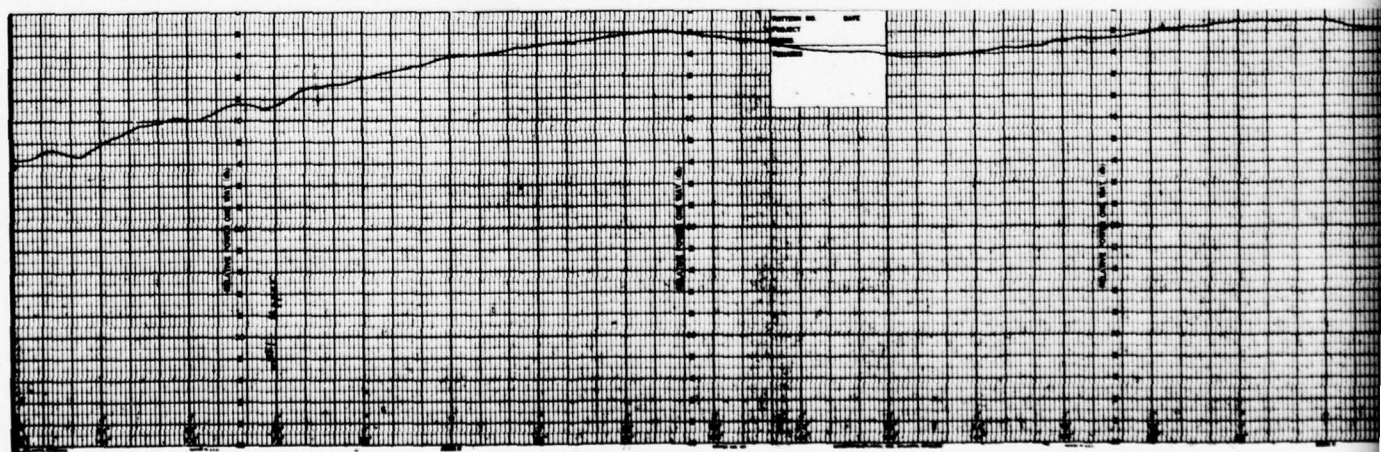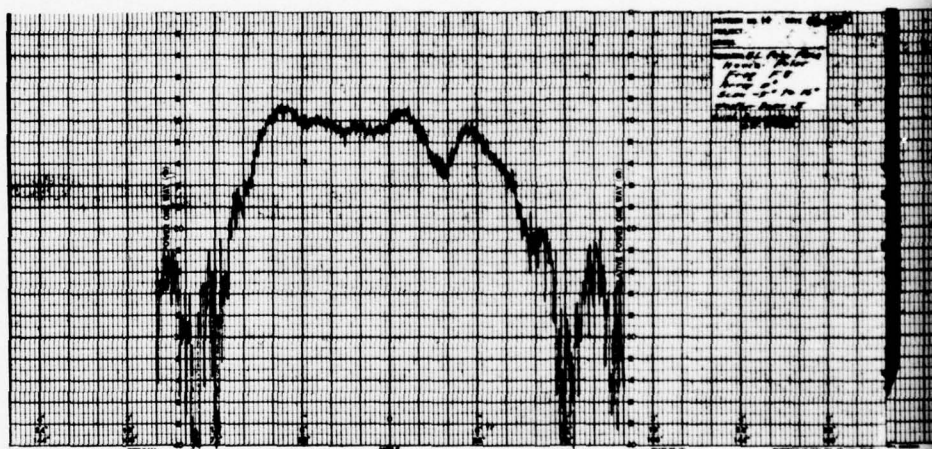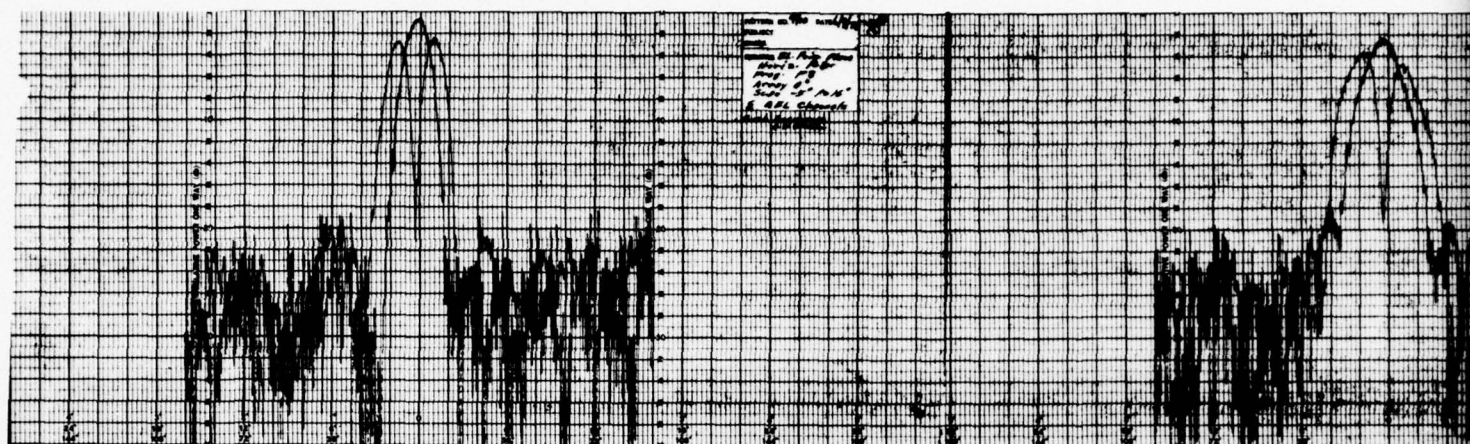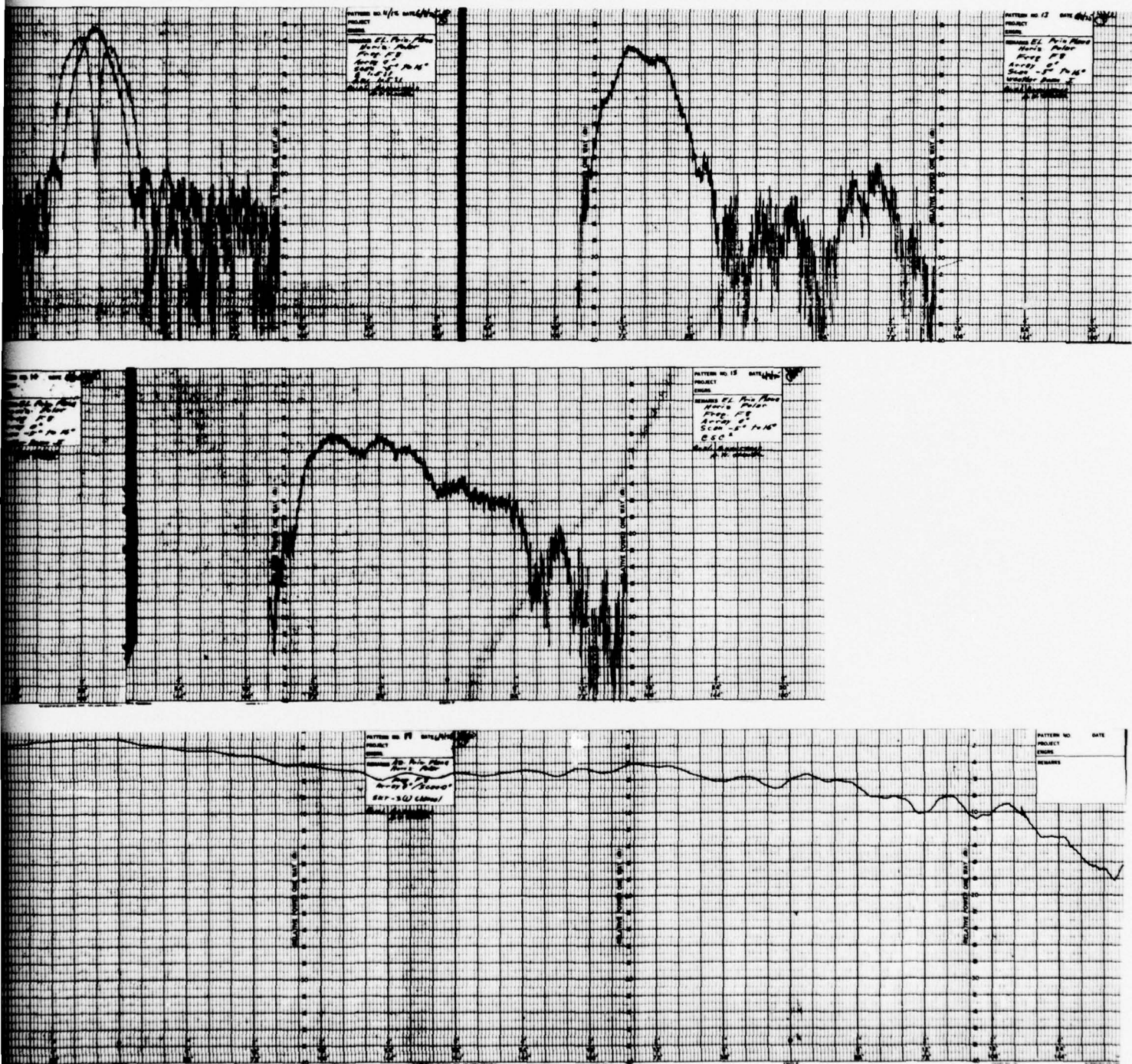
1

Figure 12-1. Receive Antenna Patterns (Sheet 9 of 21)

PATTERN NO.   DATE
PROJECT
ENGRS.
REMARKS

Figure 12-1. Receive Antenna Patterns (Sheet 10 of 21)

12-11

PATTERN NO. 2302A DATE 6/17/?
PROJECT
ENGRS.
REMARKS EL Prin Plane
Horiz Polar
Freq F15
Scale G°
Scan 5° to 15°
E ΔEL Channels
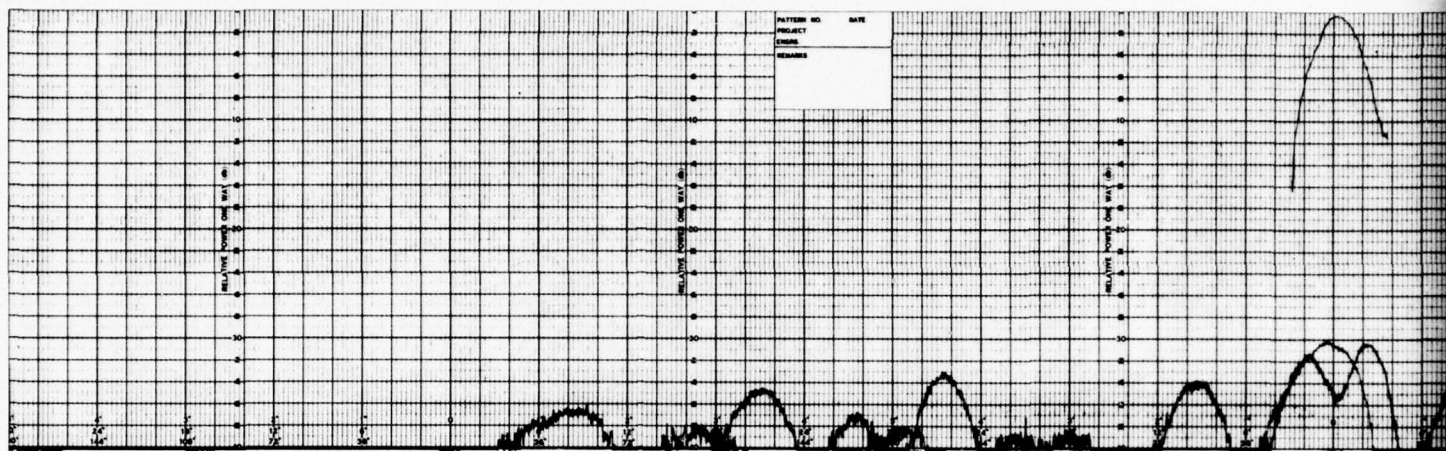
Figure 12-1. Receive Antenna Patterns (Sheet 11 of 21)

1
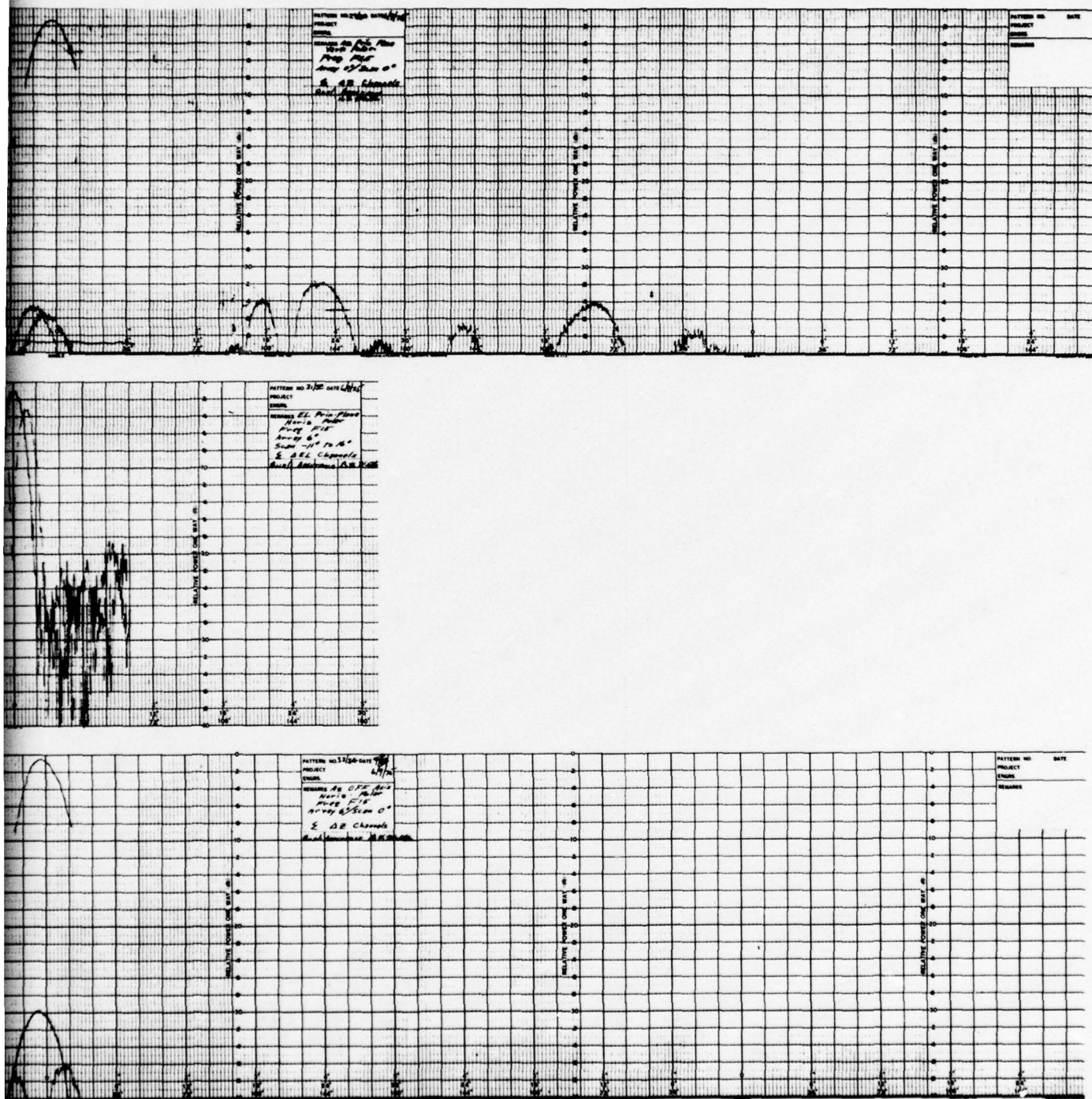
Figure 12-1. Receive Antenna Patterns (Sheet 12 of 21)

12-13

RELATIVE POWER ONE WAY db

RELATIVE POWER ONE WAY db

RELATIVE POWER ONE WAY db

RELATIVE POWER ONE WAY db

RELATIVE POWER ONE WAY db

ANGLE

ANGLE

1

Figure 12-1. Receive Antenna Patterns (Sheet 13 of 21)
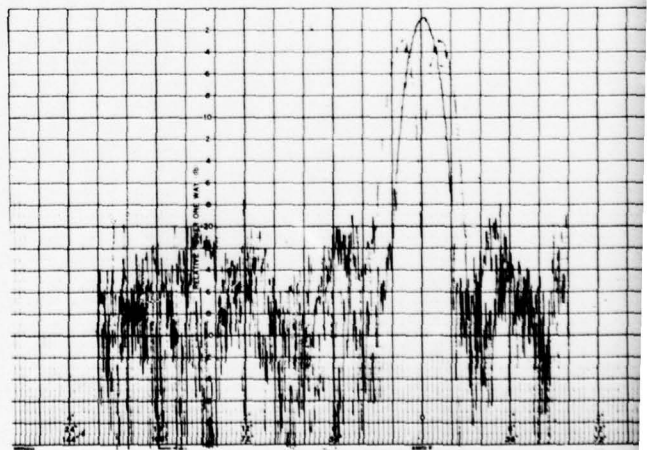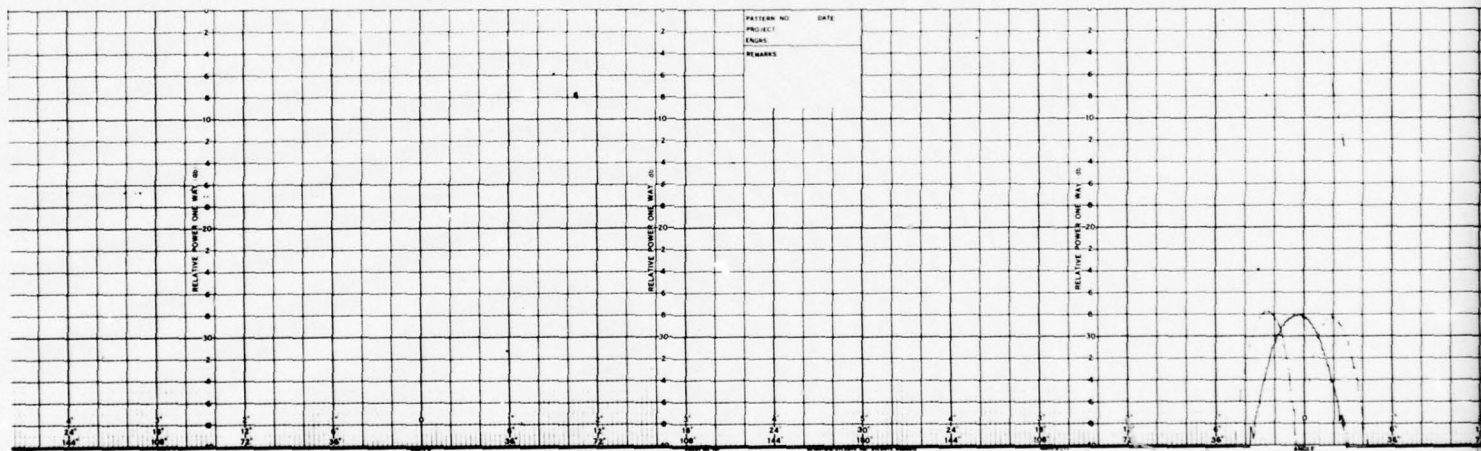
Figure 12-1. Receive Antenna Patterns (Sheet 14 of 21)

Figure 12-1. Receive Antenna Patterns (Sheet 15 of 21)

Figure 12-1. Receive Antenna Patterns (Sheet 16 of 21)

12-17
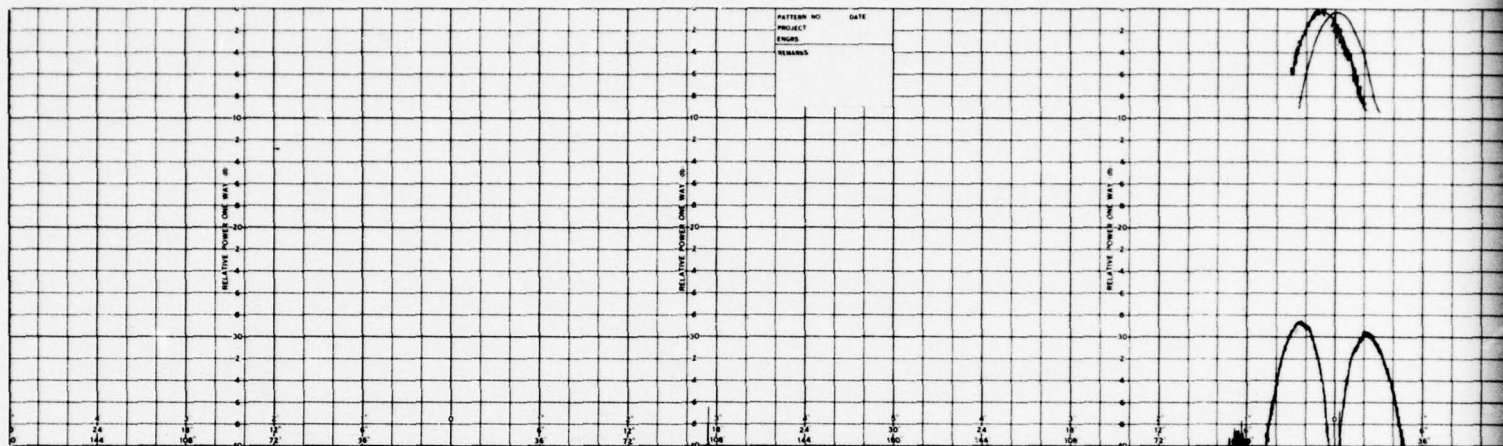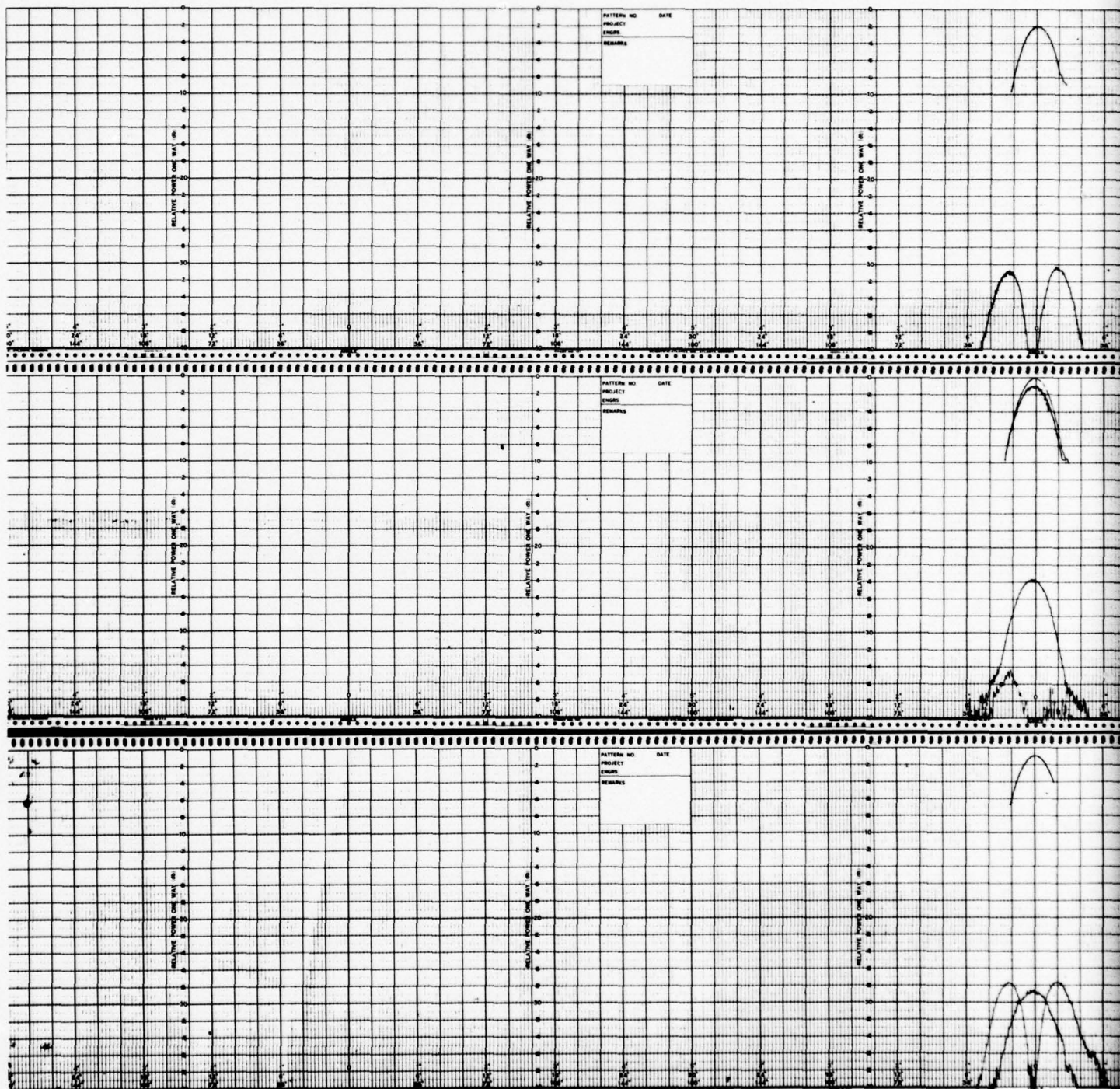
Figure 12-1. Receive Antenna Patterns (Sheet 17 of 21)
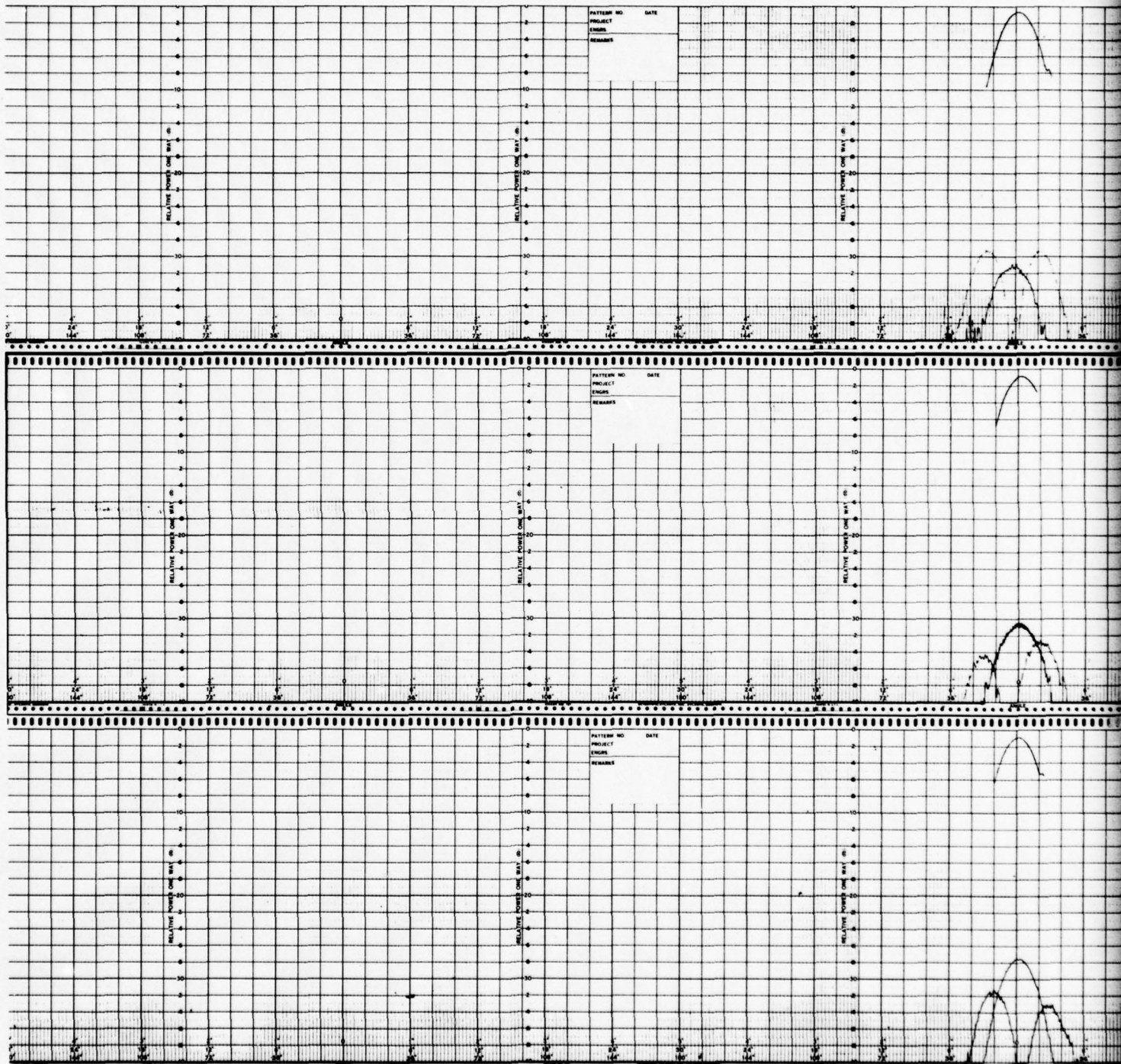
Figure 12-1. Receive Antenna Patterns (Sheet 18 of 21)

Figure 12-1. Receive Antenna Patterns (Sheet 19 of 21)

PATTERN NO. 73 DATE 4/11/70
PROJECT TPS-59
ENGRS
REMARKS F8
EL Prin Plane
Array -1° to 40°
Scan 0°
Σ Channel
Hor. Pol.
Dual Resurface

PATTERN NO. 74
PROJECT
ENGRS
REMARKS F8
Array -1°
Scan 0°
Scan Angle
Hor. Pol.
Dual Resurface

PATTERN NO. 76 DATE 4/11/70
PROJECT
ENGRS
REMARKS F8
EL Prin Plane
Array -1° to 40°
Scan 0°
ADL Channel
Hor. Pol.
Dual Resurface

PATTERN NO. 77
PROJECT
ENGRS
REMARKS F8
EL Prin
Array -1°
Scan 0°
Low Angle
Hor. Pol.
Dual Resurface

PATTERN NO. 79 DATE 4/11/70
PROJECT
ENGRS
REMARKS F8
SET 1 (1)
EL Prin Plane
Array -1° to 40°
SR 0°
Hor. Pol.
Dual Resurface

PATTERN NO.
PROJECT
ENGRS
REMARKS F8
SET 1 (1)
EL Prin
Array -1°
Scan 0°
Hor. Pol.
Dual Resurface

Figure 12-1. Receive Antenna Patterns (Sheet 20 of 21)

12-21

Figure 12-1. Receive Antenna Patterns (Sheet 21 of 21)

Pattern Number	Beam Type	Frequency	Polarization	Array Tilt Angle (θ_T)	Scan Angle Relative to Broadside	Pattern Type
1	Normal Transmit	F8	Horizontal	0°	0°	Azimuth Principal Plane (Static)
2	Normal Transmit	F8	Horizontal	0°	−16 to +16°	Elevation Principal Plane (Dynamic)
3	Weather Beam I	F8	Horizontal	0°	−16 to +16°	Elevation Principal Plane (Dynamic)
4	Weather Beam II	F8	Horizontal	0°	−16 to +16°	Elevation Principal Plane (Dynamic)
5	Cosecant Beam	F8	Horizontal	0°	−16 to +16°	Elevation Principal Plane (Dynamic)
6	Broaden Beam (1.5:1)	F8	Horizontal	0°	−16 to +16°	Elevation Principal Plane (Dynamic)
7	Normal Transmit	F1	Horizontal	0°	−16 to +16°	Elevation Principal Plane (Dynamic)
8	Broaden Beam (1.5:1)	F1	Horizontal	0°	−16 to +16°	Elevation Principal Plane (Dynamic)
9	Normal Transmit	F15	Horizontal	0°	−16 to +16°	Elevation Principal Plane (Dynamic)
10	Broaden Beam (1.5:1)	F15	Horizontal	0°	−16 to +16°	Elevation Principal Plane (Dynamic)
11	Normal Transmit	F15	Horizontal	6°	−16 to +16°	Elevation Principal Plane (Dynamic)
12	Normal Transmit	F1	Horizontal	6°	−16 to +16°	Elevation Principal Plane (Dynamic)
13	Normal Transmit	F1	Horizontal	6°	−16 to +16°	Elevation Principal Plane (Dynamic)
14	Normal Transmit	F1	Horizontal	12°	−16 to +16°	Elevation Principal Plane (Dynamic)

Figure 12-2. Transmit Antenna Patterns (Sheet 1 of 5)

Pattern Number	Beam Type	Frequency	Polarization	Array Tilt Angle (θ_τ)	Scan Angle Relative to Broadside	Pattern Type
15	Normal Transmit	F15	Horizontal	12°	−16 to +16°	Elevation Principal Plane (Dynamic)
16	Normal Transmit	F15	Horizontal	12°	−16 to +16	Elevation Principal Plane (Dynamic)
17	Normal Transmit	F15	Horizontal	−1 to +40°	0°	Elevation Principal Plane (Static)
18	Normal Transmit	F8	Horizontal	−1 to +40	0°	Elevation Principal Plane (Static)
19	Normal Transmit	F1	Horizontal	−1 to +40	0°	Elevation Principal Plane (Static)

Figure 12–2. Transmit Antenna Patterns (Sheet 2 of 5)

PATTERN NO. 2   DATE 7/4/45
PROJECT TRI-59
ENGR.
REMARKS: Army Tilt Angle of
F8
Elevation Pln, Pln
Transmit II
Dynamic Before

PATTERN NO. 5   DATE 7/5/45
PROJECT
ENGR.
REMARKS
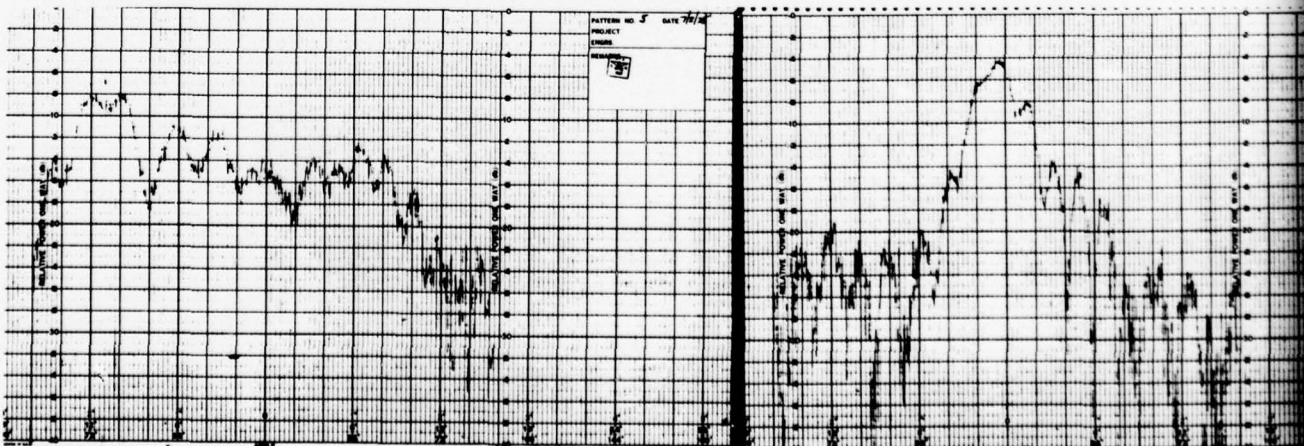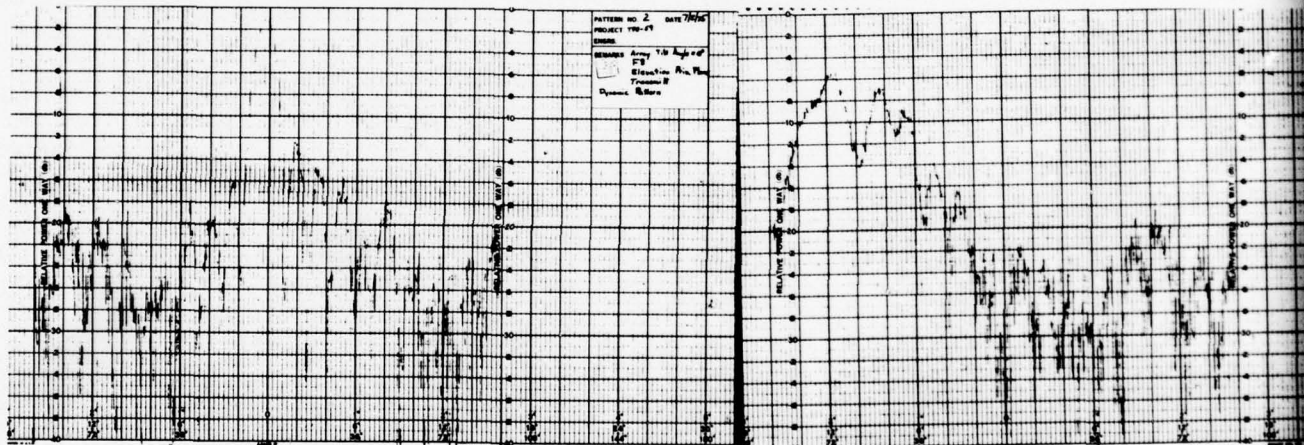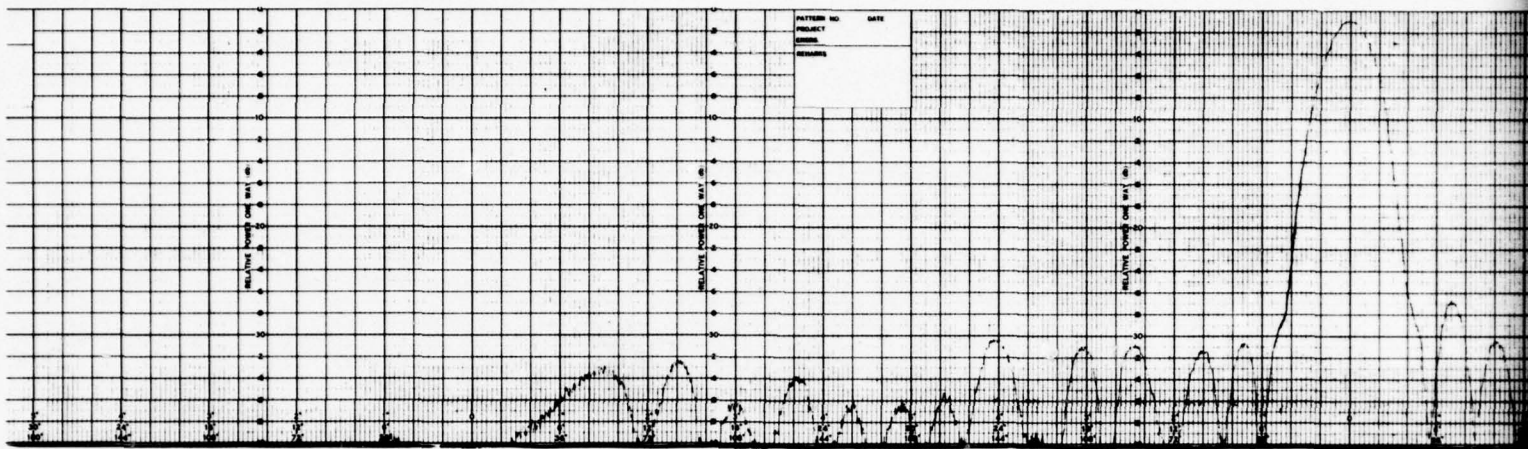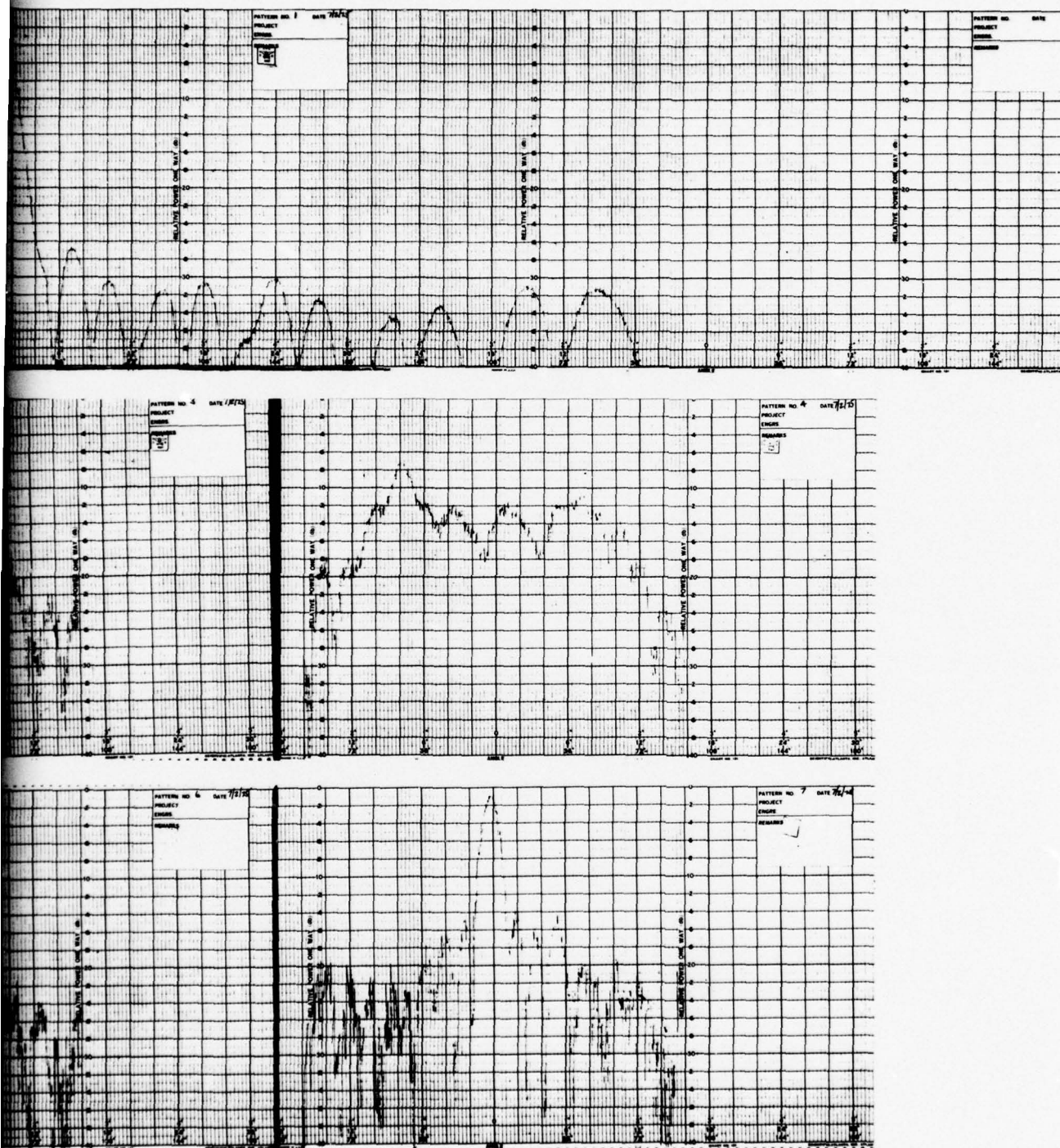
Figure 12-2. Transmit Antenna Patterns (Sheet 3 of 5)

12-25
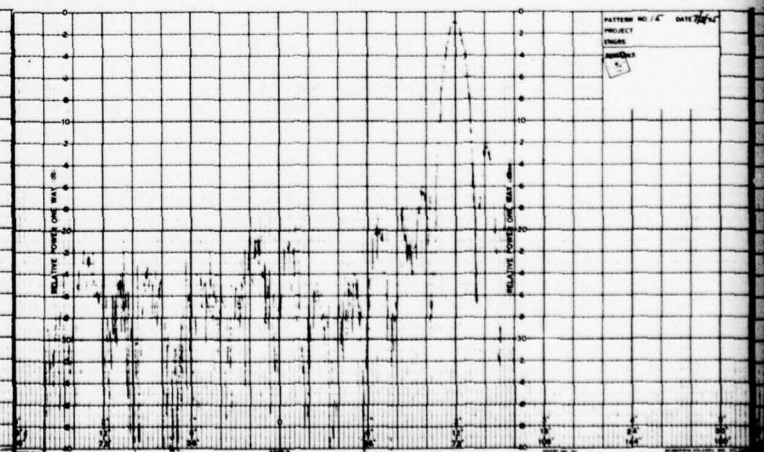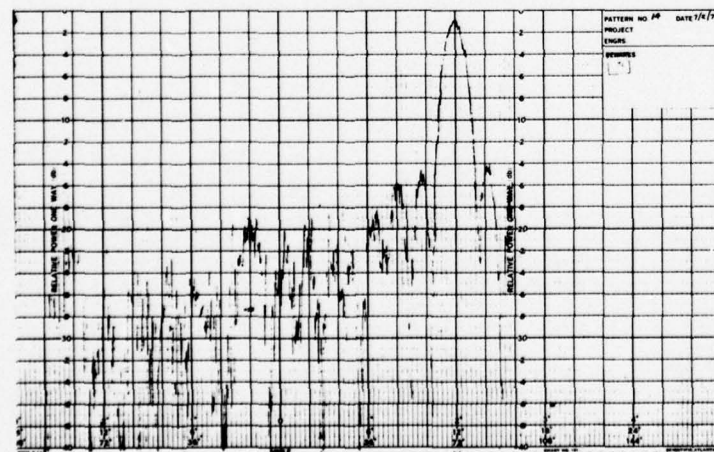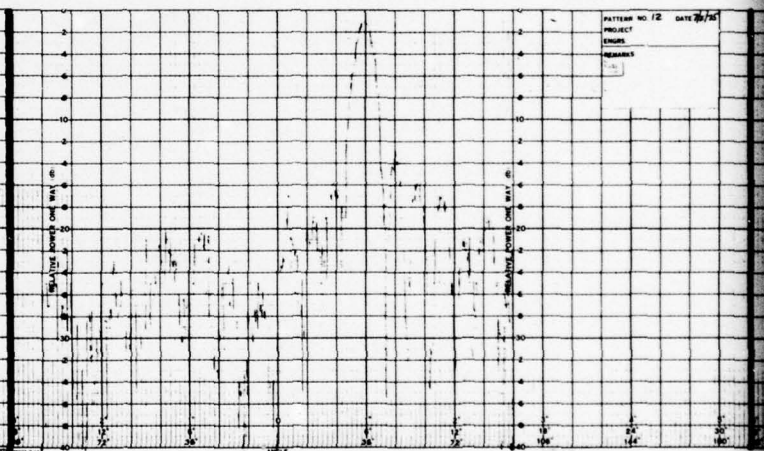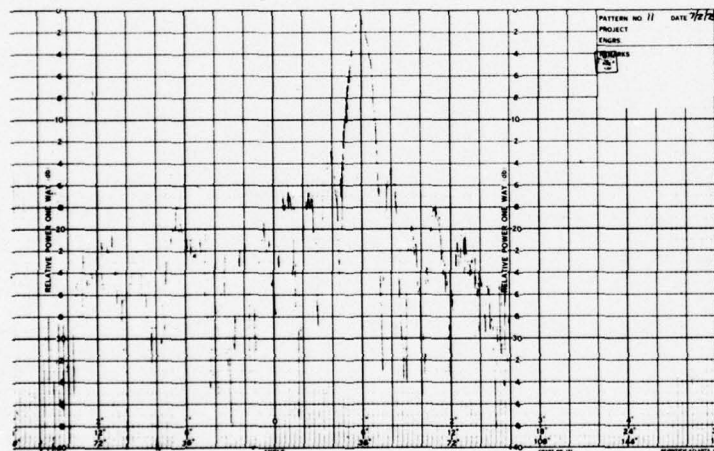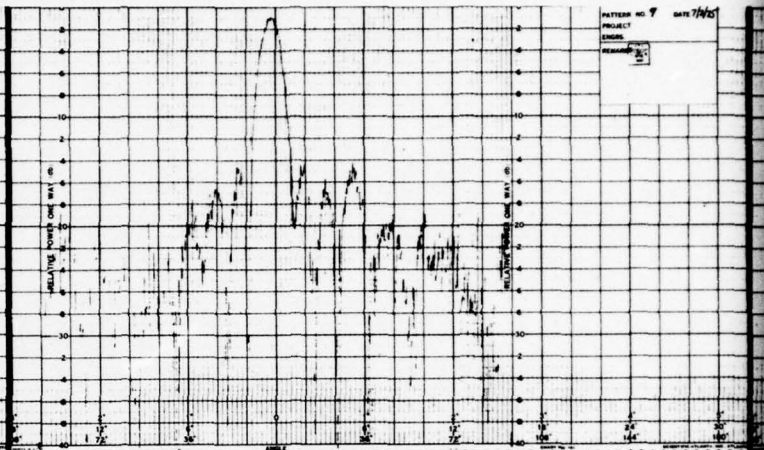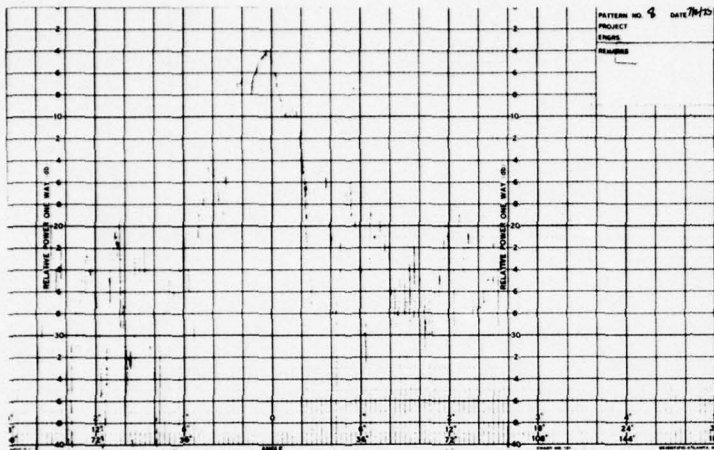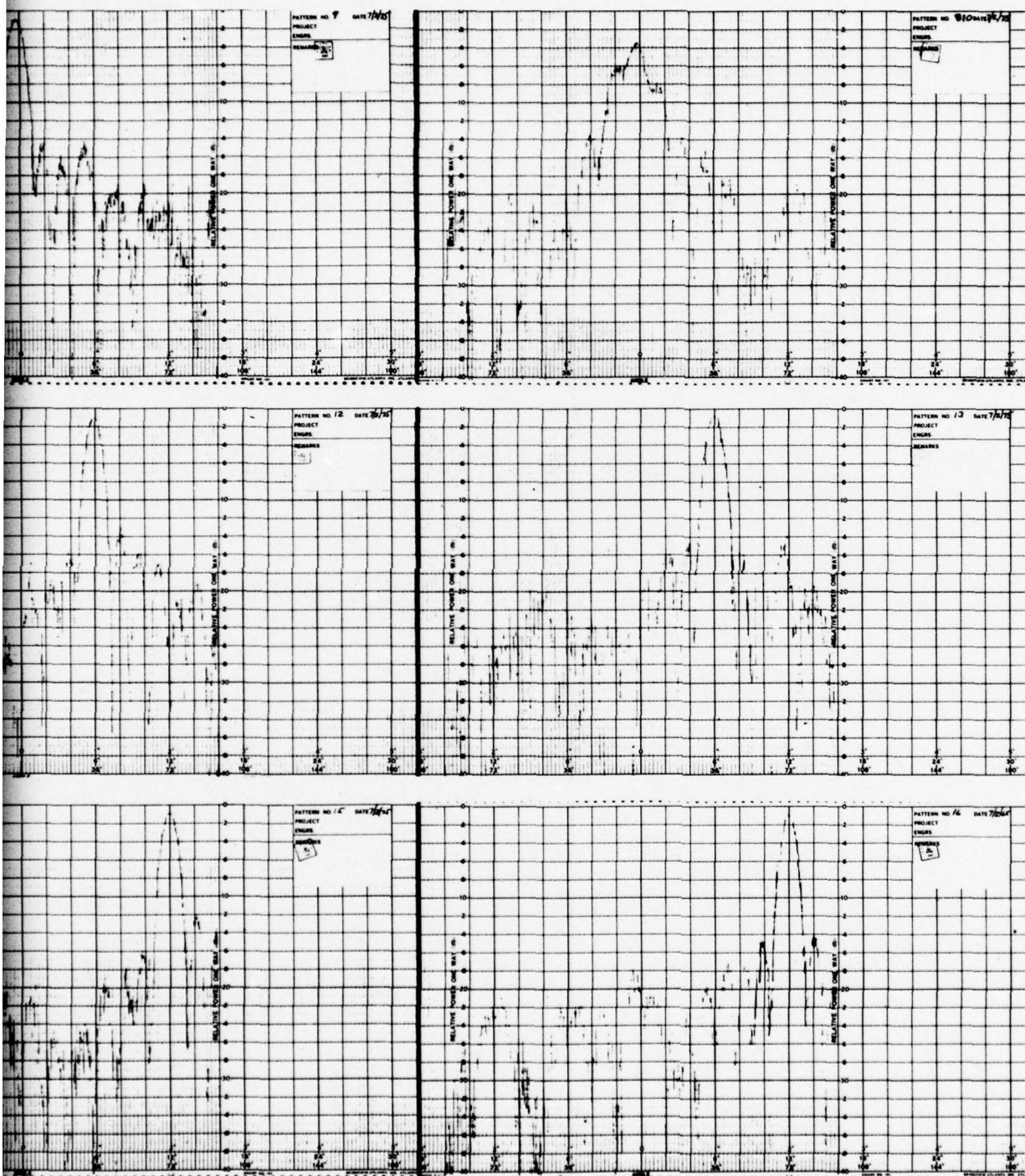
Figure 12-2. Transmit Antenna Patterns (Sheet 4 of 5)

12-26
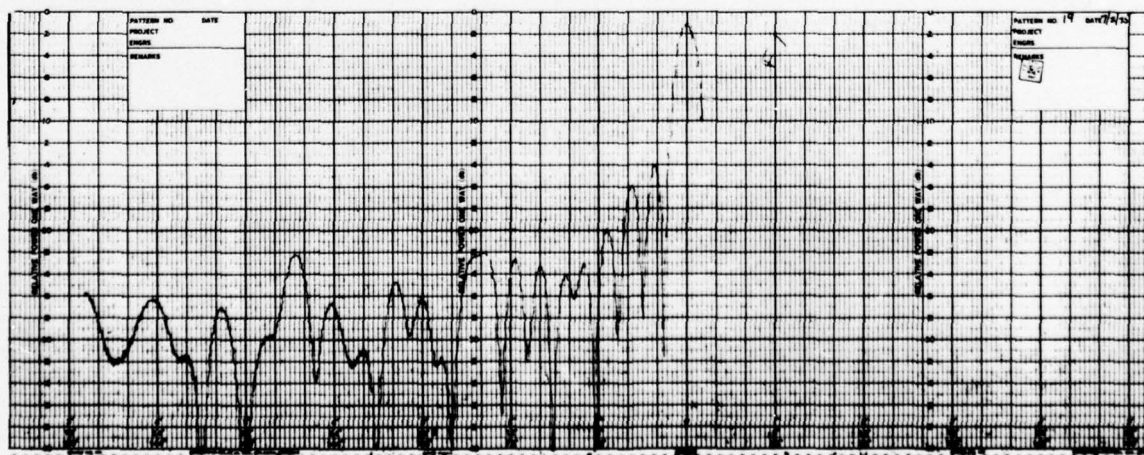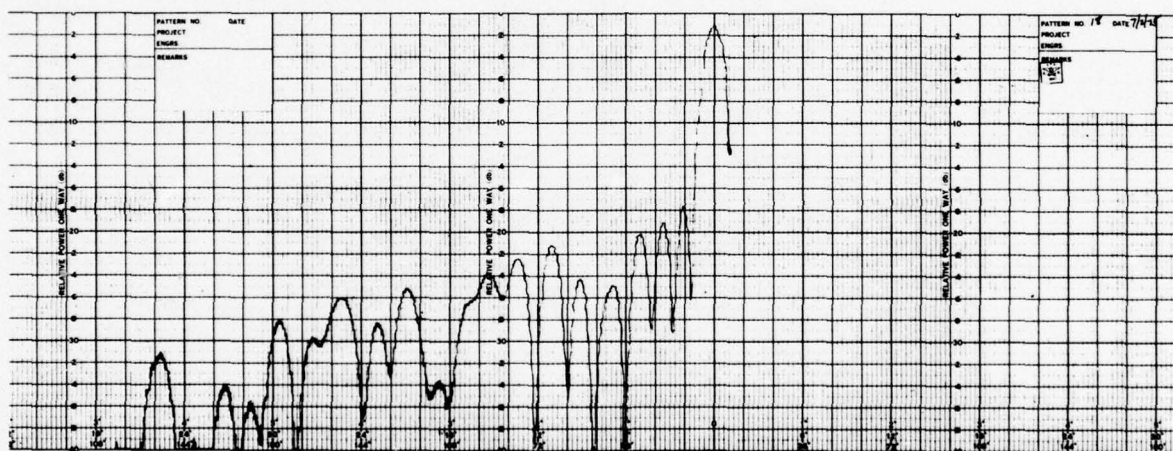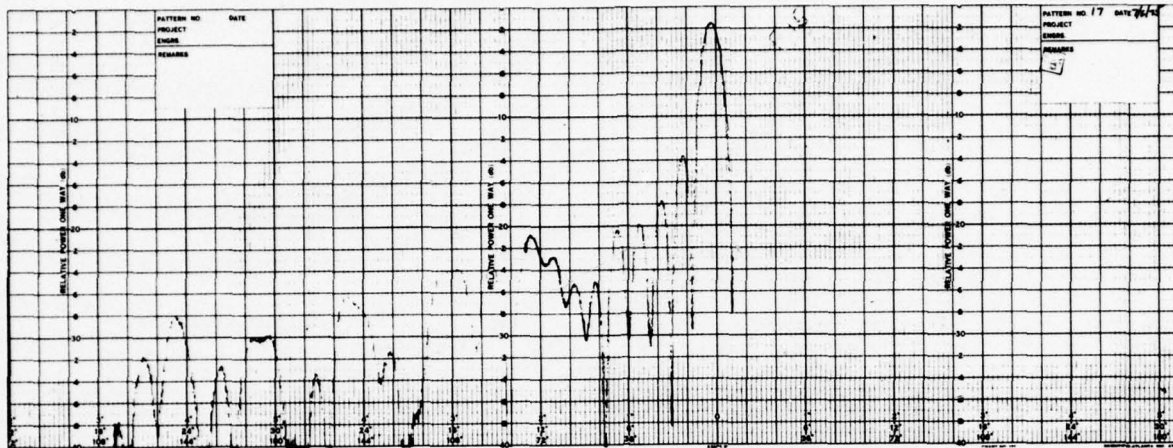
Figure 12-2. Transmit Antenna Patterns (Sheet 5 of 5)

For all electronically scanned (dynamic) patterns the beam is scanned from -16 degrees to +16 degrees with respect to the array normal direction. Note that -16 degrees is the right extreme of each dynamic pattern. The range of the scan angle listed in the indices in Figures 12-5 and 12-6 is that for which multipath effects from the valley floor are negligible.

Some preliminary data indicated that an array row phase calibration technique was needed before the antenna patterns could be recorded. It was decided that the phase of each row would be measured for all seven signal paths, and at all 20 frequencies. A computer program was generated which utilized both the RF signal generation and the phase measuring capability of the AN/TPS-59(XN-1) system to make the row phase measurements. Phase stable cables and directional couplers were used to distribute RF signals to and from the row under test. The measurements were stored in appropriate look-up tables for use as phase correction during normal system operation. This phase calibration procedure was completed on 4/23/75.

An important aspect of the pattern measurement tests was the status of each row signal path during the pattern measurement procedure. Each day prior to any pattern measurements the status of each signal path was checked using a performance monitoring computer program. In Table 12-1 the days in which the antenna pattern were measured are listed along with any row signal paths that were not functioning properly.

Table 12-1. Equipment Status

Measurement	Date	Row Status (Rows Not Functioning)
Receive Antenna Patterns	6/4/75	18, 41, 54
Receive Antenna Patterns	6/5/75	41, 54
Receive Antenna Patterns	6/6/75	1, 41, 54
Receive Antenna Patterns	6/9/75	41
Receive Antenna Patterns	6/10/75	41
Receive Antenna Patterns	6/11/75	41
Transmit Antenna Patterns	7/2/75	42
Receive Gain Measurement	7/16/75	11, 42

12.4.2.   Discussion of Results.

12.4.2.1.   Sidelobe Levels.

In an effort to determine how close the AN/TPS-59(XN-1) measured sidelobe performance compared to the expected values several receive elevation pattern calculations made with the aid of a digital computer. A set of amplitude and phase readings for each row path were generated at F2 by the use of the sum monitor test channel for each row. It should be noted that this measurement does not include the row feed networks, the circulators, and the bandpass filters. This test data was generated on 6/27/75. Both static and dynamic elevation sum and difference patterns were then calculated from this data. The calculated elevation static sum and difference patterns at frequency F2 are shown respectively in Figures 12-3 and 12-4. The calculated elevation dynamic sum and difference patterns at frequency F2 are shown respectively in Figures 12-5 and 12-6.

The calculated dynamic patterns were generated assuming a 4-bit phase shifter and 0.05 degree elevation scan steps. Only row 42 was missing (zero amplitude) for this calculation. These dynamic pattern calculations (Figures 12-5 and 12-6) compare closely to the measured patterns Number 43 and 44 in Figure 12-1.

Table 12-2 shows a summary of the dynamic elevation plane pattern measured sidelobe levels. Also included in the table are the results of the calculated dynamic patterns at frequency F2. The measured results agree favorably with the calculated expected results. For example, the measured peak sum sidelobe level at F1 is 18 dB while the expected calculated value at F2 is 20 dB. The measured number of points which exceed the 25 dB Y99 specification limit is 48 at F1 whereas 35 points are expected from the calculated pattern at F2. Table 12-2 also summarizes the percentage of measured sample points less than 25 dB sum or 20 dB difference for the elevation sum and difference patterns along with an estimation of the total number of points within specification over all visible space. It should be noted that the Y99 specification over all visible space is met for all the measurements made.
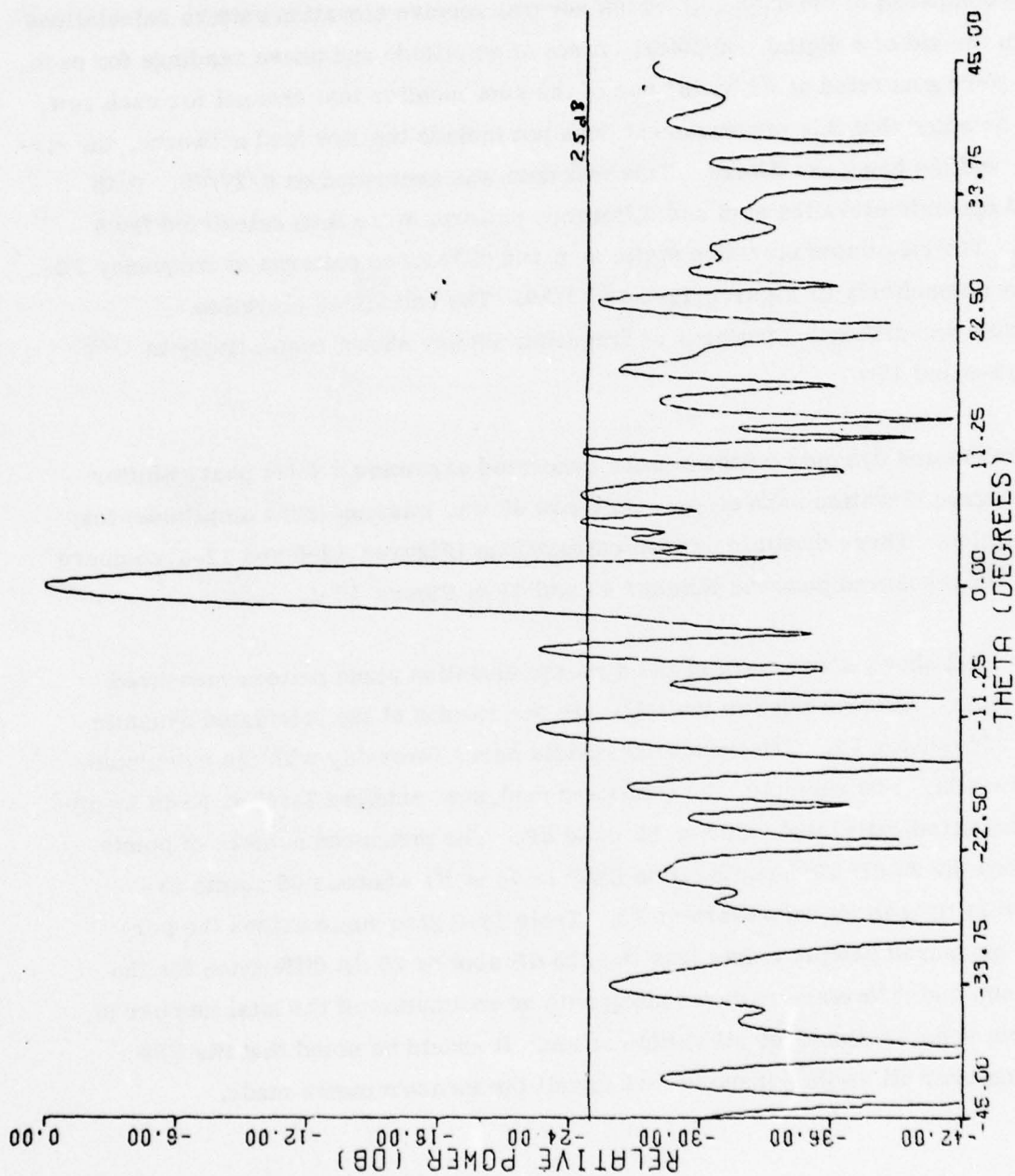
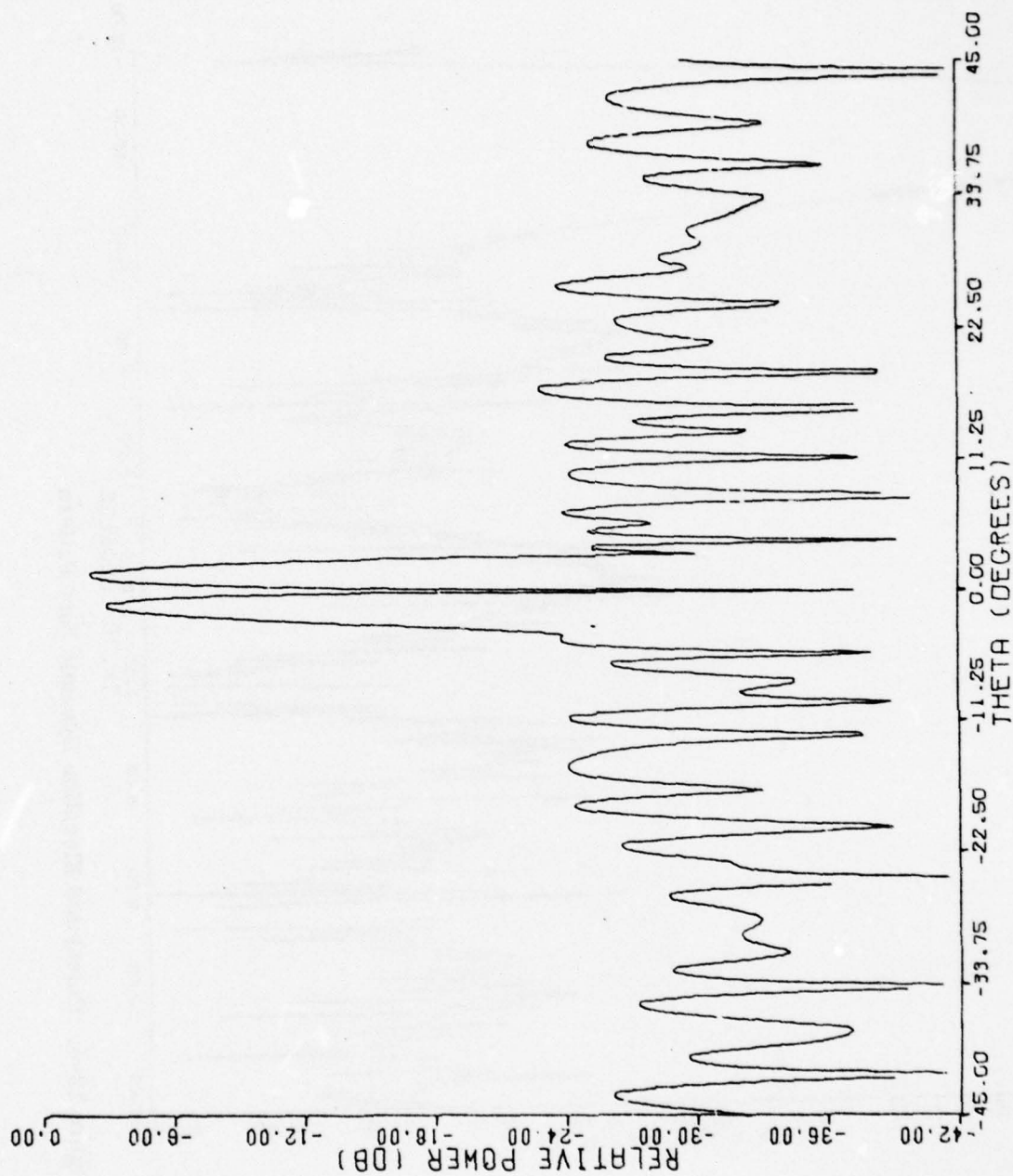Figure 12-3. Calculated Elevation Static Sum Pattern

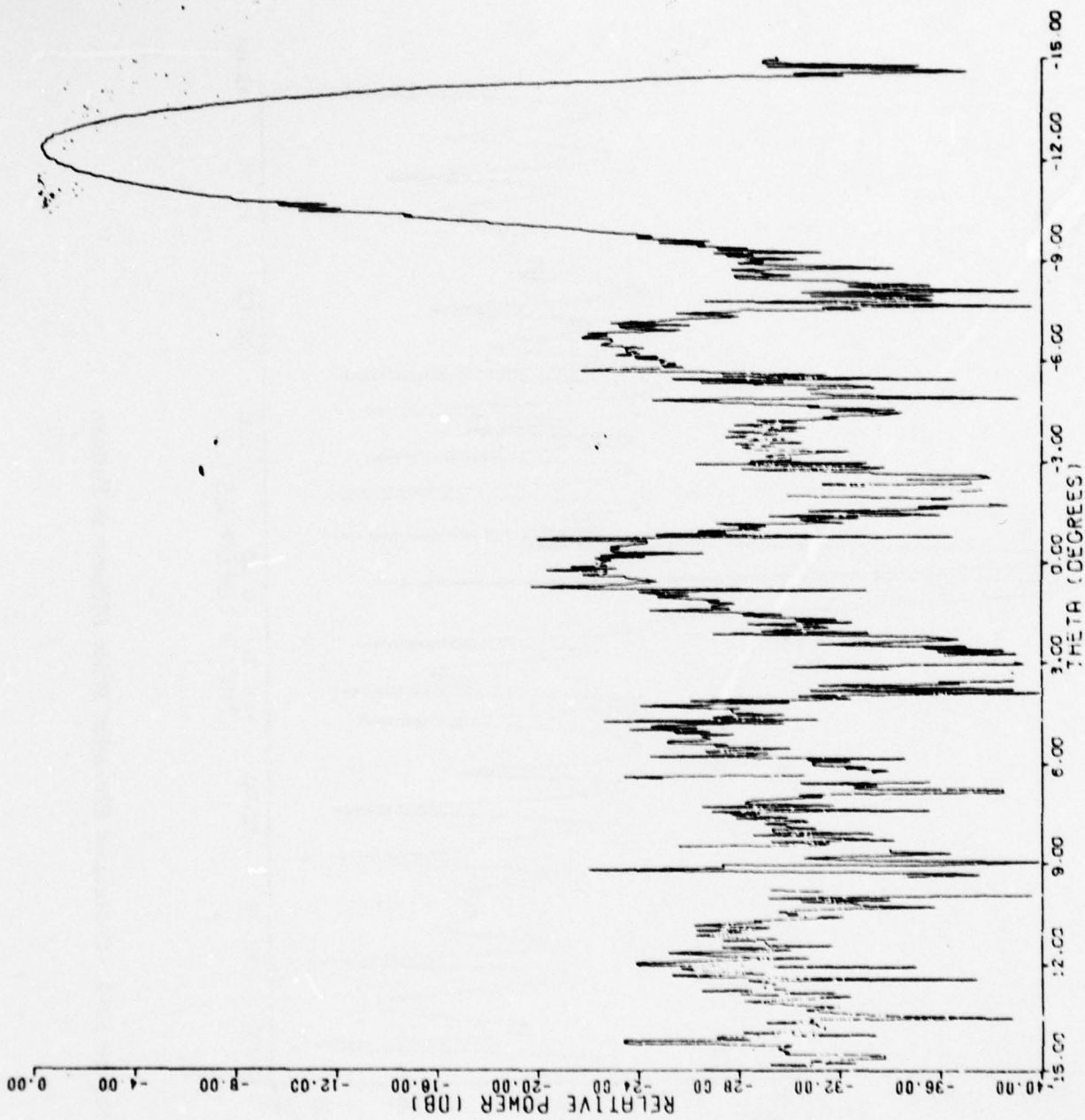Figure 12-4. Caclulated Elevation Static Difference Pattern

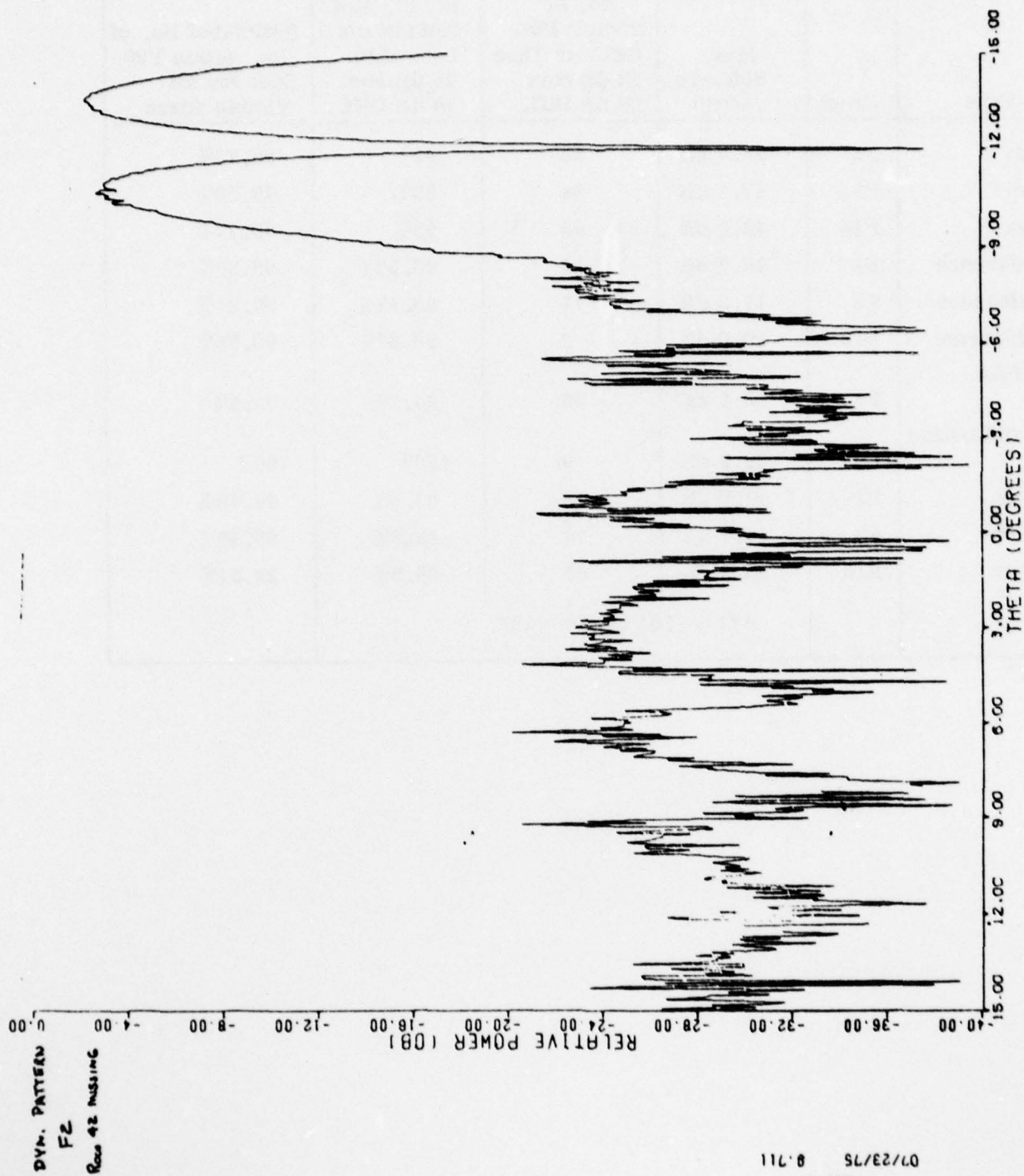Figure 12-5. Calculated Elevation Dynamic Sum Pattern

Figure 12-6. Calculated Elevation Dynamic Difference Pattern

12-33

Table 12-2. Elevation Plane Dynamic Pattern Sidelobe Level Summary

Beam Type	Freq.	Max. Sidelobe Level	No. of Sample Pts. Greater Than 25 dB Sum 20 dB Diff.	El. Pl. % of Sample Pts. Less than 25 dB Sum 20 dB Diff.	Estimated No. of Pts. within Y99 Spec for all Visible Space
Receive Sum	F1	18.0 dB	48	92%	99.73%
Receive Sum	F8	17.4 dB	84	86%	99.53%
Receive Sum	F15	19.0 dB	42	93%	99.77%
Receive Difference	F1	16.7 dB	14	96.67%	99.92%
Receive Difference	F8	17.3 dB	11	98.17%	99.94%
Receive Difference	F15	19.0 dB	2	99.67%	99.99%
Calculated Sum Receive	F2	20.0 dB	35	94.2%	99.8%
Calculated Difference Receive	F2	20.2 dB	0	100%	100%
Transmit Sum	F1	13.0 dB	99	83.5%	99.45%
Transmit Sum	F8	11.1 dB	97	83.8%	99.46%
Transmit Sum	F15	13.2 dB	88	85.3%	99.51%
		Array Tilt Angle = 12°			

Table 12-3 shows a summary of the measured static pattern sidelobe levels for all the different beam types that were measured. As expected, the azimuth plane sidelobe levels are least affected by random array excitation errors with only a few sidelobes exceeding the Y99 specification limits. For example, only one sum azimuth sidelobe exceeds the 25 dB Y99 specification and it has a value of 24.6 dB.

The AN/TPS-59(XN-1) array excitation errors are highly correlated in the elevation plane. This fact is evident from the higher sidelobe levels noted in Table 12-3 for the elevation plane. It should be noted that due to the array forward tilt angle limitation only half of the static elevation patterns were measured (-1 to +40 degrees). Consequently, the number of elevation plane sidelobes greater than the Y99 specification listed in Table 12-3 is assumed to be double that which was measured. The calculated elevation plane sum pattern (Figure 12-3) shows an expected maximum sidelobe level of 22.6 dB and 5 sidelobes greater than the Y99 specification of 25 dB. This compares with the measured data in Figure 12-1, Pattern Number 82, where it is estimated 8 sidelobes exceed the 25 dB level with a maximum level of 20 dB.

Table 12-3 lists the estimated number of sidelobes in visible space along with the percentage of measured sidelobes which meet the particular Y99 specification level (25 dB sum, 20 dB difference). In all cases the antenna sidelobe level easily meet the Y99 specification levels.

12.4.2.2. Gain Measurements.

On 7/16/75, the AN/TPS-59(XN-1) system antenna gain was measured for the receive sum channel and the low angle lower beam channel. These measurements were made at the base of the column feed at frequency F8. The measurement method consisted of measuring the RF power out the base of the column feed and comparing it to the power out of a Narda Model 646 Standard gain ham.

In order to evaluate the actual antenna gain the gain or loss of each component in the signal path leading to the base of the column feed must be known. The average gain value for these components was estimated from factory data.

Table 12-3. Principal Plane Static Pattern Sidelobe Level Summary

Beam Type	Freq.	No. of El. Plane Sidelobes > 25 dB Sum 20 dB Diff.	Maximum El. Plane Sidelobe Level	No. of Az. Plane Sidelobes > 25 dB Sum 20 dB Diff.	Maximum Az. Plane Sidelobe Level	Estimated Total No. Sidelobes in Vis. Sp.	No. of Sidelobes in Y99 Spec
Receive Sum	F1	8	20.0 dB	1	24.6 dB	4314	99.79%
Receive Sum	F8	4	23.0 dB	0	26.5 dB	4536	99.91%
Receive Sum	F15	6	19.0 dB	0	26.0 dB	4757	99.87%
Transmit	F1	22	13.0 dB	1	-	4314	99.47%
Transmit	F8	18	16.5 dB	0	26.0 dB	4536	99.60%
Transmit	F15	22	12.0 dB	0	-	4757	99.54%
Azimuth Diff.	F1	8	-	0	20.0 dB	4314	99.81%
Azimuth Diff.	F8	4	-	0	21.2 dB	4536	99.91%
Azimuth Diff.	F15	6	-	2	18.7 dB	4757	99.83%
Elevation Diff.	F1	4	18.2 dB	1	-	4314	99.88%
Elevation Diff.	F8	0	21.1 dB	0	-	4536	100%
Elevation Diff.	F15	2	18.0 dB	0	-	4757	99.96%
Low Angle Upper	F1	16	14.0 dB	1	-	4314	99.61%
Low Angle Upper	F8	10	18.0 dB	0	-	4536	99.78%
Low Angle Upper	F15	22	18.0 dB	0	-	4757	99.94%
Low Angle Lower	F1	18	12.8 dB	1	-	4314	99.56%
Low Angle Lower	F8	12	13.0 dB	0	-	4536	99.74%
Low Angle Lower	F15	16	13.0 dB	0	-	4757	99.66%
Calculated Elevation Sum	F2	5	22.6 dB	-	-	4345	99.86%
Calculated Elevation Diff.	F2	0	22.8 dB	-	-	4345	100%

The antenna gain was calculated from the data at the base of the column feed by subtracting the component gains from the measured gain. The calculated antenna gain for the sum receive channel is then $G_\Sigma = 53.7 - (19-.65-3.7-.15) = 39.2$ dB. This compares well to the expected value of 39.17 dB. The calculated antenna gain for the low angle lower beam is $G_{LA} = 52.7 - (18.7-.65-5.08-.15) = 39.88$ dB which also compares well with the expected value of 39.82 dB. The measured gain at the base of the column feed (53.7 dB Σ or 52.7 dB low angle) is referenced to an isotropic radiator.

12.4.2.3. Antenna Beamwidths.

The antenna 3 dB beamwidths were extracted from the pattern data in Appendix A and B. The 3 dB beamwidth data is summarized in Table 12-4 for a frequency of F8. From the table it can be seen that the measured values for the different system beam types agree well with the expected beamwidth values. It should be noted that the low angle beam squint listed in Table 12-4 is the difference in the pointing directions of the low angle upper and lower beams.

12.4.2.4. Antenna Cross-Polarization Levels.

Of the 12 cross-polarized receive antenna patterns measured, only one showed any level of cross-polarization greater than 30 dB. The sum elevation cross-polarization pattern at frequency F8 showed a peak level of 28 dB (referenced to the sum peak). It should be noted that in any cross-polarization, the transmit dipole orientation is extremely critical, which could result in some measurement error. It is concluded that considering possible measurement error the AN/TPS-59(XN-1) antenna easily meets the 30 dB cross-polarization requirement.

12.4.2.5. Difference Pattern Angular Sensitivity.

The expected elevation angluar sensitivity can be determined from the calculated difference pattern in Figure 12-2. From this pattern an angular sensitivity of 0.052 volts/volt/miliradian is indicated. From the measured pattern in Figure 12-1 Number 85, analmost identical sensitivity is measured.

Table 12-4. Principal Plane Beam Width Summary

Beam Type	Specification	Measured Value
Azimuth Sum Receive	3.2° Max	3.2°
Elevation Sum Receive	1.65° Nom	1.7°
Elevation Sum Transmit	1.3° Nom	1.3°
Low Angle Receive Upper Beam	1.4° Nom	1.4°
Low Angle Receive Lower Beam	1.3° Nom	1.3°
Low Angle Beam Squint	.85° Nom	1.1°
Elevation Receive Sum (1.5:1) Broadened Beam	2.5° Nom	2.3°
Measurement Frequency: F8		

The expected azimuth angular sensitivity was also calculated from factory measured row feed data at frequency F8. This calculation showed a result of 0.0314 volt/volt/mr. The measured value indicated in Figure 12-1, Pattern number 18, is 0.034 volt/volt/mr.

It is concluded that both azimuth and elevation angle sensitivity agrees well with expected values.

12.4.2.6.   Set-3 Antenna Measurements.

The Set-3 subarray antenna patterns were measured with the subarrays mounted on the AN/TPS-59(XN-1) antenna. Very little change in performance was noted when the results were compared to isolated Set-3 subarray patterns measured on 5/15/75. It was noted, however, that during this measurement the Set 3, Serial No. 2 and Serial No. 3 were mounted upside down. This means that in Figure 12-1 elevation patterns No. 80 and No. 81 the elevation angle is offset by 12 degrees due to this mounting error which has since been corrected.

12.5.   CONCLUSIONS.

The measured azimuth principal plane sidelobes show excellent agreement with the unerrored design values. This data along with the off-axix sidelobe measured data indicates an average azimuth sidelobe level due to random elements error of about -56 dB.

The AN/TPS-59(XN-1) system configuration which scans only in the elevation plane has amplitude and phase excitation errors which are highly correlated at the row level. Consequently the principal plane elevation sidelobe level shows the most degradation due to system random errors. Calculations have shown that the measured elevation pattern performance agrees well with the expected calculated pattern performance.

The AN/TPS-59(XN-1) measured sidelobe performance was compared to Y99 specification levels for both the dynamic and static pattern situations. It was concluded that in every instance for all the different beam types and frequencies that the AN/TPS-59(XN-1) sidelobe performance easily meets the Y99 specification level for all visible space. Measured beam widths, angular sensitivity, and cross-polarization levels also meet specification levels.

13.0.   NOISE TEST.

13.1.   PURPOSE.

This test was conducted as part of the Pre-Service Acceptance Test Procedures to demonstrate that the AN/TPS-59(XN-1) acoustic noise levels do not exceed the requirements of BUMEDINST 6260.6B in sound level and duration of exposure for normal operations and maintenance.

13.2.   SCOPE.

The test consisted of sound level measurements made in and around the shelters and other operating components of the system, in various operating configurations. The AN/TPS-59(XN-1) shall have passed this test if the interior sound levels do not exceed 90dBA test with air conditioners and generators operating; and the exterior sound levels do not exceed 90 dBA not including air conditioners and generators.

13.3.   TEST METHOD.

The test was conducted in accordance with paragraph 4.12 of the Pre-Service Acceptance Test Procedure.

13.4.   RESULTS.

Table 13-1 presents the data measured at the points shown in Figures 13-1 through 13-3. The measurements indicated a background noise level in the shelters, with all equipment off, of 36 dBA. The diesel generators added 16 to 18 dB of noise. The fans increased the noise ratio by another 26 to 28 dB. However, the noise level in the shelters never exceeded the 90 dBA maximum allowable level for continuous exposure. Comparisons of noise levels in the shelter, with the air conditioners and diesels running, with and without the system operating, showed an average increase in noise level of 13 to 15 dB due to the operation of the system.

Measurements made external to the shelters showed very little increase in noise due to system operation. The only exception was the noise increase on the array due to array fans (5 to 9 dB). The 90 dBA noise level was exceeded at the diesel generators (measurement positions 11 and 12 of figure 4.12-3). This condition was known prior to the actual measurements, in that acoustically protective headphones were issued to those maintenance personnel that worked on the generators.

13-1

Date _11 Sept-77_

Time _1300_

. Table 13-1. System Audio Noise Test Data Sheet

Wind Velocity _5-15 MPH_   Barometric Pres _29.37 in Hg_

Wind Direction _South_   Humidity   _62%_

Temperature _80°F_

<u>NOTE</u>: All sound level readings are in DBA

Ambient Noise

Shelter 1 position 3 _36_

Shelter 2 position 3 _36_

With Diesel Power

Shelter 1 position 3 _52_

Shelter 2 position 3 _54_

With Fans And Diesels Running

Shelter 1 position 4 _78_

position 6 _77_

Shelter 2 position 4 _82_

position 6 _81_

With Air-Conditioners And Diesels Running

Shelter 1		Shelter 2	
Position 1	_63_	Position 1	_60_
2	_63_	2	_60_
3	_61_	3	_63_
4	_61_	4	_62_
5	_61_	5	_62_
6	_61_	6	_63_

11 Sept. 75

Table 13-1. System Audio Noise Test Data Sheet (Continued)

All Systems Operating

Shelter 1

Position 1	76	90 dBA max
2	76
3	76
4	77
5	75
6	77

Shelter 2

Position 1	75	90 dBA max
2	75
3	75
4	74
5	74
6	75

Outside Sound Levels (including Generators and Air Conditioners)

	With System Operating (RF Inhibited)	Without System Operating	Difference (90 dBA max)
1	70	68	2
2	68	69	-1
3	71	71	0
4	78	81	-3
5	83	83	0
6	80	80	0
7	79	78	1
8	81	76	5
9	67	67	0
10	82	79	3
11	95	95	0
12	95	95	0
13	80	80	0
* 14	81	78	3
15	81	80	1

* FRONT OF UNIT 5

13-3

11 Sept. 75

Table 13-1. System Audio Noise Test Data Sheet (Continued)

Antenna Maintenance Platform (including Generators and Air Conditioners)

With AC Power Applied to the Antenna	Without AC Power Applied to the Antenna	Difference (90 dBA max)
Top 80	71	9
Middle 81	73	8
Bottom 81	76	5

Ronald A Joseph
Test Director

RJ LaVine 11 Sept. 75
Government Witness
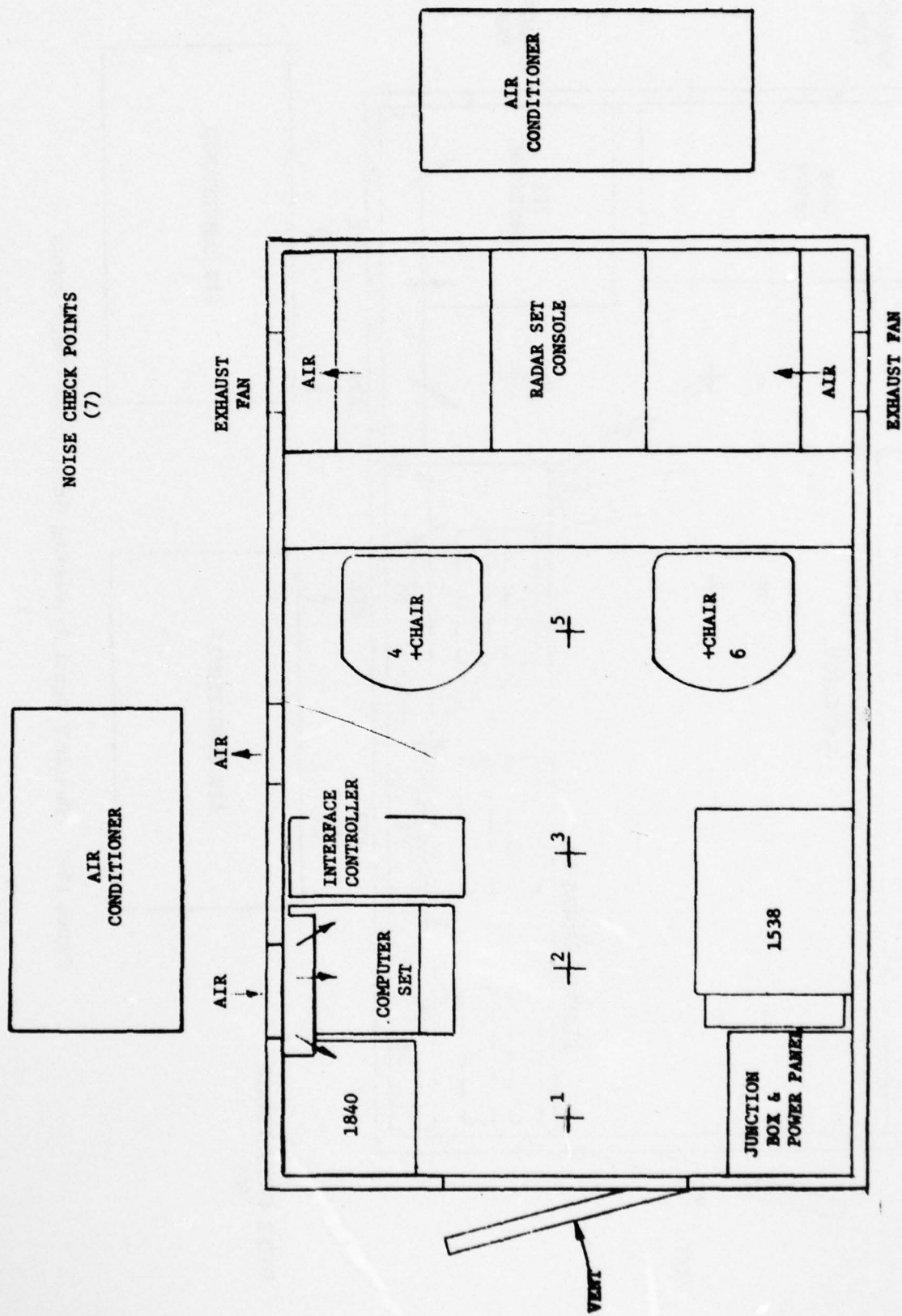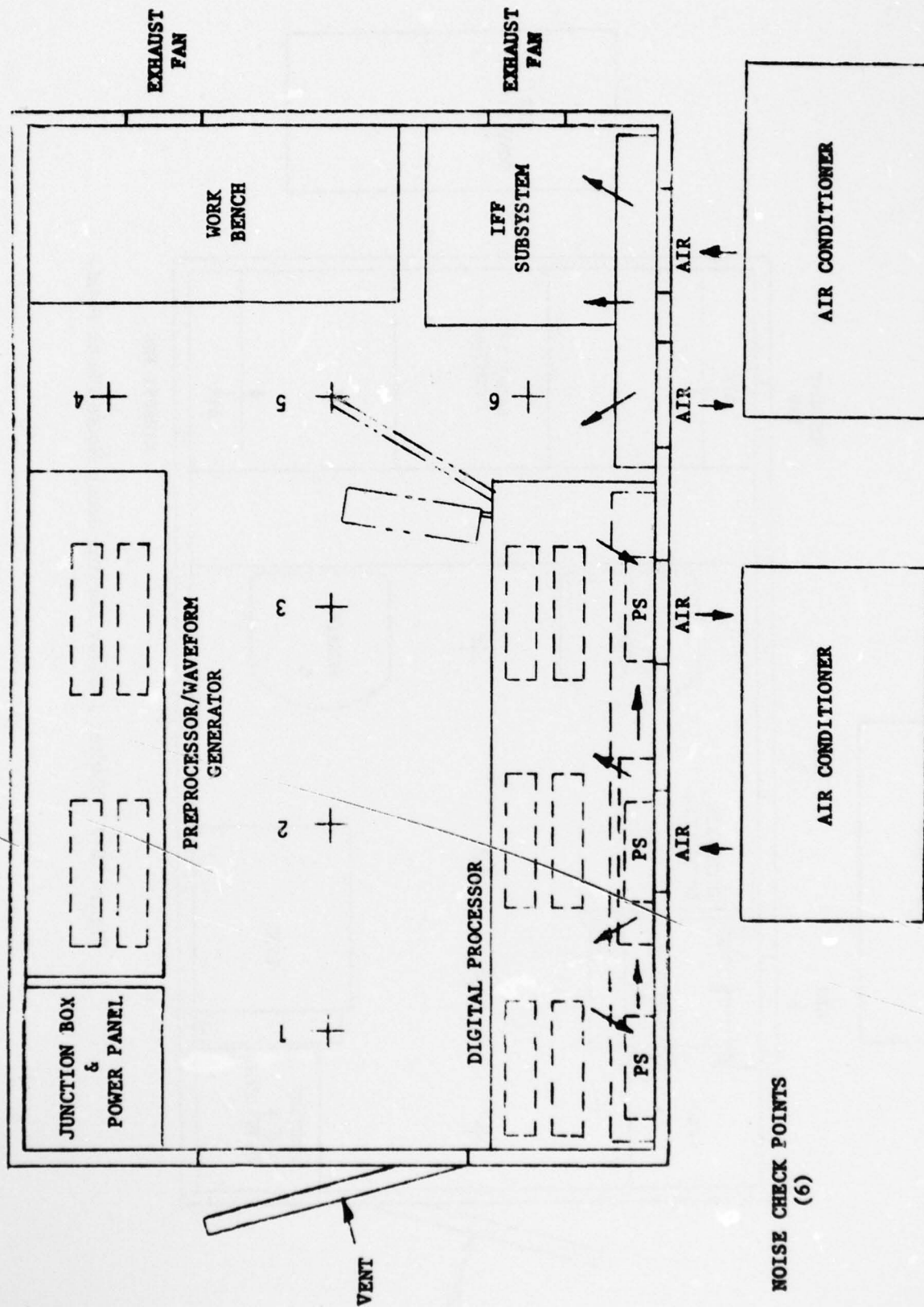
Figure 13-1. Shelter 1 Radar Control Group Noise Check Points

Figure 13-2. Shelter 2 Signal Processing Group Noise Check Points
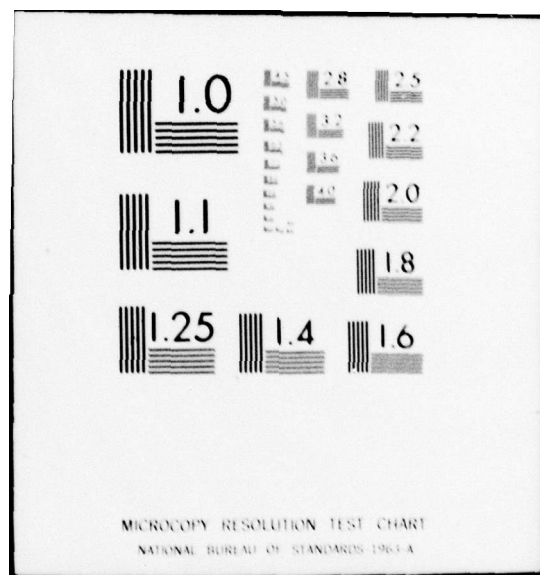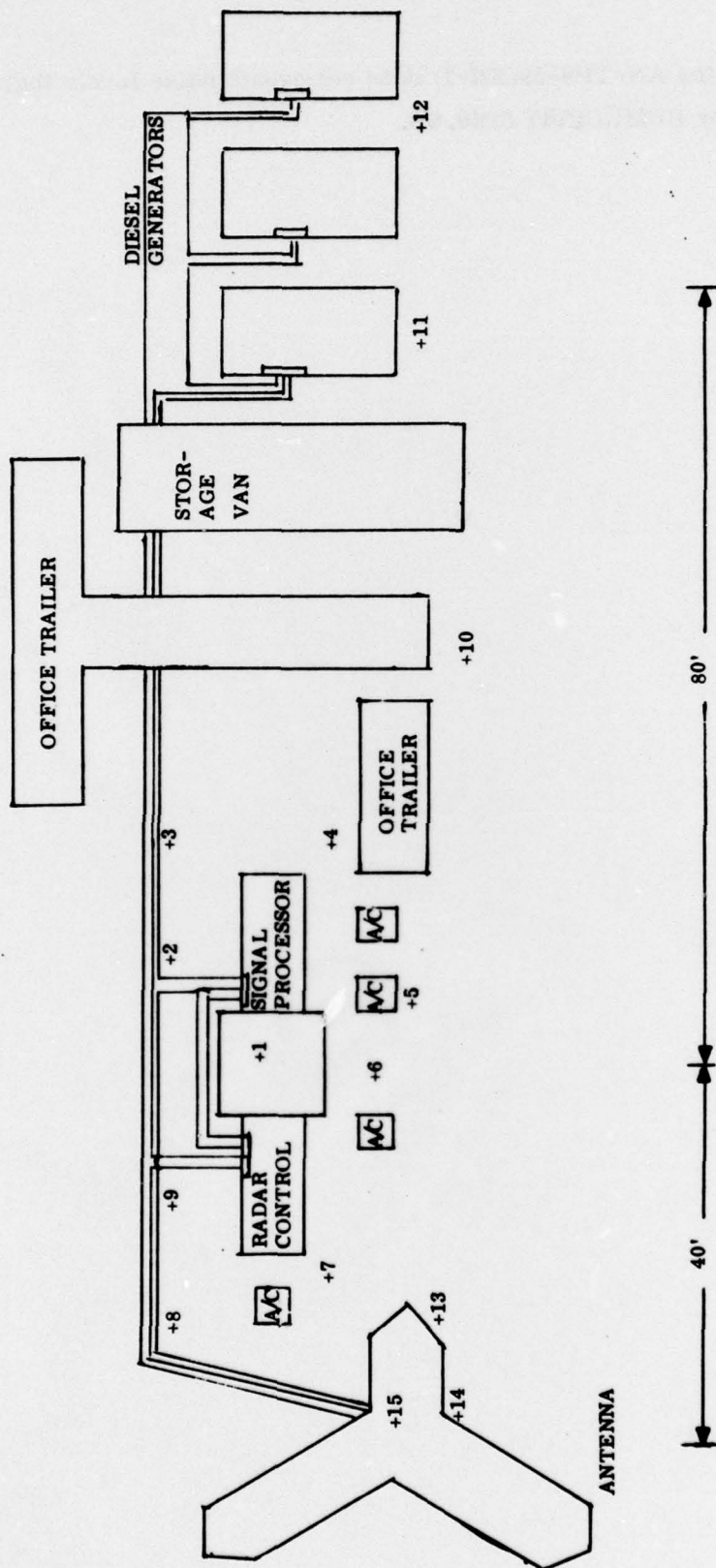
MICROCOPY RESOLUTION TEST CHART
NATIONAL BUREAU OF STANDARDS-1963-A

Figure 13-3.   Radar External Noise Check Points

13-7

14.0. PRELIMINARY EMI TEST.

Due to the nature of the data, the results and conclusions of this test are supplied as a separate classified report "AN/TPS-59 Radar Preliminary Electromagnetic Compatibility Test" dated December, 1976.

13.5. CONCLUSIONS.

The operation of the AN/TPS-59(XN-1) does not create noise levels that exceed the 90 dBA limit set by BUMEDINST 6260.6B.

14.0. PRELIMINARY EMI TEST.

Due to the nature of the data, the results and conclusions of this test are supplied as a separate classified report "AN/TPS-59 Radar Preliminary Electromagnetic Compatibility Test" dated December, 1976.

15.0. INTERCHANGEABILITY DEMONSTRATION.

This demonstration was to have been conducted as part of the maintainability demonstration. Due to method used for simulating faults during the maintainability demonstration and the limited spare parts that were available at the time, this demonstration will be conducted in a future phase of the contract.

16.0.   SURFACE EXAMINATION.

The AN/TPS-59(XN-1) was located in the Central New York environment for approximately one year during which time it was subjected to the vagaries of summer heat and humidity and the long winter months of snow, sleet and rain.   Examination of the surfaces exposed to the elements showed no significant deterioration.

17.0. SALT SPRAY TEST.

Salt spray tests were conducted in accordance with approved test procedure SK 732016A2363, Rev. 1. Test results were submitted in report TCL 8450 "Salt Spray Tests on AN/TPS-59(XN-1) Antenna, Transmitter and Shelter Sample Materials" on 21 January 1974.

18.0. TAOC INTEGRATION DEMONSTRATION.

Integration of the AN/TPS-59(XN-1) with TAOC is being accomplished at MCTSSA, Camp Pendleton, CA. in accordance with the Pre-Service Acceptance Test Procedure. The results and conclusions of this demonstration will be submitted as a separate report upon completion of the integration demonstration.